SUITABILITY OF HYBRID ELECTRIC POWERTRAINS WITH ELECTRIC TURBOCHARGER

Suitability of Hybrid Electric Powertrains with Electric Turbocharger

By
Syed Kamran Arshad-Ali

A dissertation submitted in fulfillment of the
requirement of the degree of

Master of Applied Science

Presented to the Faculty of the

Department of Mechanical Engineering

At

McMaster University

Hamilton, Ontario

McMaster University MASTER OF APPLIED SCIENCE (2015) Hamilton, Ontario

(Mechanical Engineering)

TITLE: Suitability of Hybrid Electric Powertrains with Electric Turbocharger

AUTHOR: Syed Kamran Arshad-Ali, B.Eng (McMaster University)

SUPERVISORS: Dr. Ali Emadi, Dr. S.R. Habibi

NUMBER OF PAGES: 130

Lay Abstract

Turbochargers on internal combustion engines can utilize a portion of waste exhaust energy to pump more air into the cylinder leading to greater power and efficiency. A modern high performance 4-cylinder turbocharged engine is capable of replacing a V6 engine of much higher cylinder displacement. However turbocharged engines suffer from 'turbo lag' when the engine cannot immediately produce power. An electric turbocharger can virtually eliminate this 'turbo lag' as well as generate electricity from excess energy the turbocharger does not use. Electric turbochargers have been development by researchers and various automotive manufacturers. However the potential effects of such a system within the framework of a hybrid electric powertrain in a consumer vehicle has not been quantified. The objective of this research is to use high fidelity models to investigate the effects of an electric turbocharger system within a hybrid powertrain.

Abstract

This research investigates the effects of an electric turbocharger in a hybrid electric powertrain. First generic vehicle models are created and run to understand the overall powertrain requirements of torque, power and energy of a performance consumer vehicle. Then a low fidelity baseline model of a conventional vehicle is created in Simulink to serve as a baseline measure.

To analyze an electric turbocharger system a high-fidelity model in AMESIM of a 4 cylinder turbocharged engine was modified. This engine model was analyzed using virtual dynamometer tests and a simplified look-up table based controller was developed for the electric motor within the electric turbocharger. Next this engine model was inserted within three different types of hybrid powertrain architectures models in AMESIM. Each hybrid powertrain required a unique supervisory controller which was developed using Stateflow in Simulink. These controller algorithms were imported into AMESIM and the model was simulated over standard drive cycles. Since a very wide variation of electrification level exists within hybrid powertrains the supervisory controllers are calibrated for charge-sustaining simulations. This allows for impartial comparisons across the hybrid architectures. Lastly a track drive cycle was developed to understand electric turbocharger effects under high performance loading conditions.

Acknowledgements

This research was undertaken, in part, thanks to funding from the Canada Excellence Research Chairs (CERC) Program.

I would like to thank my supervisors Dr. Emadi and Dr. Habibi for giving me the opportunity to pursue this research and making my graduate research experience an enriching one.

I would like to extend my gratitude to my colleagues and fellow researchers at the McMaster Automotive Resource Centre (MARC) and JHE for their guidance and support during my research.

Special thanks are due to the members of the McMaster Formula Hybrid team for an unforgettable four years.

Table of Contents

Table of Figures

Index of Tables

Symbols and Abbreviations

AFR	Air-Fuel Ratio
AWD	All-wheel Drive
BSFC	Brake Specific Fuel Consumption
CAFE	Corporate Average Fuel Economy
Cd	Coefficient of drag
CS	Charge-Sustaining
CD	Charge-Depleting
ECU	Engine Control Unit
EPA	Environmental Protection Agency
EV	Electric Vehicle
F_{aero}	Aerodynamic Load
F_{grade}	Road gradient load
$F_{rolling\ resistance}$	Rolling Resistance Load
F_{tr}	Tractive Force
HEV	Hybrid Electric Vehicle
HWFET	Highway Fuel Economy Driving Schedule
ICE	Internal Combustion Engine
I/O	Input/Output
M	Mass
MGU-K	Motor-generator unit kinetic
MGU-H	Motor generator unit heat
MJ	Mega Joule
MPG	Miles per Gallon
MPGe	Miles per Gallon Gasoline Equivalent
p	Pressure
PI	Proportional Integral
PM	Particulate Matter

r	Universal Gas Constant
S_c	Single Piston Displacement
SOC	State of Charge
T	Temperature
TDI	Turbocharged Direct Injection
TCU	Transmission Control Unit
UDDS	Urban Dynamometer Driving Schedule
V	Volume
V_p	Mean Piston Velocity
WOT	Wide-Open Throttle

1. Introduction

The start of widespread industrialization over 150 years ago led to a great increase in the amount of carbon dioxide and other pollutants collecting in the atmosphere. The consequences have been increased global temperatures and climate change leading to widespread social, economic and environmental consequences. Various efforts around the world from regulatory bodies and other organizations are aimed at reducing worldwide emissions. The transportation industry as one of the leading emitters of harmful pollutants has fallen within the scope of these efforts. In every major market around the world fuel efficiency and emissions regulations for passenger light vehicles are either being proposed or already in effect.

Automotive companies have begun planning for these stricter regulations in two strategies. One is to explore new technologies focused on vehicle electrification. The other is to increase efficiency of components within the conventional powertrain. Manufacturers for over 10 years have been developing newer, smaller, more fuel efficient engines to meet consumer demand and regulatory pressure. Typically larger engines are being replaced by an equivalent, smaller displacement, turbocharged one. One of the new technologies being explored in this area are electric turbochargers. Electric turbocharging involves attaching a very high speed electric motor onto the turbocharger shaft. With an electric motor 'turbo lag', lack of pressure at the intake leading to lower power, can be virtually eliminating. The system can also convert excess exhaust energy to electrical energy for later use. Electrical turbocharger systems are currently only in use within motorsports, in

Formula 1 and certain LMP1 cars. The technology is slated for release in consumer performance vehicles in the coming years.

Considerable work has already been done on using an electrical turbocharger system with a conventional powertrain in consumer applications. However its usage in a hybrid electric powertrain has not been explored apart from in motorsports applications. This research will explore the feasibility and potential benefits of an electrical turbocharger system within the wider energy framework of a hybrid electric powertrain in a consumer performance vehicle.

Vehicle Fuel Economy and Emissions Targets

The growing social movement towards a sustainable future has led to a need in the automotive industry to build increasingly fuel-efficient vehicles. The Obama administration in the US has set a 54.5 mpg standard efficiency target for cars by 2025 [1]. This is essentially double the average of current models on the market today. It will be very difficult for conventional gasoline powered cars to reach such a target in only ten years without significant technical innovation. The standard also stipulates a yearly compliance target specifying on average an annual improvement of 2 mpg. The table below is from the United States Environmental Protection Agency Regulatory Announcement document specifying its required CO_2 emissions and Corporate Average Fuel Economy (CAFE) targets [1].

Table 1: Projected Fleet-Wide Emissions Targets

	2016 base	2017	2018	2019	2020	2021	2022	2023	2024	2025
Passenger Cars (g/mi)	225	212	202	191	182	172	164	157	150	143
Light Trucks (g/mi)	298	295	285	277	269	249	237	225	214	203
Combined Cars & Trucks (g/mi)	250	243	232	222	213	199	190	180	171	163
Combined Cars & Trucks (mpg)	35.5	36.6	38.3	40.0	41.7	44.7	46.8	49.4	52.0	54.5

These fuel economy limits are enforced via fines of $5.5 per 0.1 mpg violation based on the average fleet mpg rating of all vehicles sold in a calendar year by the manufacturer. For example BMW in 2013 had a weighted fleet rating of 33.1 mpg, without any improvements in fuel economy they would be subject to a fine of over $357 million in 2025 [2].

This upcoming regulatory pressure is not limited to only the North American market. Policy makers around the world are pushing for stricter limits on fuel economy. Even in developing markets such as India and China strict limits similar to the CAFE targets are projected. Figure 1 below illustrates future enacted or proposed fuel economy targets from major regions worldwide [3]. The results are normalized to the standardized CAFE dynamometer test cycle.

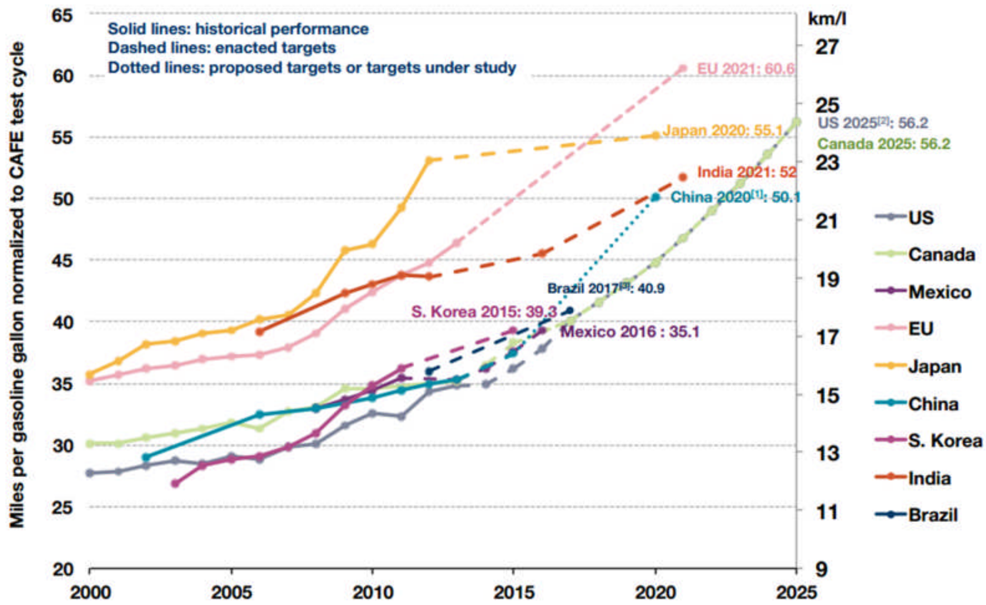

Figure 1 - Worldwide Fuel Economy Standards to 2025 [4]

Additionally regulatory bodies have enacted similar requirements for vehicle tailpipe emissions. CO_2 emissions are directly proportional to the amount of fuel burned however other harmful emissions such as hybrocarbons, Nitrogen oxide (NO_x), particulate matter and Sulfur Oxide (SO_x) are explicitly controlled. In recent years tighter emission regulations have led to further advancements in clean diesel technologies and exhaust after treatment systems.

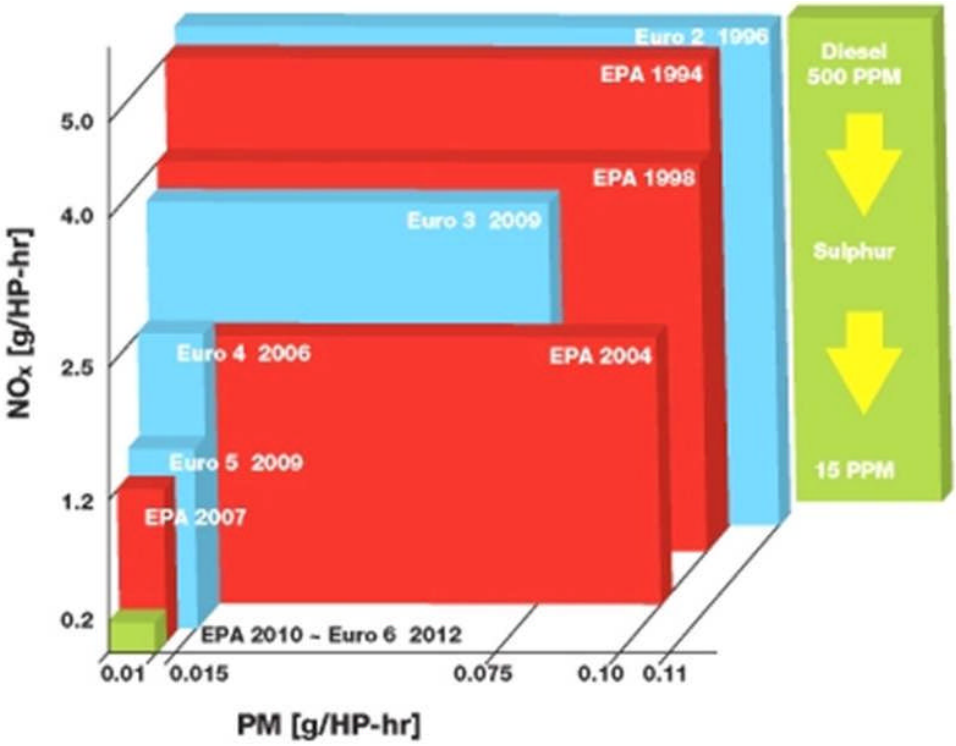

Figure 2 - Historical EPA NOx & PM Emissions Regulations [5]

Current Automotive Powertrain Trends

Fuel economy targets and increasing consumer demand for fuel efficient vehicles in the face of rising oil prices have forced manufacturers to re-engineer their offerings. In a conventional vehicle the internal combustion engine is the greatest source of inefficiency. It is expected the majority of improvements for fuel economy and emissions will come from progress in internal combustion internal combustion engines [6].

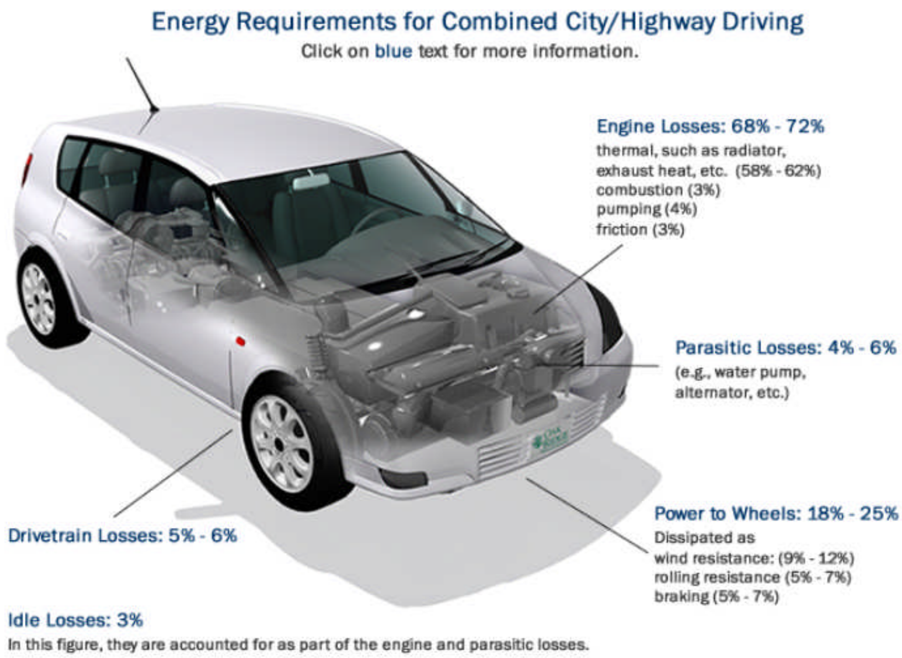

Figure 3 - Energy Split for Conventional Vehicle [7] [8] [9]

A further challenge on top of this is the increased consumer demand for performance. The average power in light-duty vehicles sold has been steadily increasing over the past thirty years. Manufacturers and consumers do not want to compromise between efficiency and performance if possible.

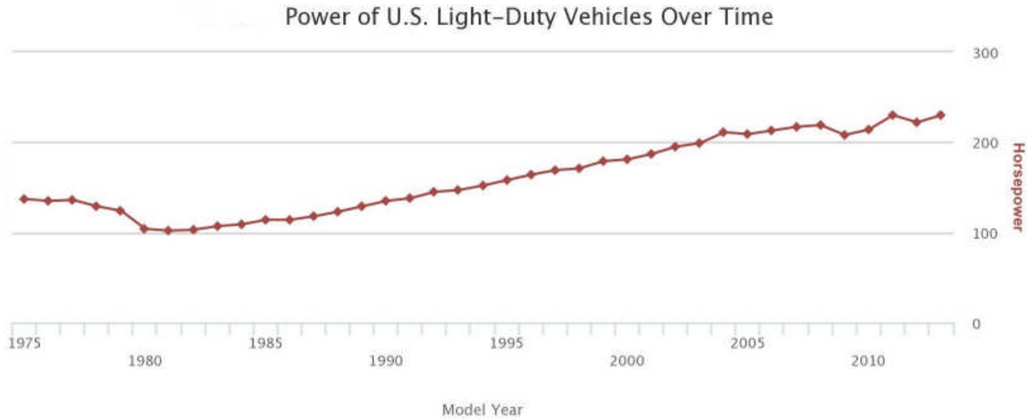

Figure 4 - Average Horsepower of Vehicles in U.S. from 1975-2015 [1]

Consequently the automotive industry have invested greatly in new engine programs designed to meet regulatory requirements. An example is the Skyactiv technology program by Mazda Motors, first seen in their vehicles in 2011. The Skyactiv program aims to increased engine fuel efficiency without sacrificing performance. Mazda`s Skyactiv engines have a high compression ratio of 14:1 compared to other engines with a compressions ratio of between 10:1 to 12:1 [10]. Compression ratio is directly proportional to the thermal efficiency of an engine therefore any increase directly translate into improved fuel economy. Typically an increased compression ratio leads to higher incidence of knocking, or premature combustion. The Skyactiv program was able to mitigate knocking through complete redesign of the exhaust system, piston heads and direct injection system [10]. The Skyactiv program to date is responsible for nearly fifteen percentage increase in vehicle efficiency [11]. Mazda reports their second generation Skyactiv gasoline engines will use homogeneous charge compression ignition (HCCI) to achieve an even higher compression ratio of 18:1 by 2020 [12].

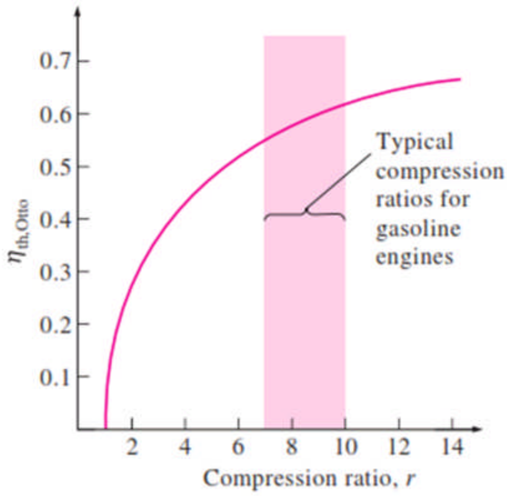

Figure 5 - Theoretical Efficiency vs. Compression Ratio for Spark-Ignition Engines [13]

Another method for increasing engine fuel economy is to employ engine downsizing. Engine downsizing is reducing the combustion chamber displacement size by using forced induction. Naturally aspirated engines use the atmospheric pressure to drive air into the combustion chamber. Forced induction engines typically use either a turbocharger or supercharger to artificially increase the pressure at the intake thereby providing more air for combustion. It has become an increasing trend in the automotive industry to replace big naturally aspirated engines with smaller more fuel efficient turbocharged ones. Large six cylinder engines can be replaced with smaller turbocharged four cylinder ones, both engine offering the same torque output. Borg Warner predicts by 2017 4-cylinder engines will have upwards of 80% of the market [14]. Companies have developed large-scale engine programs for replacing their current offerings with equivalent turbocharged engines. Ford`s EcoBoost program produces 1.3 million engines annually and is an option on almost every vehicle platform they offer [15].

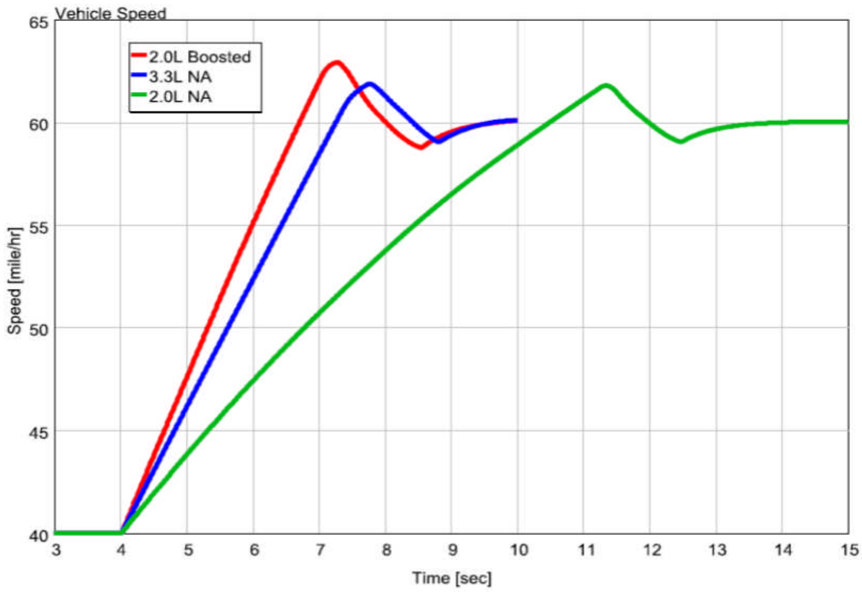

Figure 6 – Transient Response of Turbocharged vs. Naturally Aspirated Engines [14]

Another solution is to use hybrid electric powertrains which can greatly increase fuel economy and lower emissions albeit at an increased purchase price to the consumer. As of 2014 electrified powertrain vehicles comprised 2.98% of all new vehicles sold in the United States [16]. Hybrid powertrains are projected to capture an increasing amount of the market as manufacturers aim to decrease costs and move towards greater levels of powertrain integration across their model lines. Hybrid electric powertrains are discussed in greater detail in a later section.

Research Objective and Scope

The objective of this research is to quantify the suitability of electric turbocharger system within hybrid electric powertrains. Electric turbochargers offer the ability to capture a greater percentage of waste exhaust energy than conventional turbochargers. Extensive research and prototyping has already been conducted on fitting engines with electric turbochargers. This research looks at the feasibility and benefits of such a system within the wider systems interaction of a hybrid electric powertrain architecture.

First a vehicle chassis model is defined and simulated over standard drive cycles to understand power, energy and torque requirements. Then a conventional vehicle model based on this defined chassis is simulated over the same drive cycles to get baseline results for later comparisons. Next to model the E-turbocharger a predefined 1D engine model within AMESIM was modified to add the electrical system to the conventional turbocharger. The E-turbocharger model is then used within different hybrid powertrain architectures. The simulation results are compared to the baseline conventional vehicle model and to the hybrid powertrain models without E-turbocharger system to determine the system's impact.

2. Literature Review of Electric Turbochargers

Turbocharging is a common method used to increase the specific power of an internal combustion engine. The power output of an ICE is largely dependent on the amount of air it can pump per cycle. Typically a naturally aspirated engine is reliant on the atmospheric pressure to pump air. A turbocharger increases this airflow by increasing the pressure at the inlet. In a turbocharger the engine exhaust gasses that are otherwise wasted are harnessed by a turbine to drive a compressor at the inlet. By increasing the pressure at the inlet a larger mass of air is driven into the cylinder allowing for greater combustion at the higher fuel efficiency.

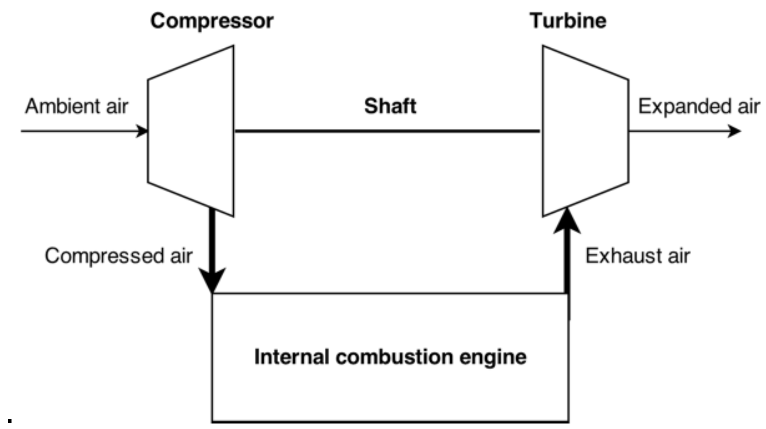

Figure 7 - Basic Turbocharger Diagram

A major disadvantage of turbocharged engines is the delayed response in power generation. If the turbine is at a lower speed it takes time for it to spin up to effectively power the compressor. This causes a delay which is commonly known as "turbo lag".

To overcome the drawbacks of large turbochargers and to also maximize exhaust energy recovery the addition of electric motors to either the turbine or compressor have been researched extensively. Adding an electric motor to the compressor will eliminate turbo lag by driving the compressor electrically during periods of insufficient turbine boost pressure.

Electrification of the turbine would allow extra energy to be harvested from the exhaust gasses. In a conventional turbocharger not all of the exhaust gasses travel through the turbine, at certain operating conditions they are diverted around using a wastegate. This is to ensure the compressor stays within its operating envelope. The compressor has three main limits, its maximum rotational velocity, the surge limit and the choke limit. The surge limit is due to an inadequate air flow rate through the compressor that triggers a complete breakdown and results in reverse flow [17]. It is found at the left hand side of a compressor operating map. The choke limit is the maximum mass flow rate the compressor can achieve and is found on the right side of a compressor operating map. Beyond this point the compressor efficiency drops dramatically due to local velocities approaching Mach 1 [18].

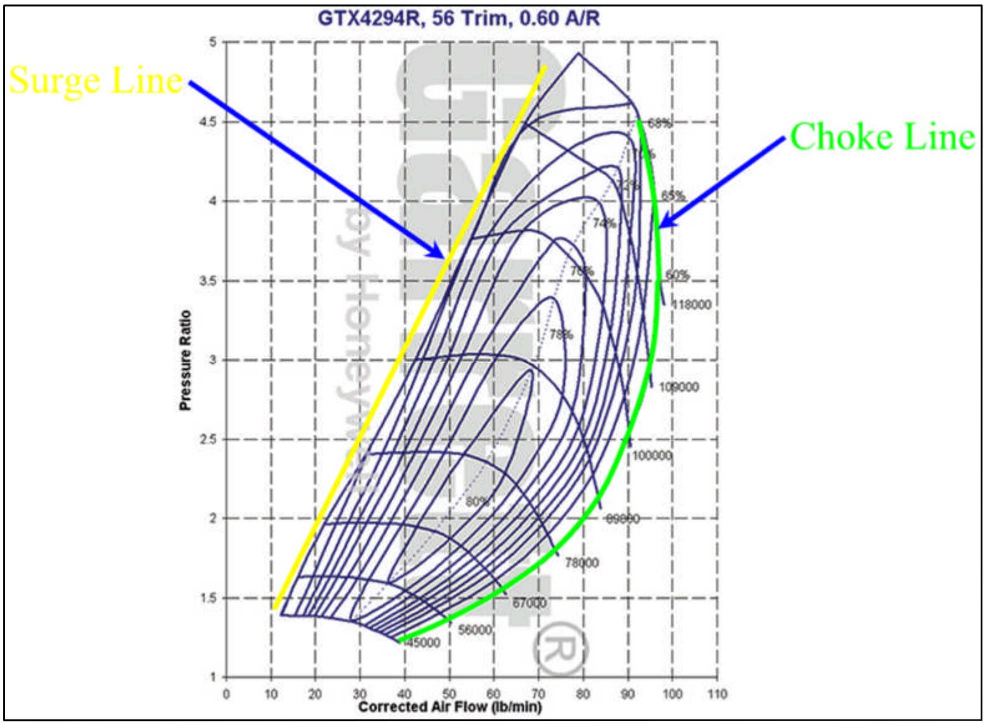

Figure 8 - Example Compressor Map with Marked Surge/Choke Limits [19]

A wastegate controls the amount of mechanical energy converted by the turbine by diverting exhaust gasses around the turbocharger. Electrification of the turbine would allow the system to generate energy without pushing the compressor past its limitations. This extra captured energy can be used later to drive the compressor or by other components in a wider electrified vehicle.

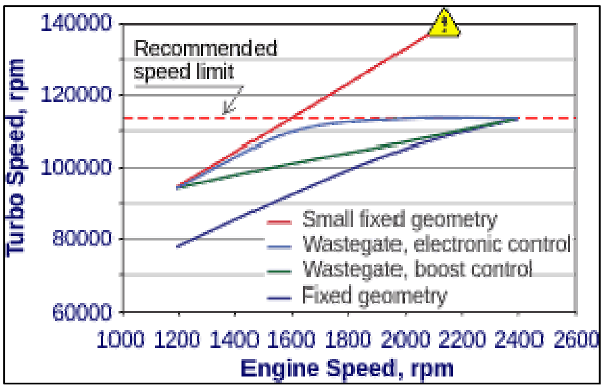

Figure 9 - Wastegate Control for Turbocharger RPM Limit [20]

There are various possible electrified turbocharger architectures depending on where the electric motor(s) is located in the system.

a) Electric motor on a separate turbine downstream of turbocharger

b) Electric motor on a separate turbine connected in parallel to turbocharger

c) Electric motor on the compressor only

d) Electric motor on the turbocharger shaft

e) Separate electric motors on both compressor and turbine

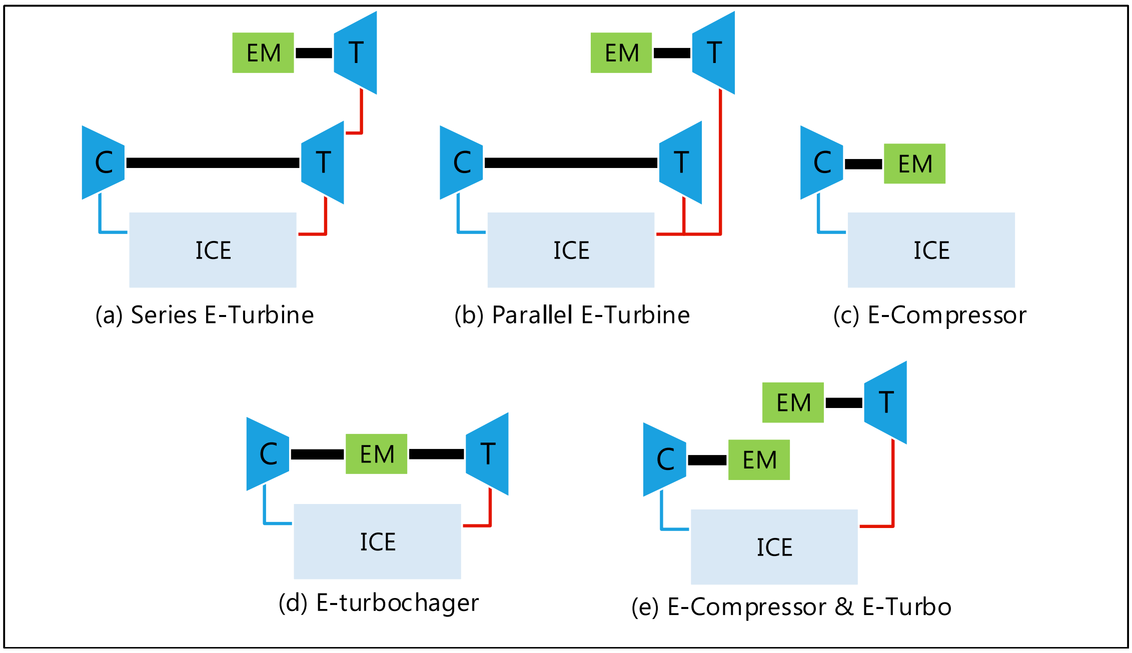

Figure 10 - Electrified Turbocharger Configurations

Configurations (a) to (c) add an electric motor to either the compressor or the turbine side. Therefore their benefits are limited to just one of the two discussed earlier. Studies have shown configurations (a) and (b) offer a decrease in brake specific fuel consumption (BSFC) even with the increased back pressure on the engine due to the extra turbine [21]. Exhaust back pressure is the resistance acting against the engine exhaust gasses flowing out. Too much exhaust back pressure will have adverse effects on engine operation leading to increased pumping work, reduced intake manifold pressure and unfavorable cylinder scavenging/ combustion effects [20].Ojeda and Rajkumar conducted research demonstrating upgrading existing turbochargers with high efficiency turbines can sufficiently decrease exhaust back pressure to accommodate an E-turbo system [22] [23]. Furthermore additional work by Weilin et. al showed the E-turbo system cannot be optimized for both vehicle high and low load drive cycles [24].

Electrification of just the compressor side is a technology projected to appear in OEM offered commercial vehicles within the next two years. Audi released information on its prototype e-compressor system fitted to a new 3.0L TDI engine monoturbo in the Audi A6 and to a 3.0L TDI engine biturbo in an Audi RS5 [25]. Audi reports the new engines improve drivability significantly in higher gear ratios and during acceleration events by virtually eliminating turbo lag. Audi is pushing to release a model with an e-compressor in 2016 [26]. Other manufacturers such as Valeo, Borg Warner and AerisTech have their own versions of the E-compressor approaching commercialization [27] [28] [29].

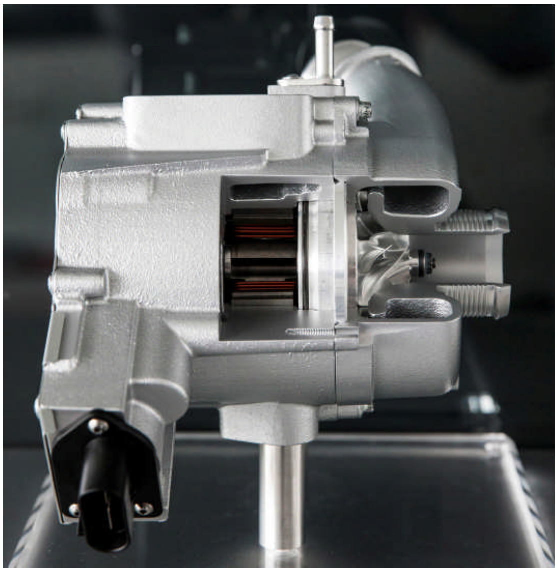

Figure 11 - Cutout of the Audi E-Compressor Prototype [26]

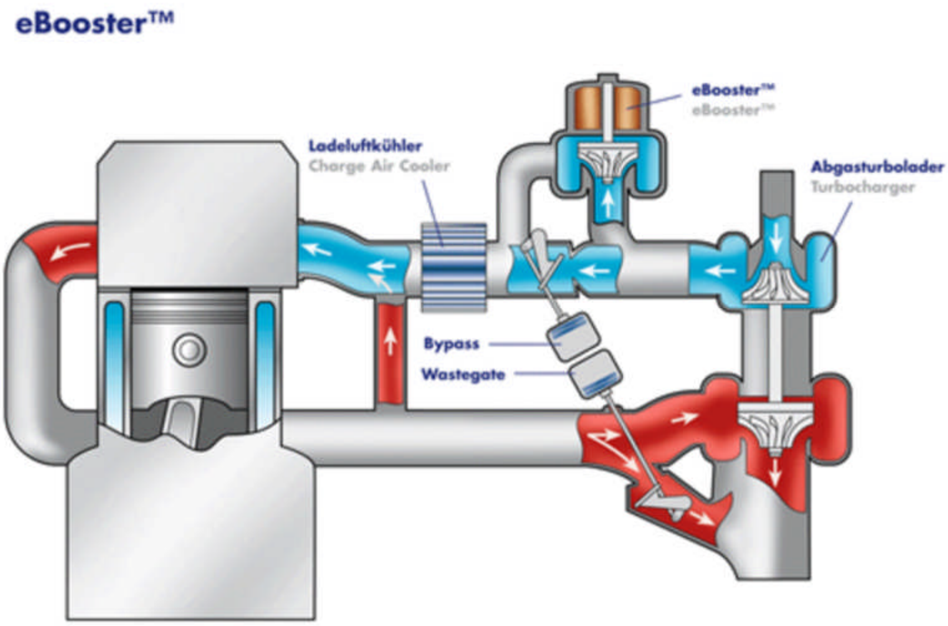

Figure 12 - BorgWarner eBooster Schematic [28]

E-turbochargers, configuration (d), are a relatively new concept. Here both the compressor and turbine are electrified via a motor mounted on the turbocharger shaft. Due to the existing mechanical connection between both compressor and turbine the electric motor cannot fulfill both its functions at the same time, ie. A shortage of boost pressure cannot overlap with excess exhaust energy. In configuration (e) an extra degree of freedom is available by delinking the turbine speed from the compressor side solving this issue. Additionally in this setup the turbine and compressor can be operating at their respective points of greatest efficiency instead of a compromised being dictated by the compressor due to inlet pressure requirements. However a major drawback within this setup is the two side now are linked electrically which introduces additional inefficiencies into the turbocharger system. In a conventional turbocharger the energy is converted from exhaust gas into mechanical energy by the turbine which transfers this energy into the compressor. The component efficiencies involved are the turbine/compressor wheels and losses within the shaft and bearings. By introducing two electric motors the energy must now be translated from the turbine into electric motor 1 then sent to electric motor 2 and applied to the compressor. Extra component efficiencies of the two electric motors plus their respective inverters are now part of the system. Configuration (e) will also require an extensive redesign of the piping on both the inlet and exhaust sides to ensure system efficiency is maximized. For these reasons and added expense of an extra electric motor this configuration is not studied. The majority of research instead is conducted using configuration (d).

With configuration (d) early experiments and studies involved large displacement engines. Caterpillar in partnership with the U.S. Department of Energy designed and tested such a system on a large displacement diesel engine for use in heavy machinery. In their testing it was found an E-turbocharger improved fuel economy by 3%-5% depending on the cycle and up to 10% at its peak efficiency point [30]. For engines with a smaller displacement Arsie et al. showed efficiency gains at normal engine loading conditions are close to negligible [31]. Only at 80% plus engine loading conditions are significant net benefits from the E-turbocharger system displayed.

An application where electrified turbochargers have been successfully implemented is in motorsports. In Formula 1 new engine regulations came into effect at the start of the 2014 season. The previous V8 naturally aspirated engines with KERS (kinetic energy recovery system) were replaced by new power units consisting of a smaller V6 engine with an E-turbocharger and a 120 kW traction electric motor mounted to the rear. The E-turbocharger (MGU-H) is allowed to capture an unlimited amount of energy from the exhaust gasses while the electric motor (MGU-K) is limited to 2 MJ energy recovery per lap and 4 MJ of energy deployment per lap.

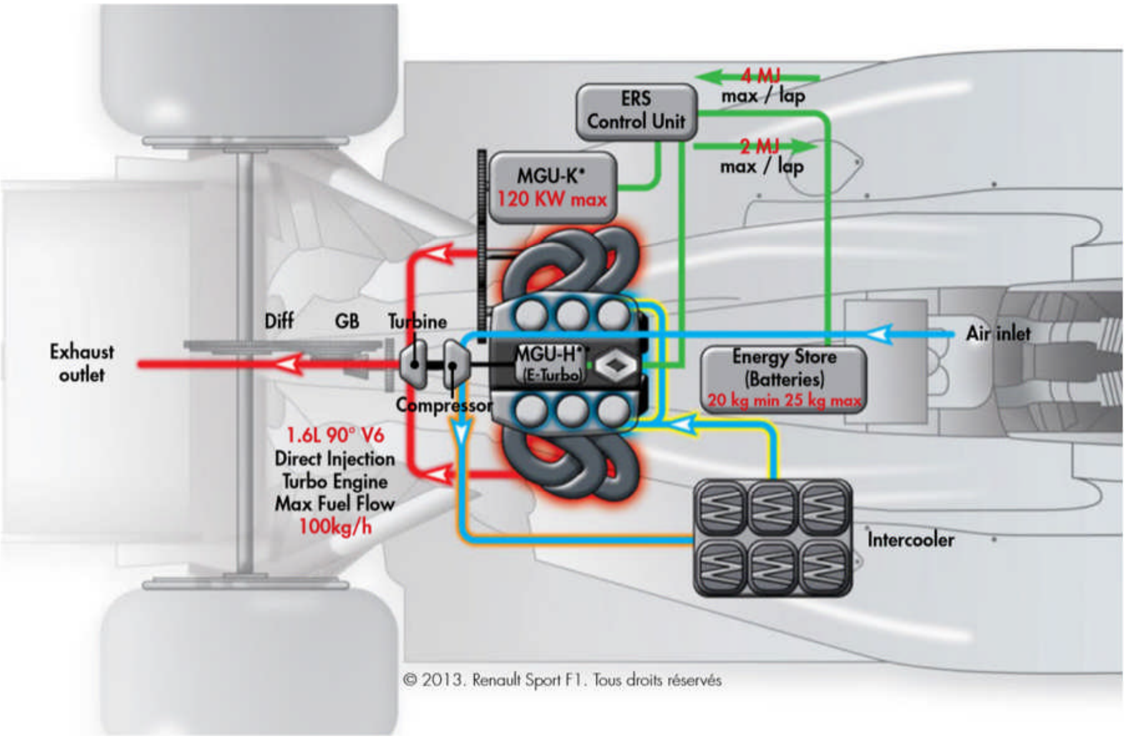

Figure 13 - 2014 F1 Powertrain Powerflow Schematic [32]

Reportedly the MGU-H unit by Magneti-Marelli Motorsport used in the Ferrari power units is capable of extracting a maximum of 90 kW of energy from the turbocharger. It is estimated with these power units the electrical system can provide power for over 30s at full output. With the MGU-H unit the hybrid system is capable of supplying a part of the extra 2MJ of energy difference from MGU-K energy regeneration and discharge limits. It allows the system to be charge sustaining at a greater total power output [33].

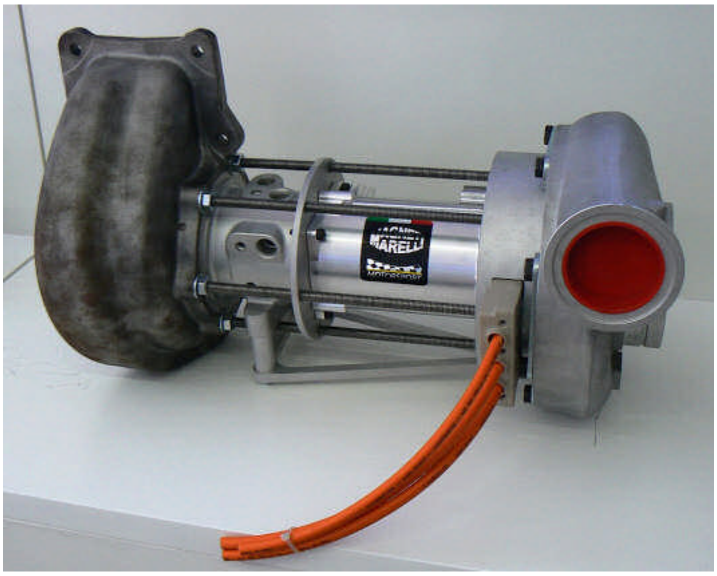

Figure 14 - Magneti-Marelli MGU-H Unit [34]

Formula 1 has demonstrated an electrified turbocharger can be an integral part within a wider hybrid electric powertrain, however whether this can translate effectively to commercial passenger vehicles is the question this research aims to answer.

3. Review of Hybrid Powertrain Architectures

Hybrid electric powertrains use one or more electric motors to provide traction to the vehicle. There are many configurations a hybrid powertrain can have, depending on the driving characteristics, costs, technical difficulty and performance requirement. In this section the most common hybrid powertrain architectures are presented and reviewed.

Parallel Hybrid

Parallel hybrid powertrains contain both the internal combustion engine and an electric motor mechanically coupled together so their torques add up at the output. The architecture is analogous to a parallel battery circuit where the currents add up at the common node. The electric motor draws its power from a battery pack, which it can also recharge by generating power from the internal combustion engine or during regenerative braking. Since internal combustion engines (ICE) are not efficient within their low rpm range, the electric motor can assist in accelerating the vehicle from rest and then allow the ICE to operate in a more efficient rpm range. Parallel hybrid powertrains are the most common and can be found in wide variety of models on the market. Due to their great variety and flexibility these powertrains can be classified by the position of the electric motor(s). Here the motor positions are classified from P1 to P4:

- P1 – Electric motor in front of ICE
- P2 – Electric motor between ICE and transmission

- P3 – Electric motor after transmission
- P4 – Electric motor at the wheel or on a separate axle from the ICE

In the P1 configuration typically a small high electric motor is mounted in place of the starter motor. It allows stop-start engine function leading to fuel saving and lower emissions by eliminating idling in stop and go city traffic. A higher power capable P1 system can also provide a small load to the engine to boost its operation into a better efficiency region in its operating map, for regenerating power during deceleration or provide a small acceleration boost. The P1 motor also replaces the conventional alternator on an engine. This architecture is exclusively used in hybrid vehicles with a small battery pack and can be found in a wide variety of vehicle platforms.

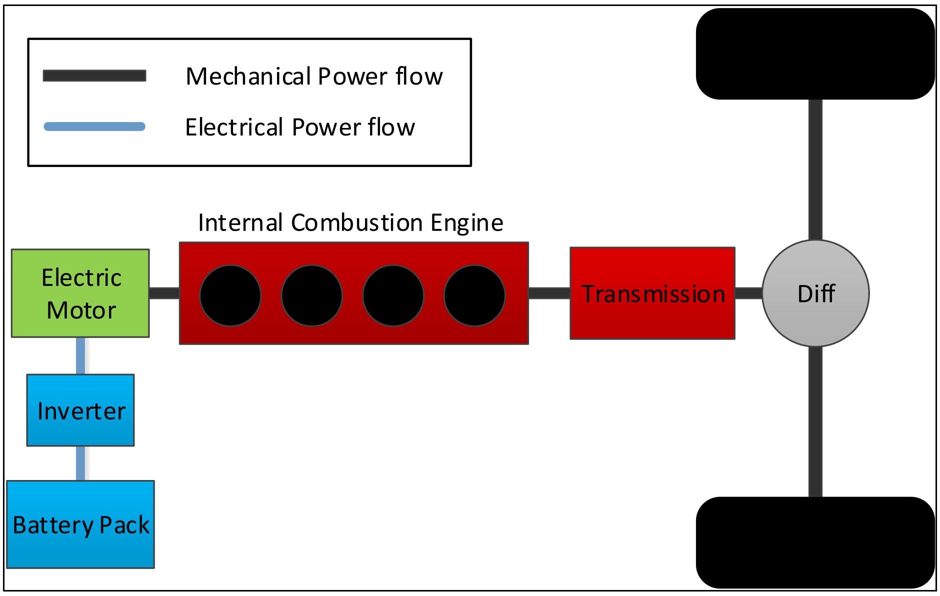

Figure 15 - P1 Motor Position

In the P2 configuration the electric motor is located in between the transmission and the ICE. There is usually a clutch separating the electric motor from the ICE to allow electric-only vehicle operation if the battery pack capacity and power output are sufficient. The motor can also load the engine to charge the battery at a faster rate since the engine can provide more power than required during low power driving situations. In this configuration the electric motor can also take advantage of the transmission torque ratios

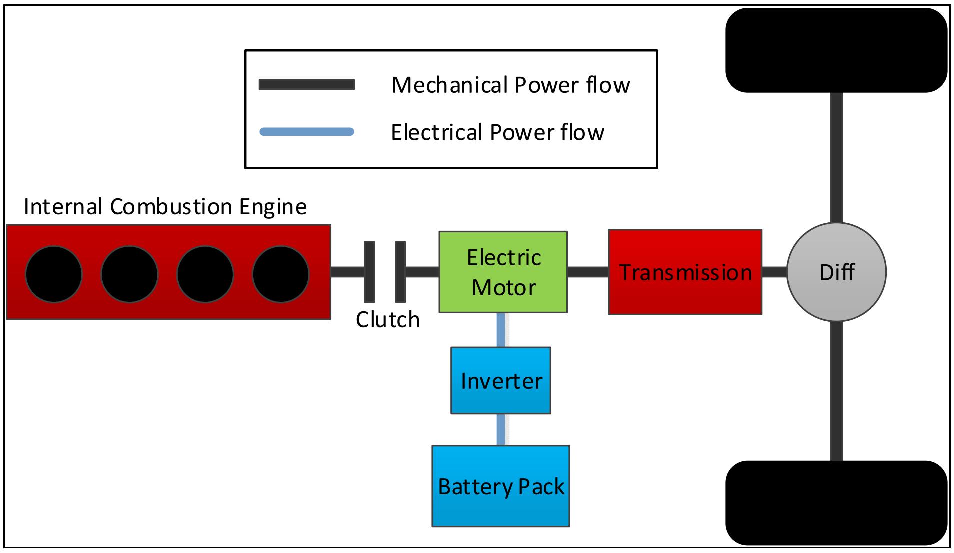

Figure 16 - P2 Motor Position

The P3 motor configuration is similar to the P2 configuration expect since the motor is placed after the transmission the torque is not multiplied but the transmission can be placed in neutral and therefore it reduces the driveline losses and inertia.

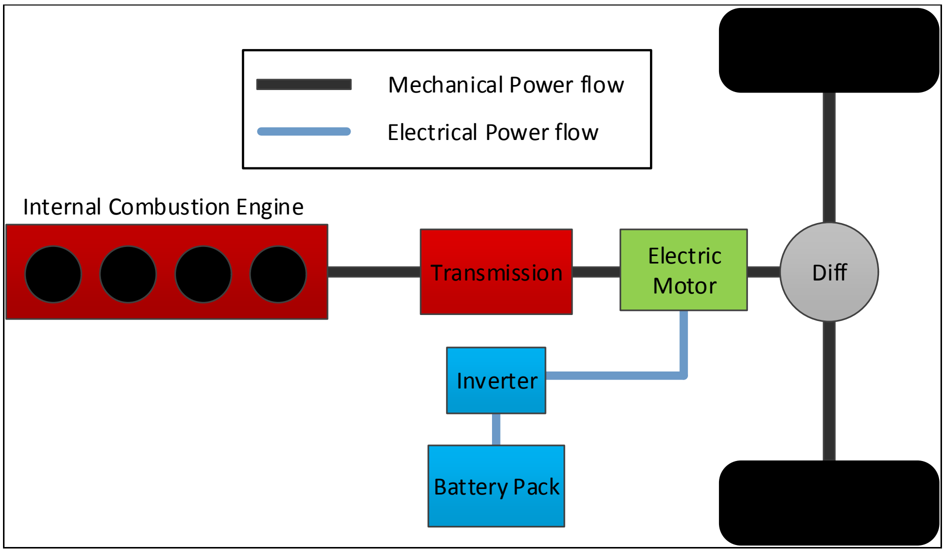

Figure 17 - P3 Motor Position

In the P4 configuration the electric motor is either placed at the wheel or on a separate axle from the ICE. This type of parallel hybrid powertrain is also referred to as 'parallel through-the-road' since the torque coupling of ICE and electric motor is at the road. This architecture is capable of the same operating modes as the other parallel hybrid powertrains. Its main advantages are the performance and handling benefits of an all-wheel drive (AWD) powertrain. Additionally, if the electric motor is placed on the front axle it can benefit from increased regenerative braking capability due to vehicle weight transfer during braking. The electric motor can also charge the battery by applying a braking torque while the engine is running.

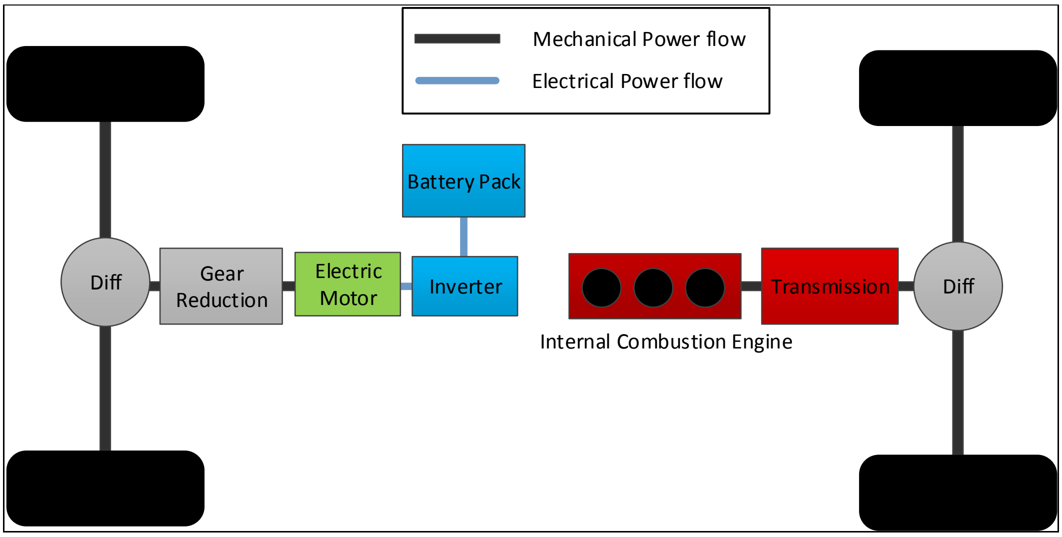

Figure 18 - P4 Motor Position

The electric motor draws its power from a battery pack, which it can also recharge by generating power from the internal combustion engine or during regenerative braking. It can also act as a starter motor. Since internal combustion engines (ICE) are not efficient within their low rpm range, the electric motor can assist in accelerating the vehicle from rest and then allow the ICE to operate in a more efficient rpm range. A common commercial implementation of this powertrain is to place an electric motor in between the internal combustion engine and transmission. The internal combustion engine can be engaged by the use of a clutch to provide extra power during highway driving or when the battery state of charge is low.

Series Hybrid

In a series hybrid the internal combustion engine acts only as a generator for replenishing the energy in the battery pack. The traction is provided purely by the use of one or more electric motors. Typically a transmission is not needed as electric motors can provide the necessary torque required by a car over a large rpm range. The internal combustion engine drives a separate generator motor providing power either for storage in the battery pack or to directly drive the traction motor. This configuration allows the internal combustion engine to run within only its high efficiency rpm range. It increases the range of the vehicle while still allowing for operation at an optimal efficiency point at all times. Since the engine is most efficient in only a narrow rpm band, the generator motor will also double as a starter motor (similar to a P1 motor in parallel hybrids), skipping the lower efficiency rpm values during engine start-up. It is common for the internal combustion engine in series hybrid to use the Atkinson thermodynamic cycle instead of the Otto cycle. Atkinson cycle further increases fuel efficiency at the cost of lower specific power.

In this configuration is it possible to have two traction motors, one for each axle, or even four traction motors, one for each wheel, as they are not connected to a combustion engine.

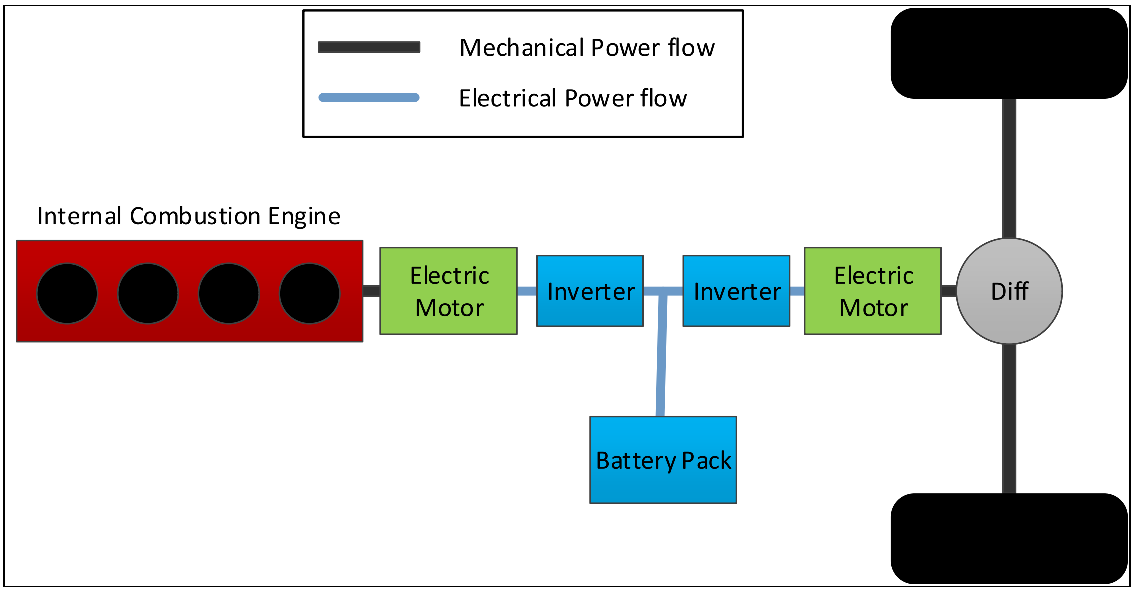

Figure 19 - Series Hybrid Powertrain Architecture

Power-Split Hybrid

A power-split hybrid allows the vehicle to be powered using either of the two power flow paths of series and parallel hybrids described previously. This is accomplished by the use of one or more mechanical power split devices connecting the internal combustion engine, a generator motor and the traction motor. The power split device, typically a planetary gear set, enables the internal combustion engine to act as either a generator as in a series hybrid or help with transferring power directly to the wheels like a parallel hybrid. Additionally, the engine does not need to be running at all times. If the battery state of charge is sufficient the engine will be turned off to conserve fuel and the car will operate with the traction motor power only. These different power modes come from locking different parts of the planetary gear set (sun, carrier, etc). A series-parallel hybrid gives a vehicle the option to use either of these power flow paths depending on the driving requirements and battery conditions.

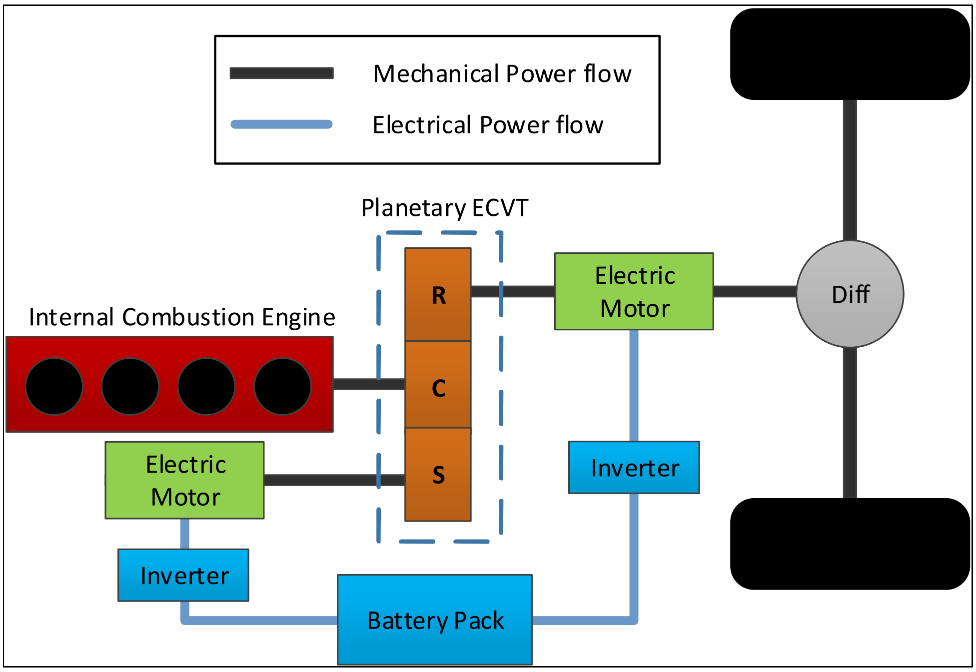

Figure 20 - Power-Split Hybrid Powertrain Architecture

The above block diagram shows the layout of a power-split hybrid. The three sources of power (generator, traction and ICE) all feed into the power split device. A central supervisory control unit determines the power blending based on the driver input. Figure 21 below shows the power split device of the 2004 Toyota Prius Hybrid.

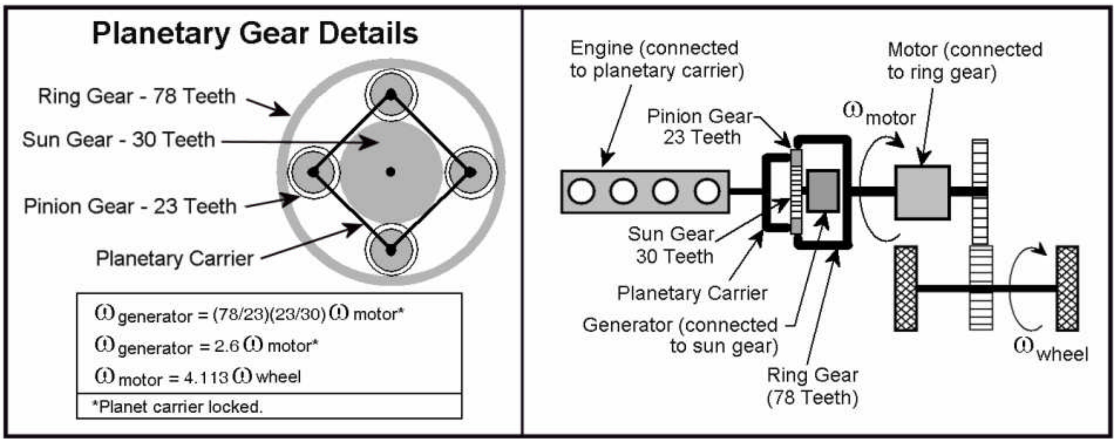

Figure 21. Power-Split Device in 2004 Toyota Prius [35]

The ring gear of the planetary gear is connected to the traction motor and the final drive. The sun gear is connected to the smaller generator motor and the pinion gear is connected to the engine. A disadvantage with this power split device is the power from the internal combustion engine cannot be fully transferred to the final drive. A fraction of it always goes into the generator motor, a power flow path which is less efficient than the purely mechanical one. This limitation was addressed in the newer 2010 Prius model that employs two power split devices interconnected to allow the generator to be bypassed when the internal combustion engine is operating.

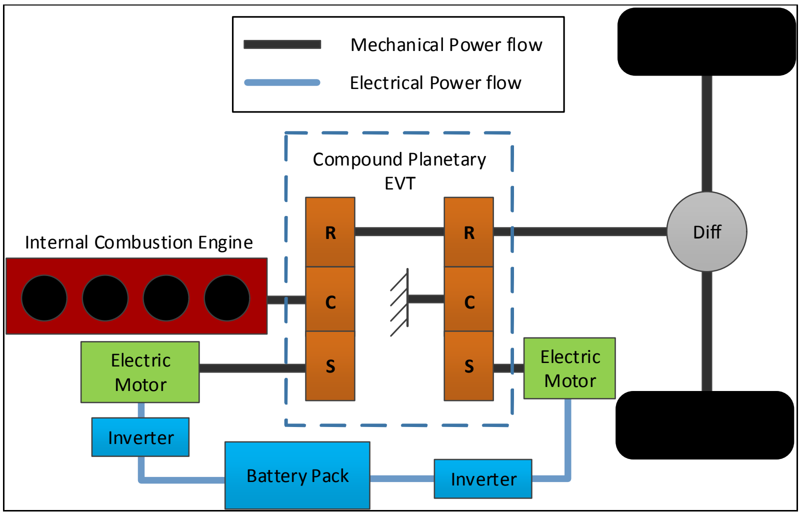

Figure 22 - Prius 2010 Power-Split Hybrid Powertrain Architecture

Electrification Level

All hybrid electric powertrains are defined by another metric, their electrification level. Electrification level is broadly defined as the percentage of electrical power to a vehicle's total power. Increasing levels of electrification lead to greater overall fuel efficiency and hence lower tailpipe emissions. A vehicle with a 100% electrification level is powered solely by electrical energy. Within hybrid powertrains electrification level usually translates into battery pack electrical capacity. A larger battery pack will allow the vehicle to operate in electric-only mode for longer and during higher velocities. Whereas smaller packs indicate limited operation where the motor can only assist the engine for limited periods or start/stop the engine. The figure below classifies hybrid powertrains and their capabilities according to the electrification level

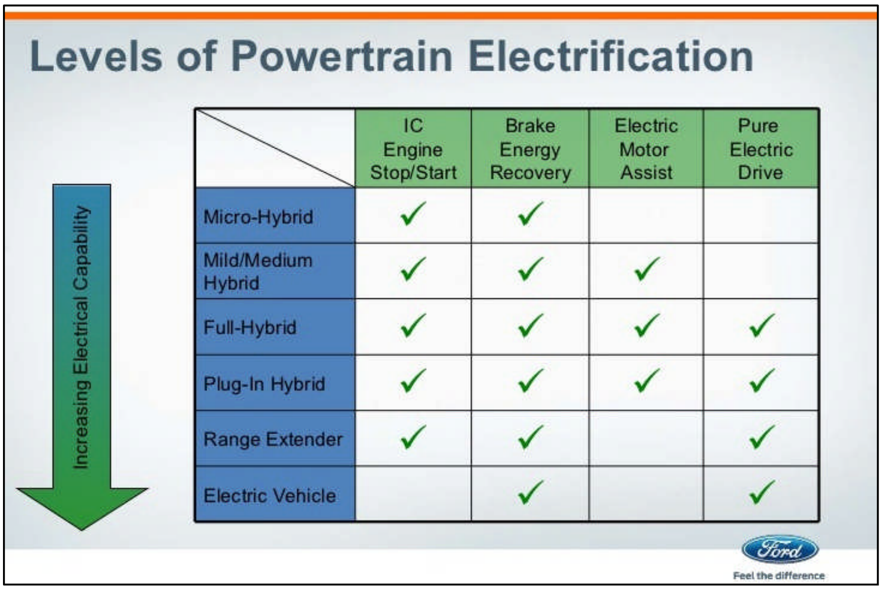

Levels of Powertrain Electrification

	IC Engine Stop/Start	Brake Energy Recovery	Electric Motor Assist	Pure Electric Drive
Micro-Hybrid	✓	✓		
Mild/Medium Hybrid	✓	✓	✓	
Full-Hybrid	✓	✓	✓	✓
Plug-In Hybrid	✓	✓	✓	✓
Range Extender	✓	✓		✓
Electric Vehicle		✓		✓

Figure 23 - Powertrain Electrification Level [36]

Any of the previous hybrid powertrain architectures discussed can also have a plug-in option. This allows vehicles to have a larger battery capacity where it would be difficult or inefficient to obtain a full charge through regenerative braking or ICE power generation. These vehicles can be plugged into a regular wall charger and recharge their batteries from the energy of the local power grid. Typically the battery pack is sized to allow electric only operation over a longer driving time with the internal combustion engine used only for extended range or during highway driving. Electric only operation is more fuel efficient and the only emissions associated with it are from the methods used to generate power for the local electrical grid. The average rating for these vehicles is just under 100 MPGe (miles per gallon gasoline equivalent) when using electric only mode, generating significant savings in fuel and emission costs [37].

4. Baseline Vehicle Model

To simulate the powertrain over standard drive cycles baseline vehicle specifications are first identified and modelled. Vehicle simulation requires several experimental coefficients to accurately capture road loading conditions. The scope of this research is to evaluate the performance of an electrified turbocharger system in higher performance vehicles. To generate specifications for a baseline vehicle the current North American muscle car market and a selection of vehicles from the 4-door luxury segment were analyzed.

In the muscle car market the 2015 model year line of the Chevrolet Camaro, Ford Mustang and Dodge Challenger are compared against each other. The entry level models from these three brands are equipped with roughly 300 horsepower (225 kW) and range from 1600 kg to 1750 kg in curb weight. Their next few respective trims have progressively higher horsepower figures and consequently better performance. These trends are illustrated in Figure 24-Figure 27.

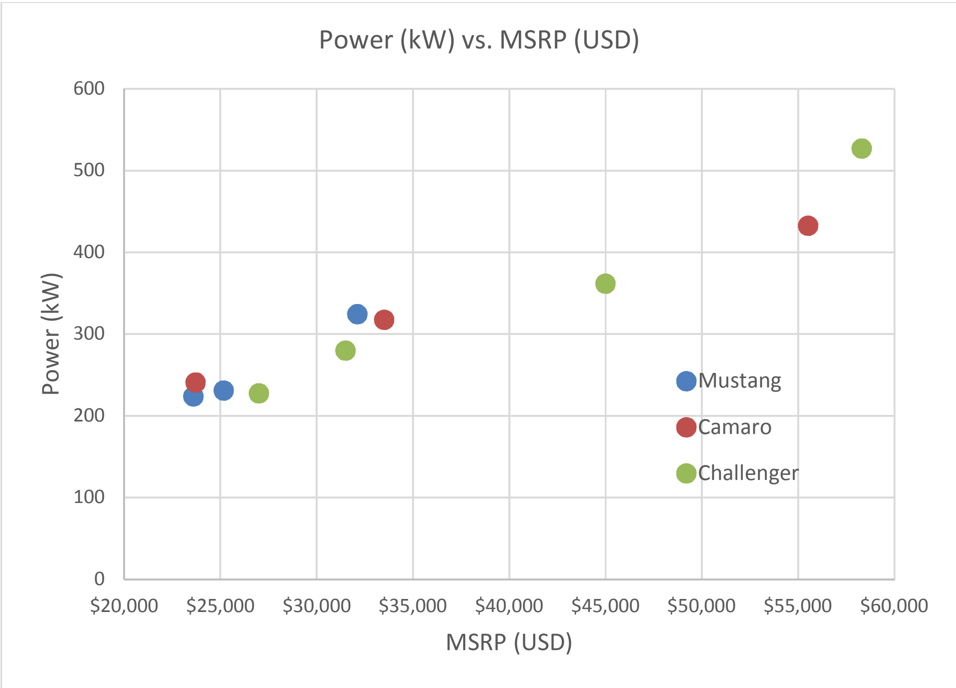

Figure 24 - Power (kW) vs. MSRP in Current Muscle Cars

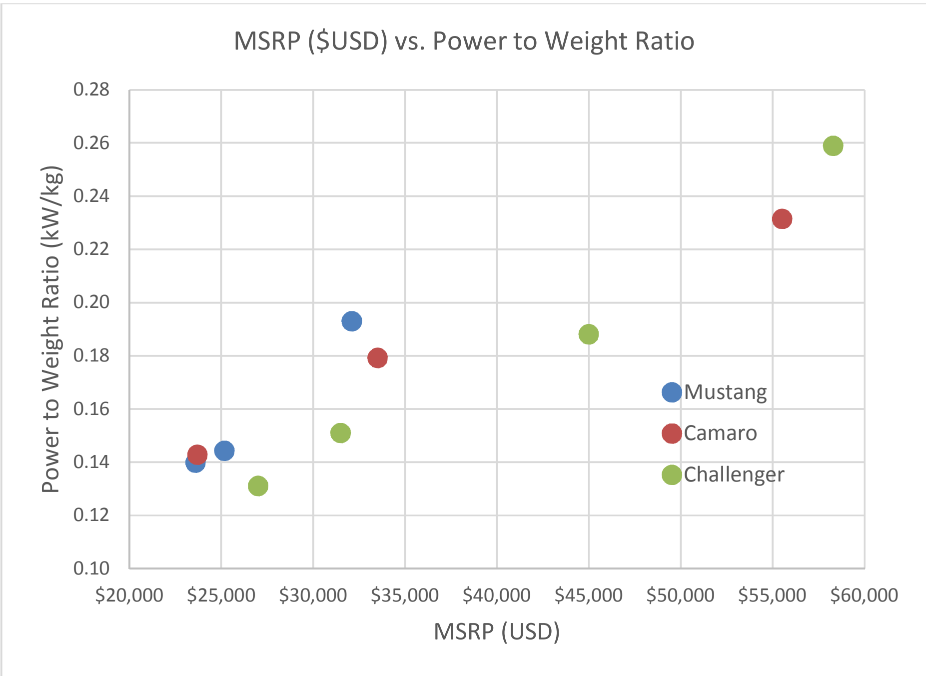

Figure 25 - Power/Weight Ratio of Current Muscle Cars

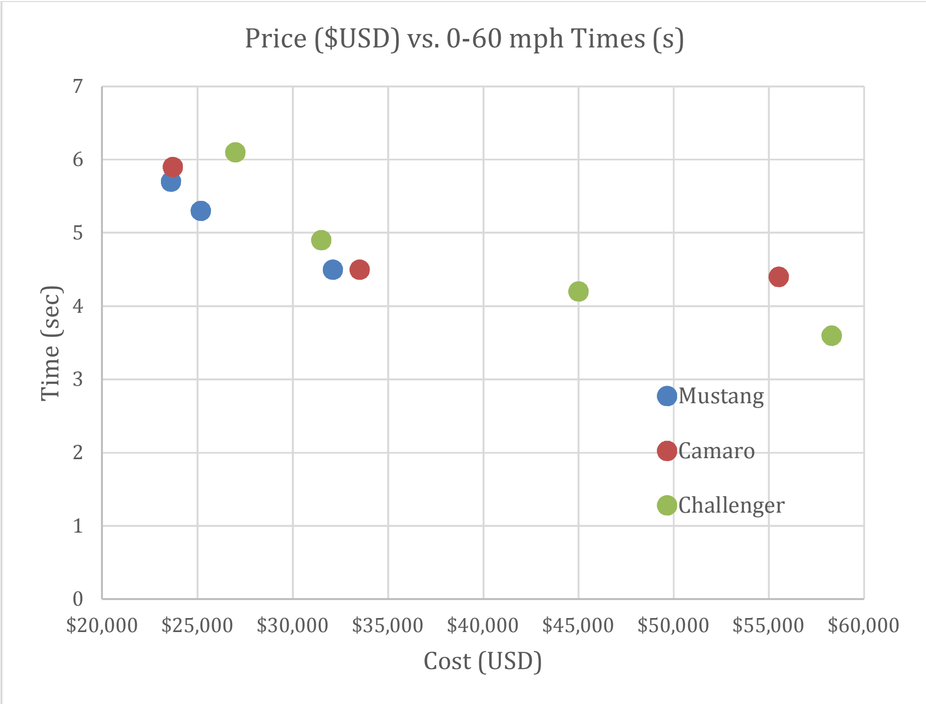

Figure 26 - Current Muscle Cars 0-60 Acceleration Times

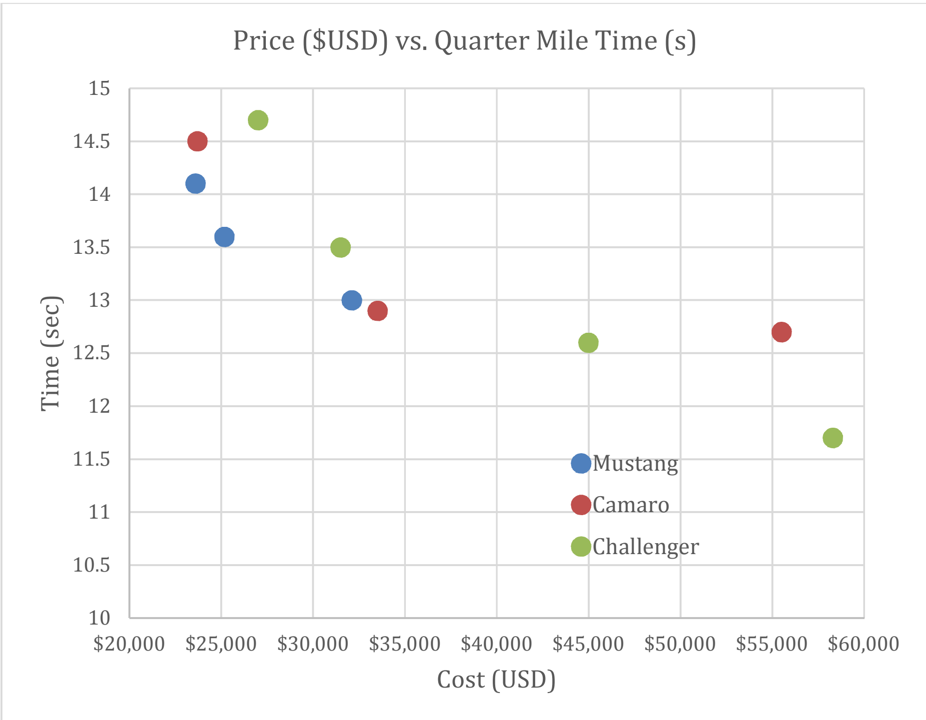

Figure 27 – Current Muscle Car Quarter-Mile Times

In the current muscle car market there are two distinct vehicle power levels at which these three manufacturers compete First at the entry level all three models compete around the 200 – 250 kW mark and around the price point of $25,000. The second level is from 275 – 325 kW and a price point of $32,500. Past this level the field is open and performance models with a power output as high as 527 kW are available. In the luxury vehicle market a similar clustering of models is observed at the 225 – 250 kW power level and a price point between $45,000 and $60,000. Therefore the baseline vehicle model specifications are based on vehicles available in these two market segments around the 225 kW level.

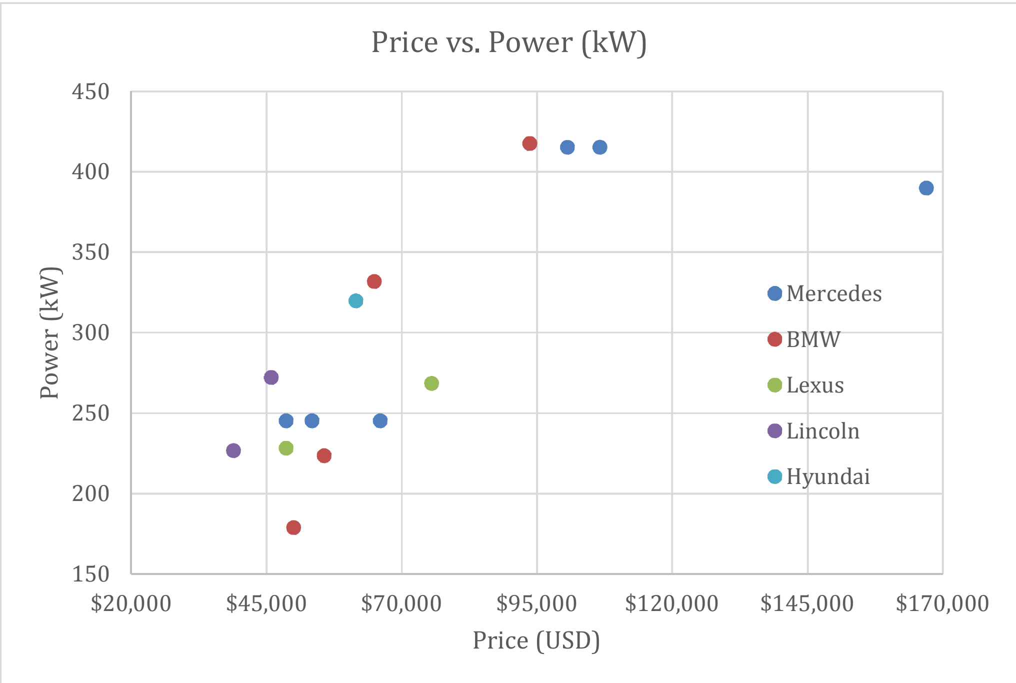

Figure 28 - MSRP vs. Power Output (kW) in Luxury 4-Door Vehicle Market

The baseline vehicle specification given below in Table 2 are determined by averaging published specifications from current available vehicles around the 225 kW power level from both the muscle car and luxury vehicle segments [38] [39] [40] [41] [42]

Table 2: Baseline Vehicle Parameters

Vehicle Parameter	Value	Unit
Mass	1674	kg
Driver Mass	80	kg
Drag Coefficient [43]	0.34	-
Frontal Area [42]*	2.2	m^2
Rolling Resistance Coefficient [43]*	0.01	-
Tire Radius	0.356	m
Tire Coefficient of Friction [43]*	1.0	-

*These specifications are estimates based on information from several literature sources

Standard Drive Cycles

To understand vehicle loading conditions and performance in normal everyday driving standardized drive cycles are used. A drive cycle is the trace of a vehicle's velocity over time. There are many standardized drive cycles defined by various regulatory bodies around the world for the purpose of emissions and fuel economy testing of automotive vehicles. In this research three standard drive cycles specified by the EPA will be used for vehicle simulations, the Urban Dynamometer Driving Schedule (UDDS), US06 cycle and the Highway Fuel Economy Test (HWFET) cycle. Figures 29 - 31 below are plots of these drive cycles.

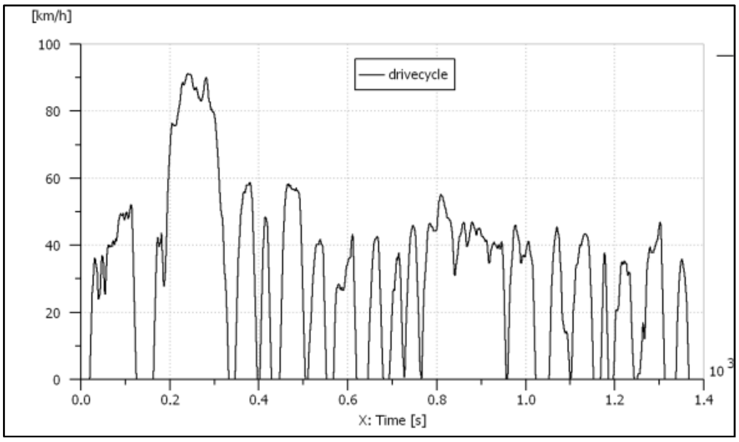

Figure 29 - UDDS Drive Cycle

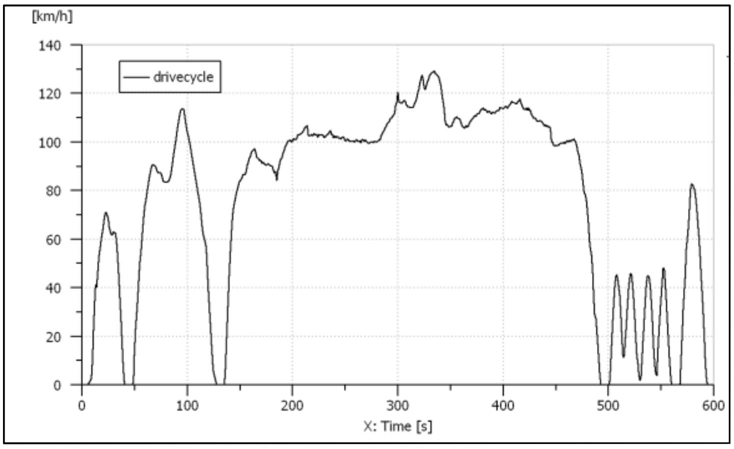

Figure 30 - US06 Drive Cycle

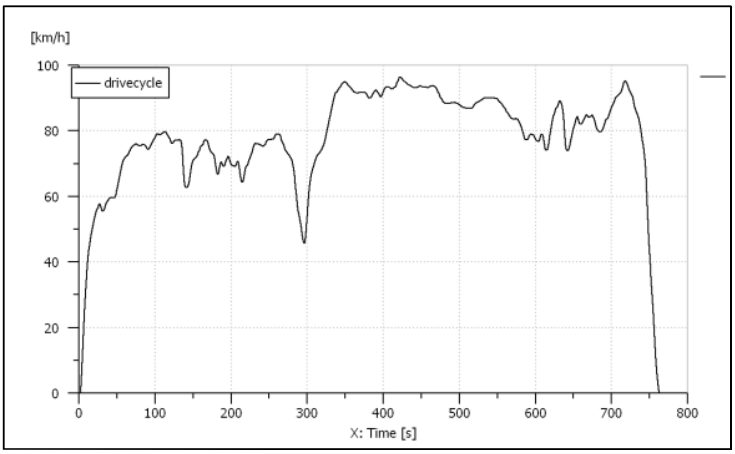

Figure 31 - HWFET Drive Cycle

The federal regulations mentioned previously in the Vehicle Fuel Economy and Emissions Targets section are based on the Corporate Average Fuel Economy (CAFE) testing procedure. In CAFE testing the combined fuel economy is a weighted average of 45% city driving and 55% highway driving. The UDDS cycle is used for city and HWFET is used for highway in the CAFE procedure. The CAFE testing standard is very different from the one used to generate fuel consumption labels for new vehicles. In the US since 2008 and in Canada since 2015 the 5-cycle method is used to generate these fuel consumption label. The 5-cycle method was introduced in response to consumer complaints of unrealistic fuel economy claims by manufacturers in particular for hybrid electric vehicles [44] [45].

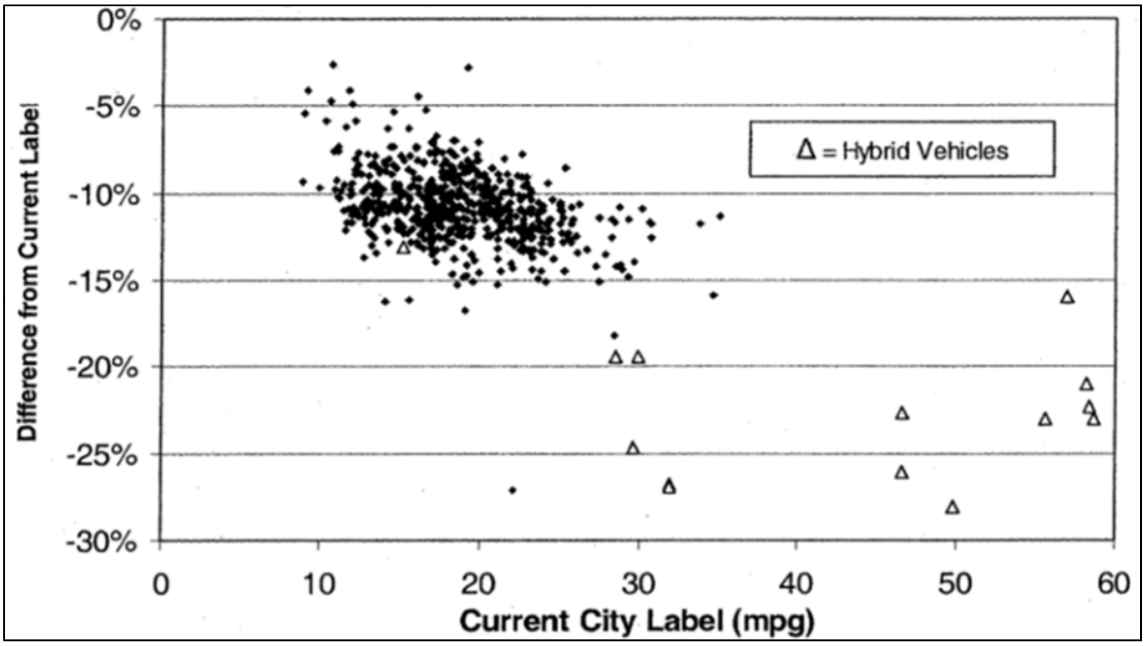

Figure 32 - Fuel Economy Difference from 2-Cycle to 5-Cycle Method [44]

The 5-cycle method contains both UDDS and HWFET cycles, but also takes into account aggressive driving behaviour with the US06 cycle, air conditioning with the

SC03 cycle and cold start effects with a cold engine UDDS cycle. Air conditioning and cold-start behaviours are difficult to simulate without high fidelity temperature and emissions models therefore in this research all vehicle simulation will be conducted over the UDDS, HWFET and US06 cycles for evaluating regular driving conditions. Temperature effects will not be considered.

Table 3: 5-Cycle Testing Details [46]

	City	**Highway**	**High Speed**	**A/C**	**Cold Temp**
Cycle Name	UDDS	HWFET	US06	SC03	UDDS
Distance	17.8 km	16.5 km	12.9 km	5.8 km	17.8 km
Top Speed	90 km/h	97 km/h	129 km/h	88 km/h	90 km/h
Average Speed	34 km/h	78 km/h	78 km/h	35 km/h	34 km/h
Maximum Acceleration	5.3 km/h/s	5.2 km/h/s	13.6 km/h/s	8.2 km/h/s	5.3 km/h/s
Number of Stops	23	0	4	5	23
Idling time	18%	0	7%	19%	18%
Engine Startup	Cold	Warm	Warm	Warm	Cold
Lab Temperature	20-30 °C	20-30 °C	20-30 °C	35 °C	-6.67 °C

Table 3 above shows a breakdown of the five tests that make up the revised testing procedure for generating fuel economy labels.

Baseline Chassis Model Simulation

To calculate the minimum tractive power and torque requirements at the wheel a 1D longitudinal model was used in Simulink [47]. The model considers forces and loads only in the longitudinal direction similar to vehicle operation on a chassis dynamometer. The model considers aerodynamic, rolling resistance, inertial and grade loads to calculate the current vehicle acceleration and from this derive the current velocity and position. In equation 1 below the inertial load is taken into account by adding it to the vehicle mass. Equations 2-4 are used to calculate the road load.

$$F_{tr} - \left(F_{aero} + F_{rolling\ resistance} + F_{Grade}\right) = \left(M_{vehicle} + M_{Inertial}\right)a \qquad (1)$$

Where F_{tr} is the vehicle tractive force and a is the vehicle acceleration

$$F_{aero} = \frac{1}{2} * Velocity^2 * C_d * Area_{Frontal} \qquad (2)$$

Where C_d is the coefficient of drag

$$F_{rolling\ resistance} = C_{RR} * M_{vehicle} * 9.81 \qquad (3)$$

Where C_{RR} is the coefficient of rolling resistance

$$F_{Grade} = M_{vehicle} * 9.81 * sin(arctan\left(\frac{\alpha}{100}\right)) \qquad (4)$$

Where α is the slope angle in %

To simulate the changing loading conditions over a dynamic drive cycle first the acceleration is calculated from the derivative of the drive cycle profile and then the current velocity is used to calculate the resistance forces. Total tractive effort force can then be integrated to calculate power and energy or multiplied by the tire radius to calculate torque. Since standard drive cycles do not specify road grade F_{Grade} is always zero.

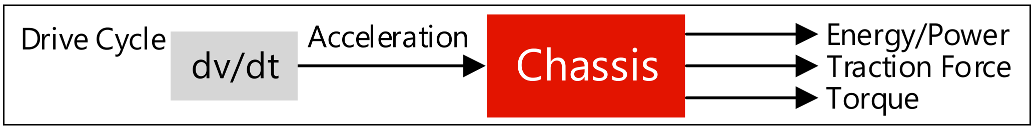

Figure 33 - Chassis Model Signal Flow

Figure 33 above is the signal flow logic of the chassis model to calculate minimum energy, power and torque requirements at the wheel for the specified drive cycle. Figure 34 below is the equivalent Simulink chassis model.

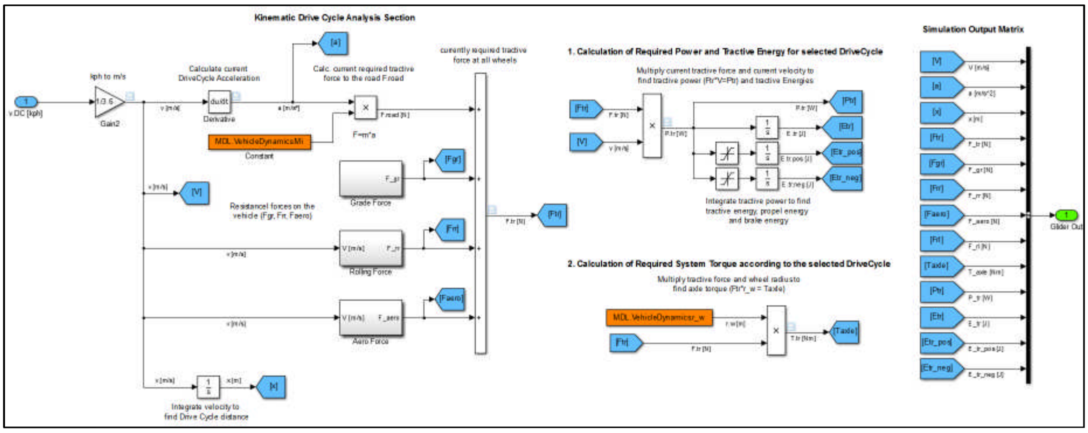

Figure 34 - Simulink Vehicle Chassis Model

The results of the chassis model simulation are given in Table 4 below. The US06 cycle has been split into two parts city (US06c) and highway (US06h). US06c contains the high acceleration portions of the cycle and US06h contains the high speed portion.

Table 4: Chassis Model Simulation Results

Drive Cycle	UDDS	HWFET	US06	US06C	US06H
Propulsive energy @ wheels [Wh/km]	141.4	126.1	212.1	302.9	186.3
Braking energy @ wheels [Wh/km]	-68.6	-15.1	-68.8	-201.4	-31.1
Net energy consumption @ wheels [Wh/km]	72.9	111.0	143.3	101.5	155.2
Average propulsive power [kW]	4.5	9.8	16.4	13.4	18.2
Average brake power [kW]	-2.2	-1.2	-5.3	-8.9	-3.0
Peak power output [kW]	42.1	34.2	102.3	101.6	102.3
Peak tractive force [kN]	3.0	2.9	7.3	7.3	6.0
Peak total torque @ wheels [Nm]	1032.7	988.5	2490.7	2490.7	2061.7

Propulsive energy is the minimum energy requirement to drive the chassis over the drive cycle profile. It consists of the energy used to oppose aerodynamic, rolling resistance and inertial losses. The simulation also calculates the minimum power output required at the wheels to meet these drive cycles. For the aggressive US06 cycle just over 100 kW is required while the HWFET needs only a third the power to meet its velocity requirement.

5. Baseline Conventional Vehicle Model Simulation

To compare hybrid electric and electric turbocharger powertrains with current vehicles a conventional baseline vehicle model is created in Simulink. The model is built on top of the 1D chassis model outlined previously. For modelling conventional vehicles 4 other sub-models have been added onto the chassis component:

1. Driver
2. Controller
3. Internal Combustion Engine
4. Transmission / Drivetrain

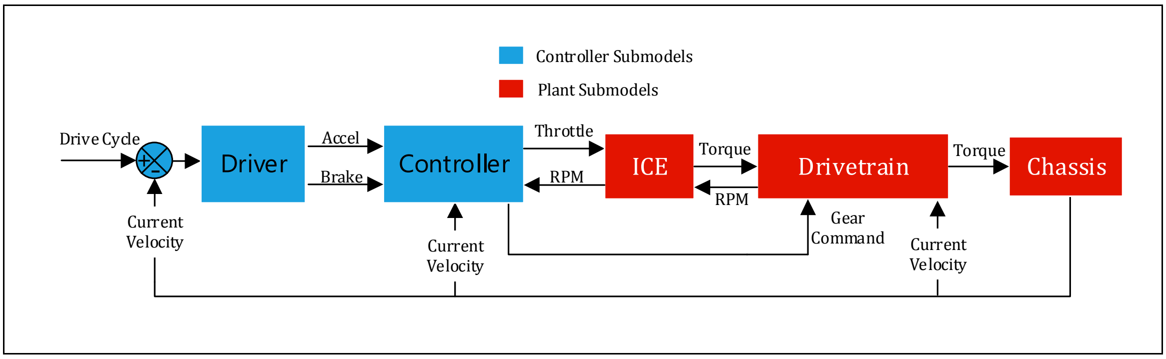

Figure 35 - Conventional Vehicle Simulink Signal Flow

The driver subsystem simulates a driver's accelerator and brake pedal position to match the current vehicle velocity to a predefined drive cycle. The driver is modelled using separate Proportional-Integral (PI) controllers for both the accelerator and brake pedals by splitting the velocity error into negative and positive signal lines. This allows both the braking and throttle to be tuned separately for each drive cycle. A small dead-band is used in the error signal to prevent chattering in the accelerator and brake signals. Additionally the chassis velocity feedback signal to the PI controllers contains a delay to prevent algebraic loops in the Simulink model.

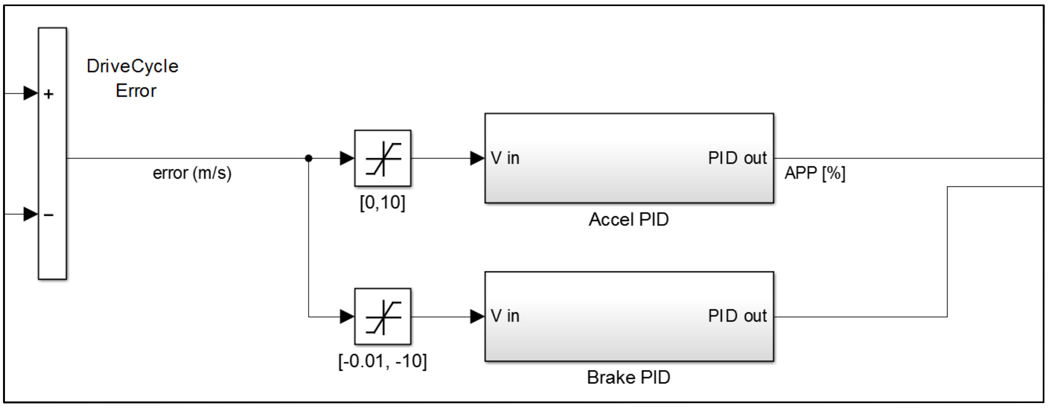

Figure 36 - Driver Simulink Model

The vehicle controller is modelled using Stateflow. It converts the driver accelerator pedal command to an equivalent engine throttle command. The controller also outputs transmission gear command to ensure engine rpm is kept within its region of greatest efficiency.

The ICE is modelled using the wide-open throttle (WOT) curve, a minimum torque curve and a fuel flow rate look-up table that is a function of the current rpm and torque. The throttle input from the controller is multiplied by the maximum output torque at the current engine rpm to generate current output torque. Then using the current engine speed rpm and current output torque the fuel flow rate is calculated from the look-up table.

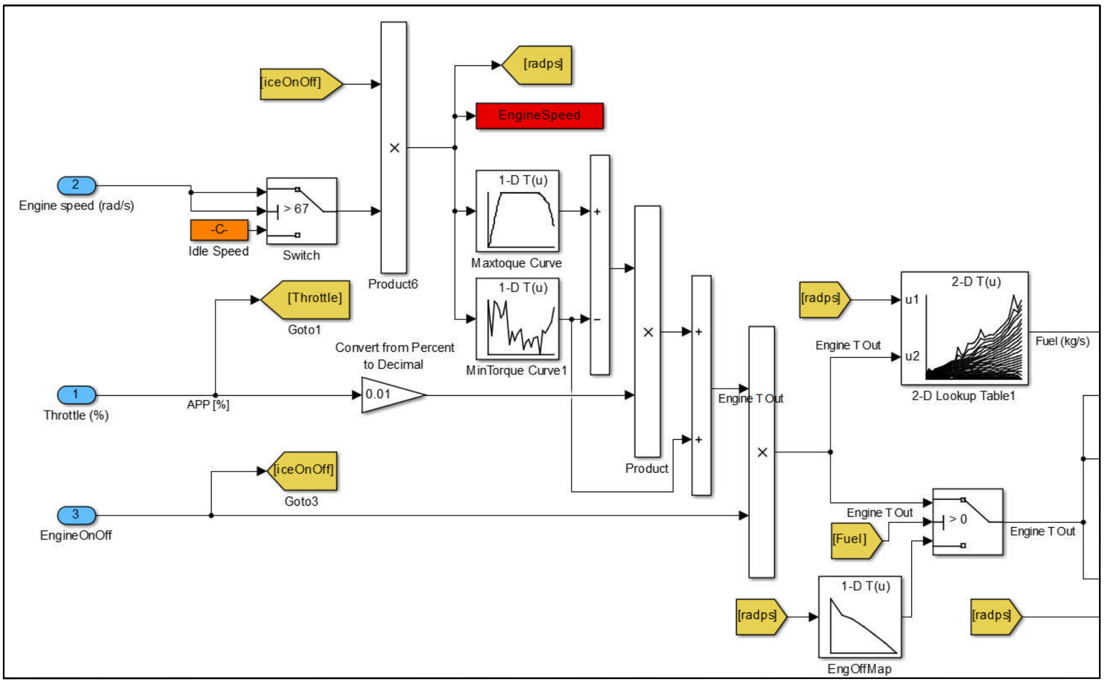

Figure 37 - ICE Component Model in Simulink

To create a representative engine model a generic fuel flow rate map was used from Autonomie. Autonomie is a powertrain and vehicle model architecture and development environment based on Simulink. It contains many pre-defined plant models of components such as engines, electric motors, transmissions, etc [48]. The generic fuel flow map was resized to a maximum engine power and torque output determined by market research. Similar to how the specification for the baseline chassis model are calculated the muscle car market and luxury vehicle market were analyzed to determine the engine size and power.

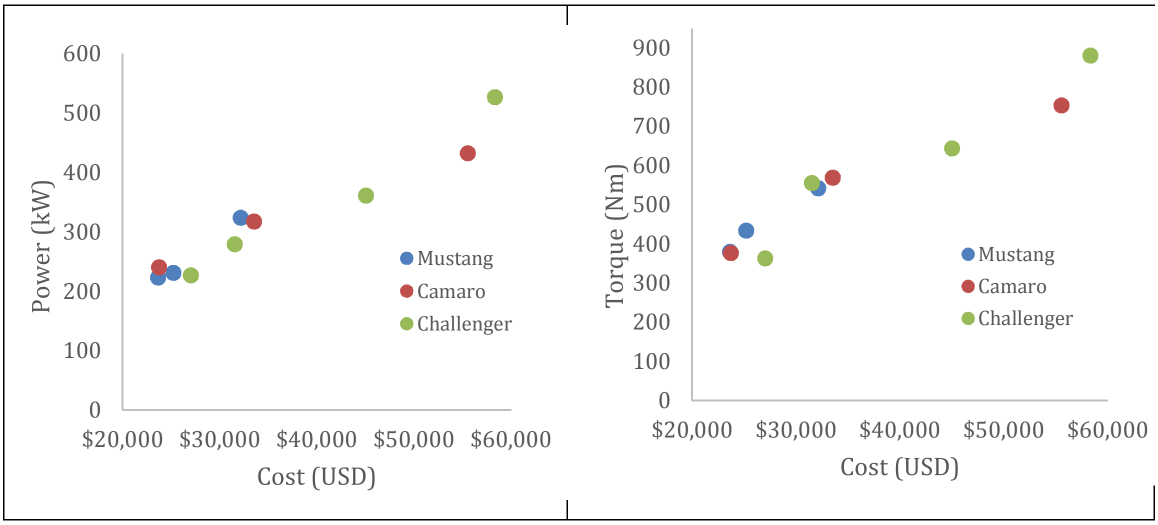

Figure 38 – Current Muscle Car Power and Torque

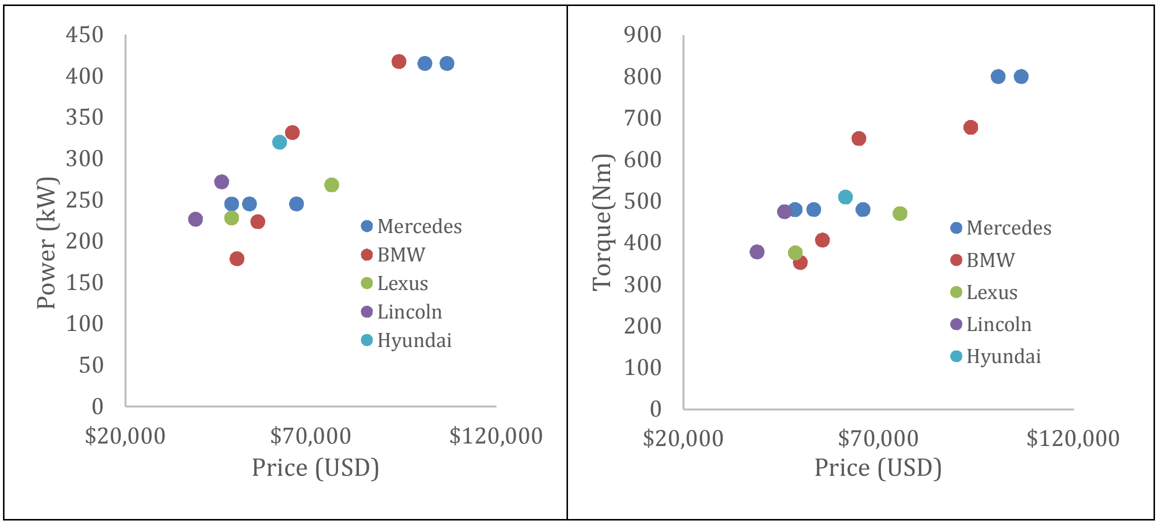

Figure 39 – Selected Current Luxury Vehicle Power and Torque

In the current luxury vehicle and muscle car markets the available powertrain options start from as low as 175 kW and up to 527 kW in the example of the 2015 Dodge Challenger Hellcat. For the baseline vehicle since the majority of the vehicle model offerings are in the lower end of this range the engine was scaled to a maximum power of 225 kW. At 225 kW the engine WOT curve scales to a maximum torque output of 387 Nm at 5200 RPM. This also correlates well with the lower end muscle car and luxury vehicle options on the market. Figure 40 is the resultant engine map with the scaled WOT curve.

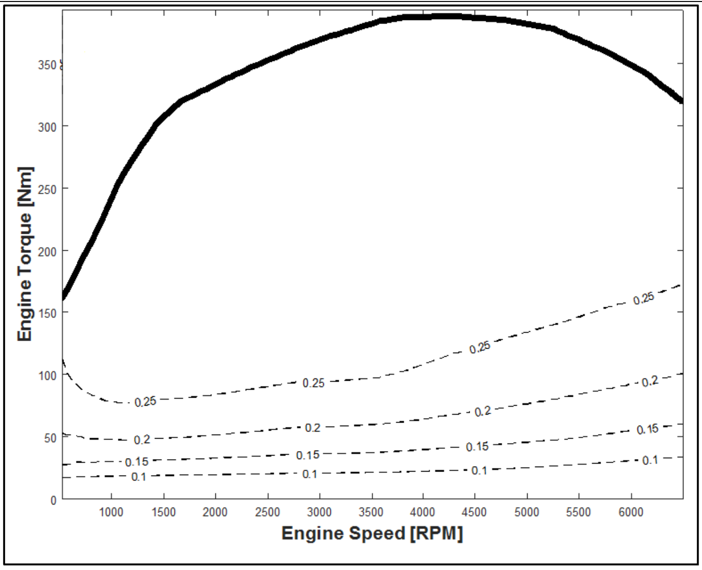

Engine Wide-Open Throttle Curve

Fuel LHV (J/kg)	44,400,000
Configuration	V6, Naturally Aspirated
Max RPM	6500
Max Torque	387 Nm
Max Power	225 kW

Figure 40 - Baseline Conventional Vehicle Engine Information

The transmission is modelled using a gain to multiply the engine output torque. A separate gain is used for each gear ratio. Additionally a delay of 0.25 seconds is also used to model the time it takes to change gears. The engine rpm is calculated in this component by dividing the vehicle speed by the tire radius then translating that number back through the driveline to get engine rpm. A constant efficiency of 92% is specified for the transmission torque output to approximate transmission losses. This value is based on dynamometer experiments carried out by Irimescu et.al [49]. The Simulink block diagram of this transmission model can be seen in Figure 41.

Transmission gear ratios are modelled after the new GM 8 speed 8L90 transmission. Gear ratios are given below in Table 5.

Table 5 - Transmission Model Gear Ratios [50]

Gears	1st	2nd	3rd	4th	5th	6th	7th	8th
	4.56	2.97	2.08	1.69	1.27	1	0.85	0.65

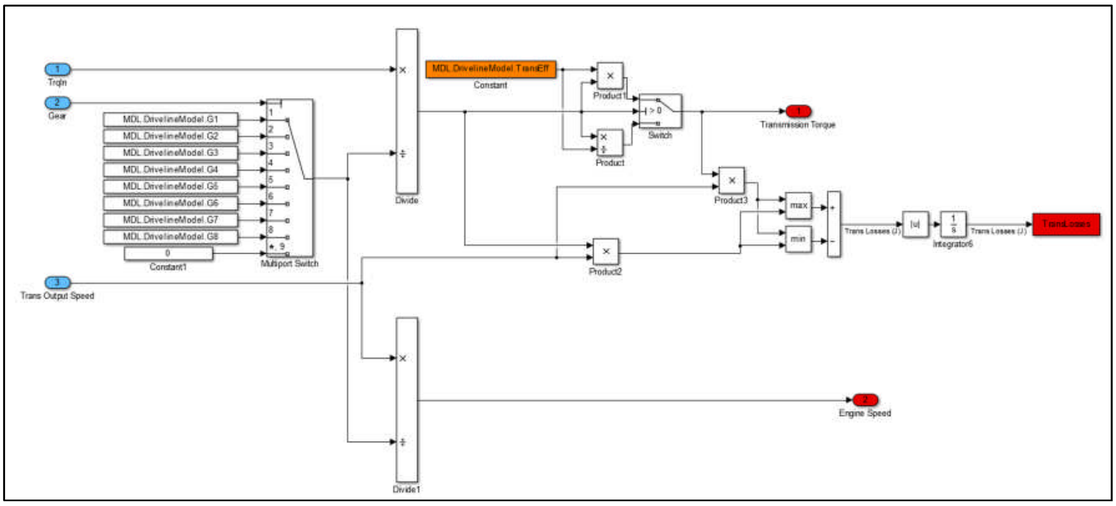

Figure 41 - Simulink Transmission Model

Baseline Conventional Model Results

The conventional vehicle is simulated over the UDDS, HWFET and US06 drive cycles. Fuel economy results in mpg and energy consumption in Wh/km are given in Table 6 below.

Table 6: Baseline Conventional Vehicle Results

	UDDS	**HWFET**	**US06**	**Combined (City 55% / Highway 45%)**
Fuel Economy (mpg)	24.5	31.8	22.4	27.8
Energy Consumption (Wh/km)	846.8	653.7	934.4	759.9

The conventional vehicle simulation results show a moderate fuel economy of approximately 24 mpg in city and US06 cycles and almost 32 mpg over highway driving. To check the accuracy of the model these fuel economy numbers are compared to published EPA values. Since the test methods are different (2 cycle vs. 5 cycle) a 12.5% penalty is imposed on these numbers. According to Figure 32 displayed in an earlier section this is a reasonable assumption for a conventional vehicle. After downscaling the combined fuel economy value of 24.3 mpg correlates well with the current trend of mpg vs. power as illustrated in Figure 42.

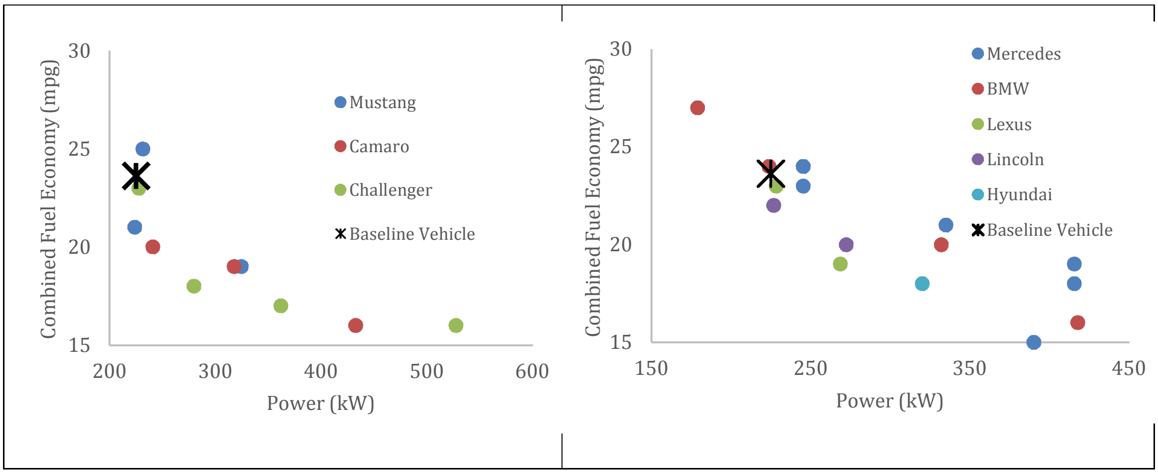

Figure 42 - Fuel Economy Comparison

In the conventional vehicle model fuel economy can be influenced by two controllable components. First the driver, modelled with a PI controller, can have problems in following the given drive cycle. The ICE, being the sole torque source, directly receives this driver command. However if there are sufficient delays in the feedback loop or the driver PI gains are not calibrated then simulation results can be flawed. To mitigate this issue the NHTSA recommended tolerance of +- 2 mph for chassis dynamometer testing are followed for all simulations conducted. If the vehicle velocity is ever outside of these limits in any drive cycle the driver PI controller gains are recalibrated until the tolerance limit is satisfied.

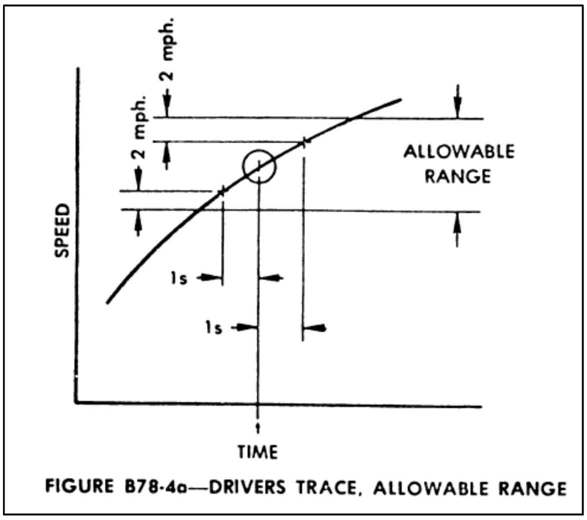

Figure 43 - Drive Cycle Error Tolerance from 40 U.S. CFR §600.109-08 [51]

The other controller which can influence performance and fuel economy results is the transmission control unit (TCU). The TCU sends a command to the transmission component to change gears. In this model the TCU is set up to upshift at 1750 rpm and downshift at 1250 rpm to keep the ICE in its efficient operating region. At high accelerator commands the upshift point changes to 4000 rpm to allow the ICE to deliver higher levels of torque.

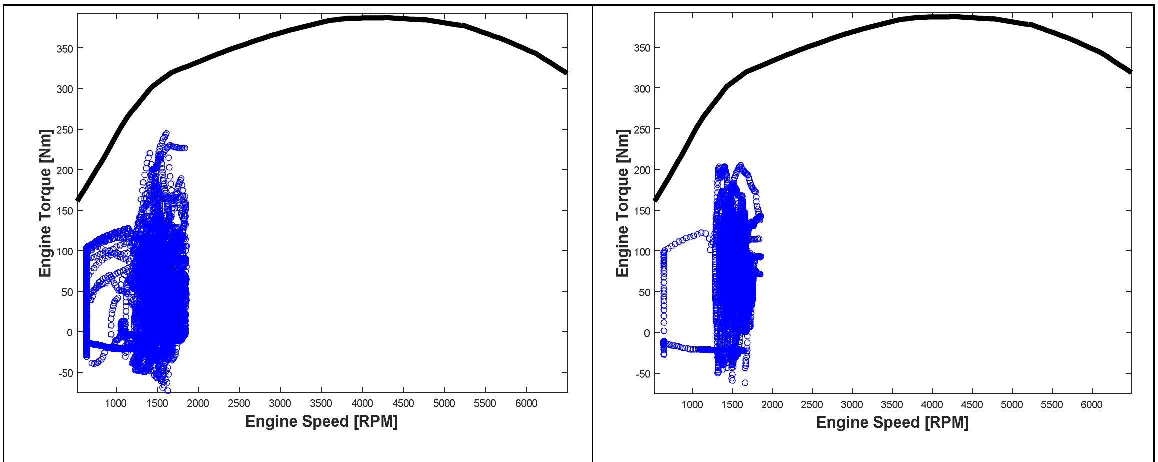

(a) UDDS

(b) HWFET

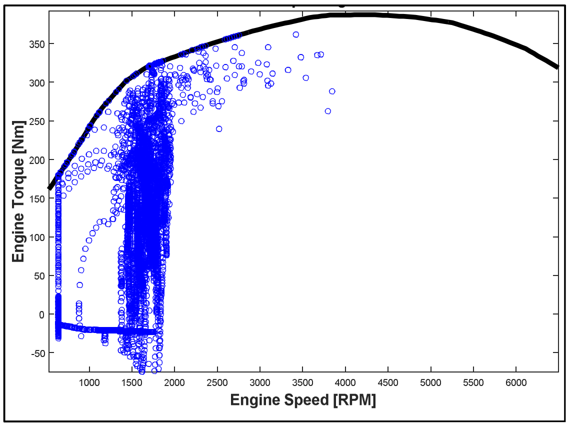

(c) US06

Figure 44 - Baseline Engine Operating Points over UDDS, HWFET & US06

Figure 44 displays engine operating points for the three simulations. Engine operation is concentrated within the mid-torque region over a relatively low rpm range of 1000-2000 for both the HWFET and UDDS cycles. The engine moves into the high torque and mid rpm range during the US06 cycle due to the high acceleration and high speed requirement of this cycle.

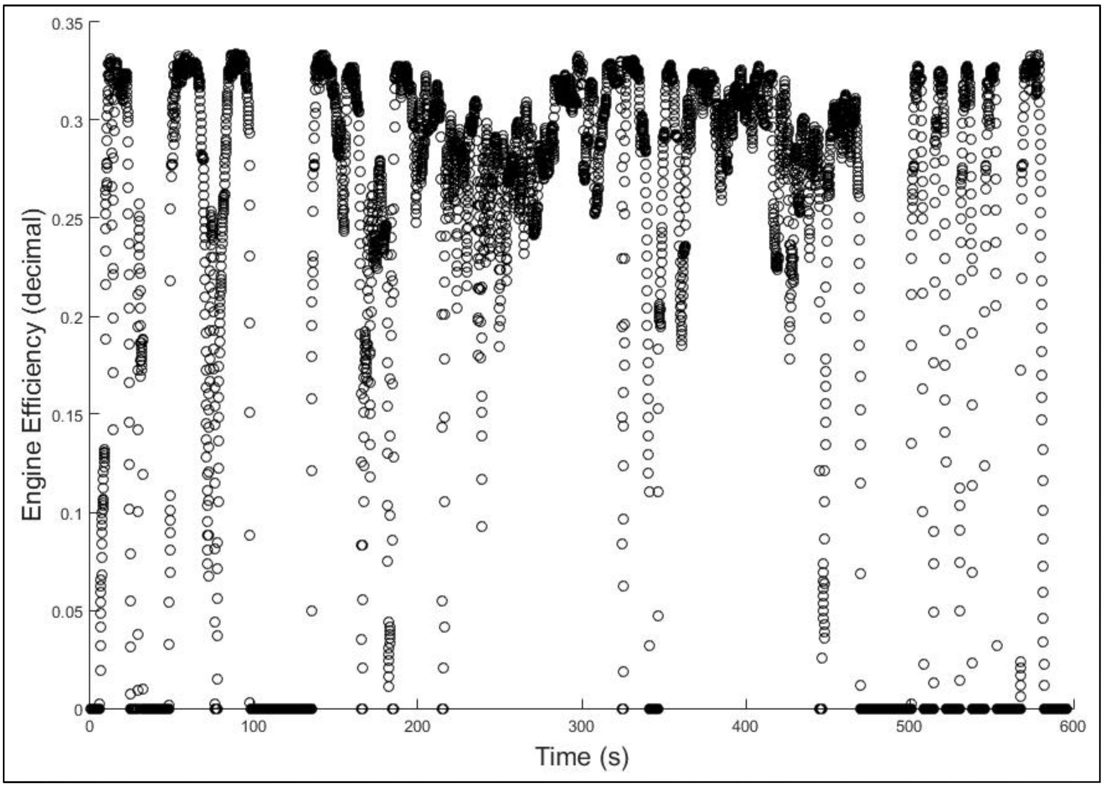

Figure 45 - Instantaneous Engine Efficiency over US06 Cycle

Figure 45 above is the instantaneous engine efficiency trace during the US06 drive cycle. Due to the eight speed transmission and relatively high torque requirement of the cycle the engine can operate in its high efficiency range over even the high speed requirement of the US06 cycle.

6. Electric Turbocharger Model

Engine Model

To evaluate the effect of an electrified turbocharger system a detailed engine model is used. The engine component is split up into three main subsystem categories: Intake, exhaust and the cylinder.

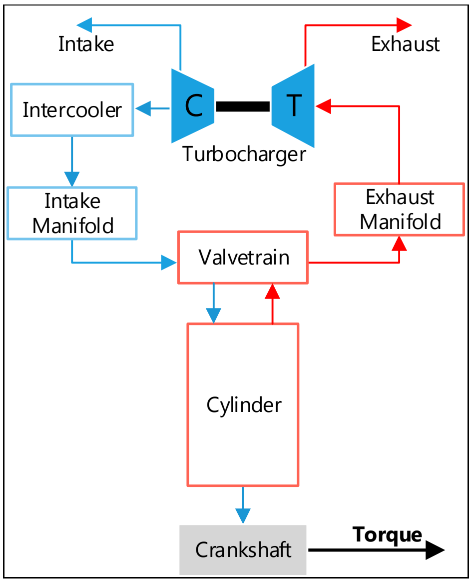

Figure 46 - Engine Configuration

The intake system is composed of the compressor from the turbocharger, the intercooler and the intake manifold. The exhaust system is composed of the exhaust manifold the turbine side of the turbocharger and the exhaust outlet. The gasses within these subsystems are assumed to be perfect and modelled as an ideal gas.

$$p \cdot V = m \cdot r \cdot T \tag{5}$$

Where p is pressure (Pa), V is the gas volume (m^3), m is the mass (kg), r is the universal gas constant (J*K/kg) and T is the temperature (K). In addition the flow is also assumed to be one-dimensional (1D), lumped (average pressure and temperature values are used) and gravity is neglected.

The modelling of gas transport is split up into three main component models:

1. Pneumatic Orifice Model
2. Pneumatic Control Volume Model
3. Pipe Model

Together these models are used to create both the intake and exhaust manifold subsystems as well as the transport of gasses in between the various subsystems in a 1D engine model.

In AMESIM the engine model uses three different types of gasses, air, fuel and burned gas. In the intake system the gas is set at 100% air. In the cylinder component fuel gas is injected based on injector timing and mean fuel rate. Here when the gaseous mixture is ignited it turns into the third gas type, burned gas. The amount of burned gas produced is dependent on the air-fuel mixture and rate of combustion. In the exhaust components generally the majority of the gas fraction is burned gas but can also contain substantial amounts of the other two gasses especially if the engine is running lean or rich. Detailed information about the gas model used can be found in the Appendix.

The inflow and outflow of gasses in the cylinder is controlled by the valves. The actuation and position of valves is defined by a valvetrain model and the global crankshaft angle ranging from 0-720° for the four stroke engine.

The valve train is modelled using test data files for the valve lift vs. crank angle. The intake and exhaust valve timing is defined within tables and by defining the IVO (intake valve opening) and EVC (exhaust valve closure) angle timings.

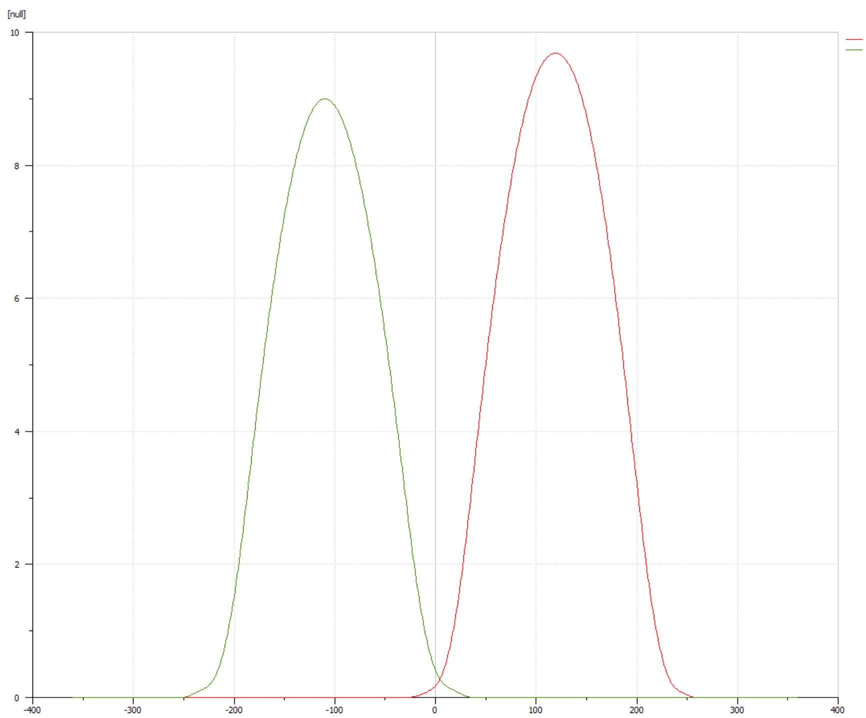

Figure 47 - Example Intake/Exhaust Valve Timing as a Function of Crank Angle

The valve flow can be modelled using the valve lift (mm) data at the crank angle.

$$Valve_{effective\_area} = flow\_coeff \cdot Area_{max} \cdot f\frac{lift}{max\ lift} \quad (6)$$

Both the intake and exhaust valve mass flow rate is calculated using the effective area.

Within the cylinder subsystem the intake air flow is mixed with injected fuel and ignited to produce power, heat and exhaust gasses. The power is transferred to a crankshaft component and the majority of exhaust gasses are sent out through the exhaust valve. The injection of fuel is modelled by defining the injection time, the static flow rate (SFR) and injector opening/closing duration.

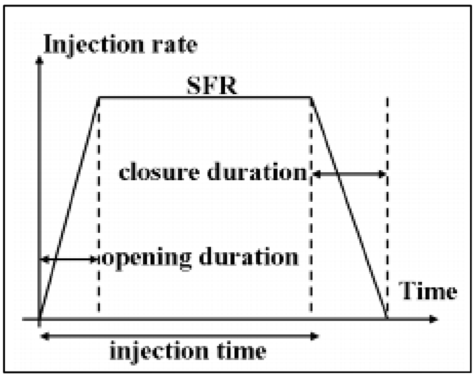

Figure 48 - Injector Timing Model

The amount of fuel injected is controlled by the air-fuel ratio (AFR) within the cylinder. Integrating SFR over two engine cycles equates to the total fuel injected for combustion.

$$\frac{\partial Q}{\partial \alpha} = Q_{total} \cdot \frac{A_1}{d_{Comb}}(1 + f_1)\left(\frac{\theta}{d_{Comb}}\right)^{f1} e^{-\lambda\left(\frac{\theta}{d_{comb}}\right)^{1+f1}} \tag{7}$$

The heat release from combustion is modelled using the Weibe equation. Here heat release is a function of the combustion duration (d_{Comb}), maximum instantaneous heat release (Q_{total}), and ignition delay parameters A_1, f_1 and λ. The Weibe model is not predictive since its parameters are fitted to experimental data and defined for one steady-state engine operating point. To adapt the model for transient predictive combustion behavior the constant fitted parameters can be replaced by a table of values. These constants are defined in a 3D look-up table and are a function of volumetric efficiency, AFR, engine speed and ignition advance [52].

Heat exchange between the combustion gases and the cylinder is also modelled. Within AMESIM heat is exchanged over three surfaces:

1. Cylinder Head
2. Cylinder Liner
3. Piston Surface

Their respective surface areas and outside temperatures are defined by the user. The temperature can either be modelled by a full lubrication and cooling circuit around the cylinders or explicitly specified. In the model used for this thesis these temperatures are explicitly specified.

A thermal model proposed by Woschni is used to calculate heat transfer [53]. It uses empirically fitted parameters along with the current cylinder pressure, temperature and volume to calculate convective heat transfer coefficient and heat flux output. The equations are reproduced below [54].

$$A_1 = C_1 V_p + C_2 V_c \left[T_1 \frac{(p - p_o)}{p_1 v_1} \right] \tag{8}$$

$$h_{convection} = 130 \frac{(pA_1)^{0.8}}{T^{0.53} B^{0.2}} \tag{9}$$

$$Q = h_{convection} \left(T_{gas} - T_{wall} \right) A_{wall} \tag{10}$$

Where:

- Vp is the mean piston velocity (m/s)
- Vc is single piston displacement (m^3)

- p1, v1 and T1 are initial pressure, volume, temperature conditions in the cylinder before start of combustion
- p and T are pressure (Pa) and temperature (K) of combustion gases within the cylinder,
- B is the cylinder bore (m)
- Twall is the wall surface temperature (K)
- Awall is the heat transfer surface area (m^2)
- C1 is a user specified coefficient. It uses 2 different values over the 4 stroke engine cycle. C1 uses one value for the intake and exhaust process and another one for the combustion, compression and expansion processes.
- C2 is a user specified coefficient also using two different values. The first value is used over the combustion and expansion process. The second is used for the intake, exhaust and compression processes.

A number of basic global engine parameters are also defined. These are used in calculation of global crankshaft angle, combustion, airflow through the engine and valve actuation. For the 4-cylinder turbocharged engine used for this research the table below summarizes these engine specifications.

Table 7: General Engine Specifications

Specification	**Value**
Number of Strokes	4
Number of Cylinders	4
Engine Architecture	in-line
Bore (mm)	83

Stroke (mm)	93
Connecting Rod Length (mm)	145
Compression Ratio	10.5
Firing Order	1-3-4-2
Number of Intake Valves per Cylinder	1
Number of Exhaust Valves per Cylinder	1
Injection Type	Direct Injection

In this thesis the included demonstration model within AMESIM of a 4-cylinder turbocharged engine is used. This model was constructed and verified using experimental test data. The engine wide open throttle curve is given in Figure 49.

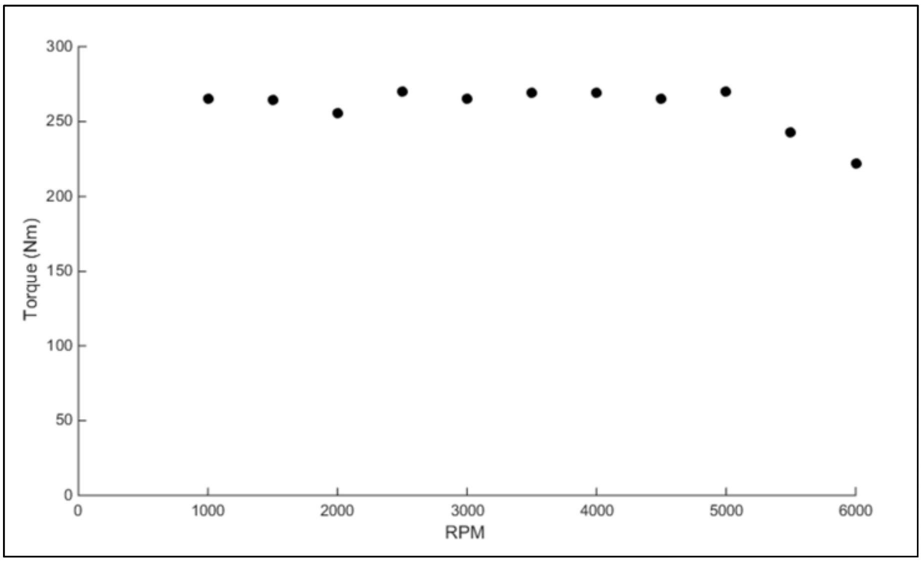

Figure 49 - AMESIM Engine Model Wide-Open Throttle (WOT) Curve

Turbocharger Model

The turbocharger is modelled by connecting turbine and compressor sub-models together. The shaft inertia and friction are also modelled.

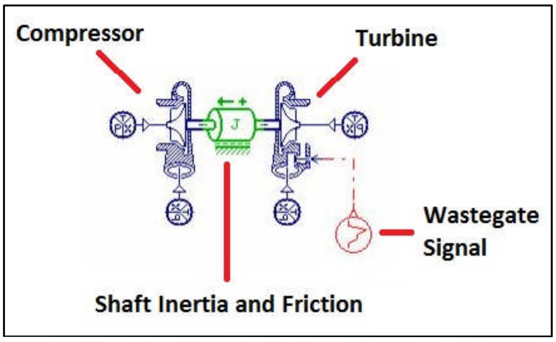

Figure 50 - AMESIM Turbocharger Model

Both the compressor and the turbine models have three ports, two pneumatic and one mechanical. The pneumatic ports are connected to the intake, exhaust and atmospheric pressure respectively for compressor and turbine. The mechanical port is where energy converted from the exhaust gasses is transferred from the turbine to the compressor.

Both the turbine and compressor are modelled using look-up tables from test data. For the compressor the pressure ratio and efficiency both as a function of mass flow rate and rotary velocity are required. From the torque applied on the shaft and the efficiency maps the mass flow rate and enthalpy flow rate can be calculated. Additionally both choke and surge limits are modelled to limit operation of the compressor. The turbine is similarly also modelled using two similar types of look-up tables: mass flow rate and efficiency as a function of pressure ratio and rotary velocity. Within this model back-flow and waste-gating is also accounted for. Both are modelled using orifices with the wastegate controllable via an external command. Thermal behavior is not modelled within the turbocharger system. Instead heat loss is encompassed within the efficiency look-up table data. Modelling heat transfer would require a much greater level of fidelity and detailed information about the turbocharger assembly and internals.

The electric turbocharger system is modelled by adding an electric motor onto the turbocharger shaft. The inertia is also increased to reflect additional motor mass. Figure 51 is the model diagram and Table 8 contains the motor specifications.

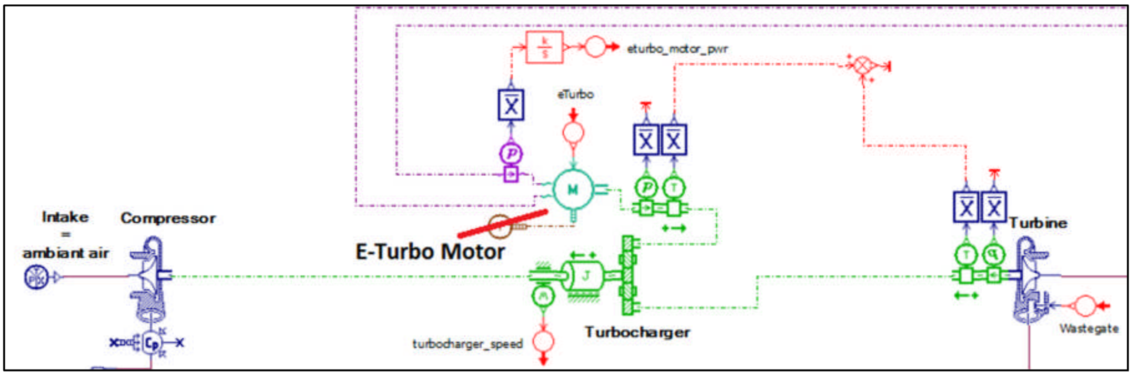

Figure 51 - E-Turbo System Model in AMESIM

Table 8: E-Turbocharger Motor Specifications

Maximum Power	Maximum Torque	Maximum Rotary Velocity	Constant Efficiency
10 kW	2 Nm	120,000 RPM	85%

Constant efficiency is used instead of a reference table of losses because a reference table for the type of compact very high speed motor could not be found.

Electric Turbocharger Controller

The electric motor in this turbocharger is controlled using a look-up table and a PI feedback loop. The motor is configured to set the turbocharger shaft speed depending on engine throttle and rpm. The motor will accelerate the turbocharger if the throttle position is 70% or above. Otherwise it is set to a lower speed taking energy away from the turbocharger. The look-up table can be seen in Figure 52. The other part of controlling the turbocharger, the wastegate, is set at 100% closed until the inlet manifold pressure increases to 2 bar then it opens up.

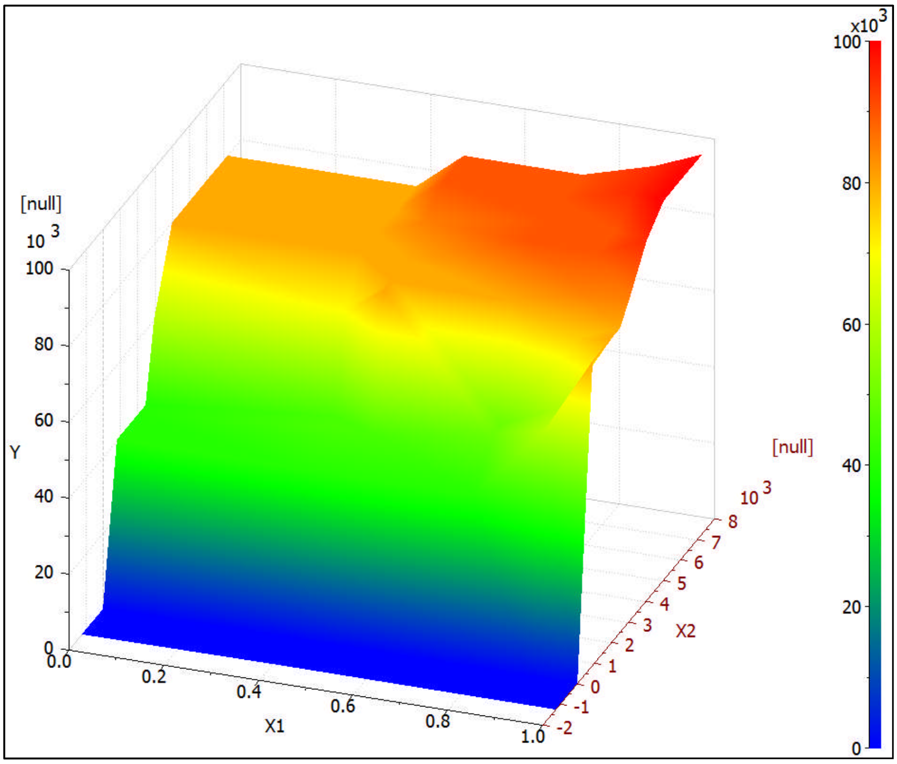

Figure 52 - Electric Turbocharger Motor Controller Look-up Table

With the electric turbocharger the engine can output full torque within 0.3 seconds compared to 0.8 seconds without electrical assist as illustrated in Figure 53 - Engine Transient Response at 2500 RPM.

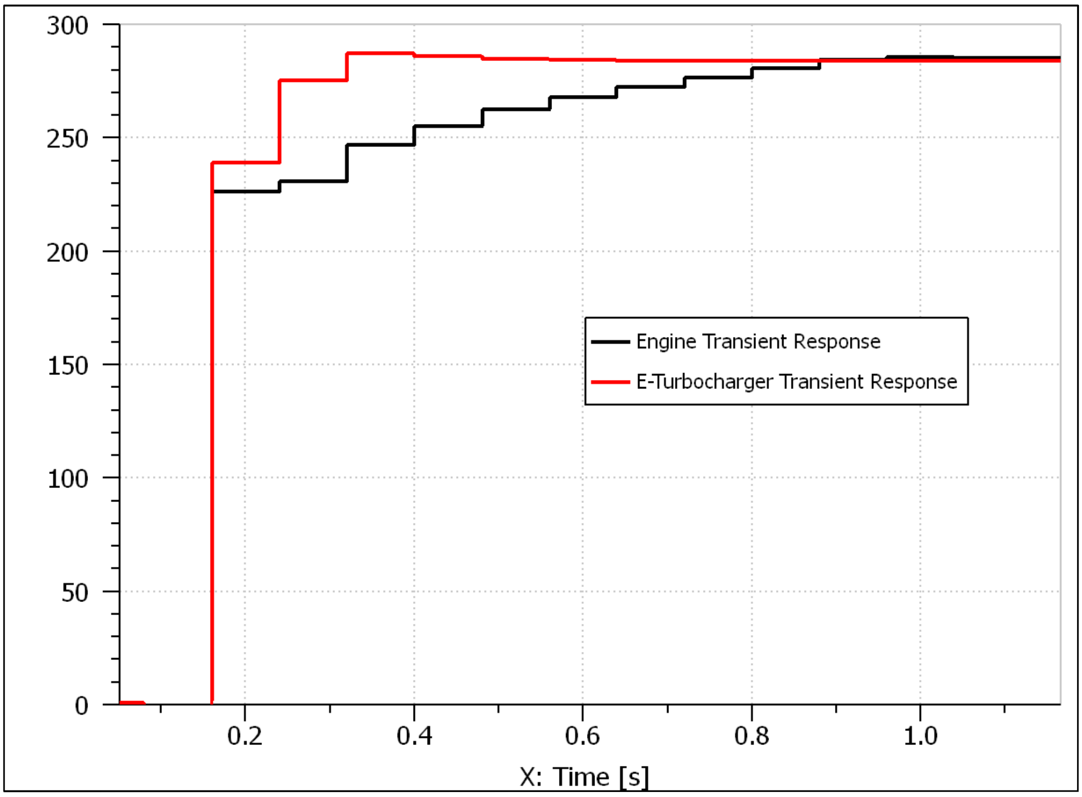

Figure 53 - Engine Transient Response at 2500 RPM (Torque averaged over engine revolution)

7. Hybrid Powertrain Architecture Modelling

Hybrid powertrain plant models are also created within AMESIM. The additional electrical and mechanical components are added onto the previously described engine model. An identical engine with electrified turbocharger is used in every hybrid powertrain modelled.

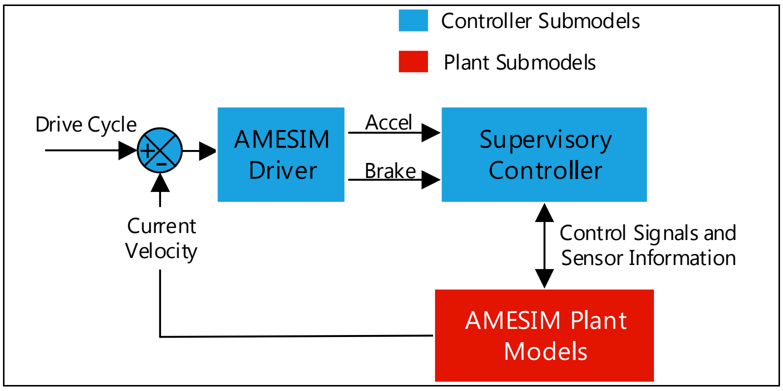

Figure 54 - Hybrid Powertrain Model Diagram

The AMESIM file contains all plant models as well as the driver subsystem. The drive cycle is selected here and the driver outputs accelerator and brake pedal commands depending on the current vehicle velocity. These commands as well as other powertrain and vehicle information is sent to a supervisory controller. The supervisory controller is created within Simulink using stateflow charts. Automatic code generation is then used to transfer the controller algorithm into C code. This code is imported into AMESIM and can interface with the rest of the system model.

To present a fair comparison between these powertrain architectures they have the same power output as the baseline conventional vehicle. Since the engines are identical the electric motor(s) specifications are adjusted to produce the same power output across all architectures simulated. Additionally all powertrain models use the same mathematical models for their individual components (ie. Electric motor, battery, etc). Only their position and specifications are changed.

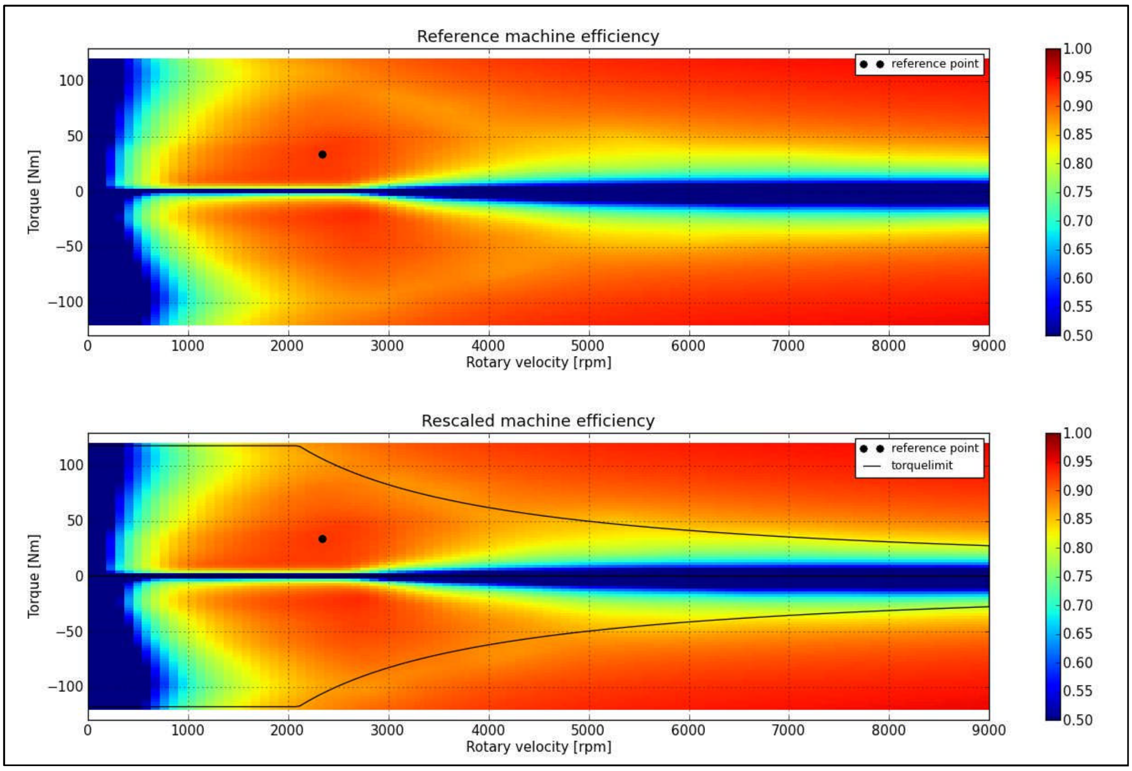

Figure 55 - Electric Motor Efficiency Map Scaling Tool

The electric motor is modelled with a reference energy loss map. This map is a function of the motor's rpm and output torque similar to how the engine was modelled in the baseline conventional vehicle. Within AMESIM a tool is used to scale this reference map for motors with differing power and torque rating. Figure 55 is a screenshot of the scaling tool.

P2-Parallel Hybrid Powertrain

The P2 parallel hybrid powertrain is modelled by inserting a clutch and electric motor in between the engine block and torque convertor sub-models. In this powertrain the power and torque of both ICE and electric motor can be added up. To meet the combined power target of 225 kW the electric motor is sized to 95kW with a resulting maximum torque output of 280 Nm and maximum speed of 8000 RPM.

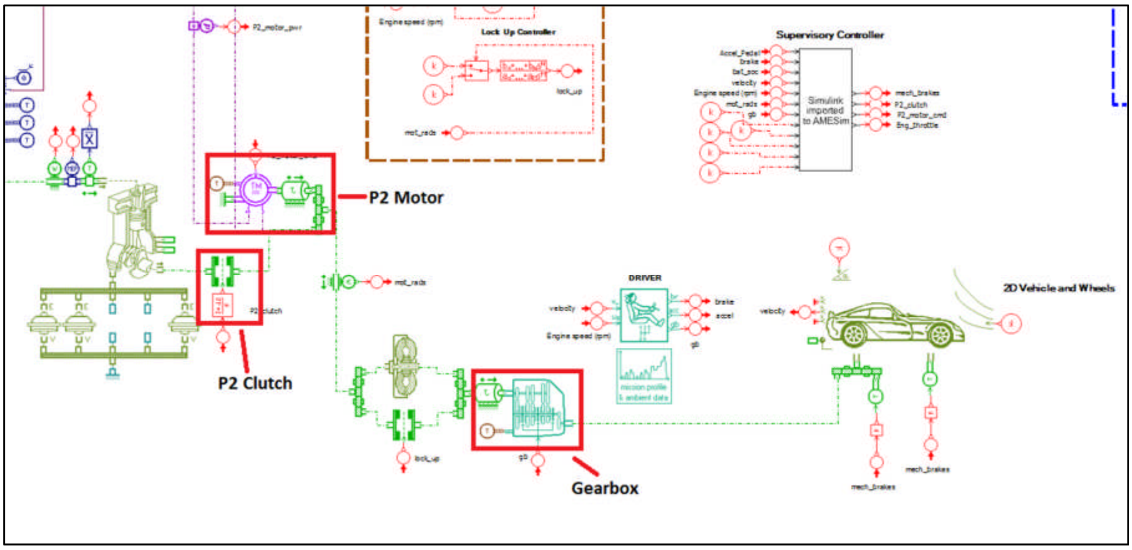

Figure 56 - P2 Parallel Hybrid Model in AMESIM

An extra inertial load of 0.05 kg*m^2 is also added to take into account the rotational mass of the electric motor. A simple battery pack model based on integrating the electrical discharge and charge power is used to calculate SOC. Figure 56 is the AMESIM sketch diagram of the P2 parallel component models and their physical signals connection.

Series Hybrid Powertrain

A series hybrid cannot directly transfer its engine power to the road. Therefore the electric motor with direct connection to the road is sized to 225 kW with a torque rating of 420 Nm. The second electric motor in this series configuration is sized to 70 kW, sufficient to meet high energy requirements of normal driving when in charge sustaining mode. The transmission in this powertrain is removed, instead the electric motor is installed in a direct drive configuration similar to most electric vehicles. A gear ratio between the series drive motor and the tires is set at 5.5:1. The figure below is the AMESIM sketch of the powertrain components for this series hybrid model.

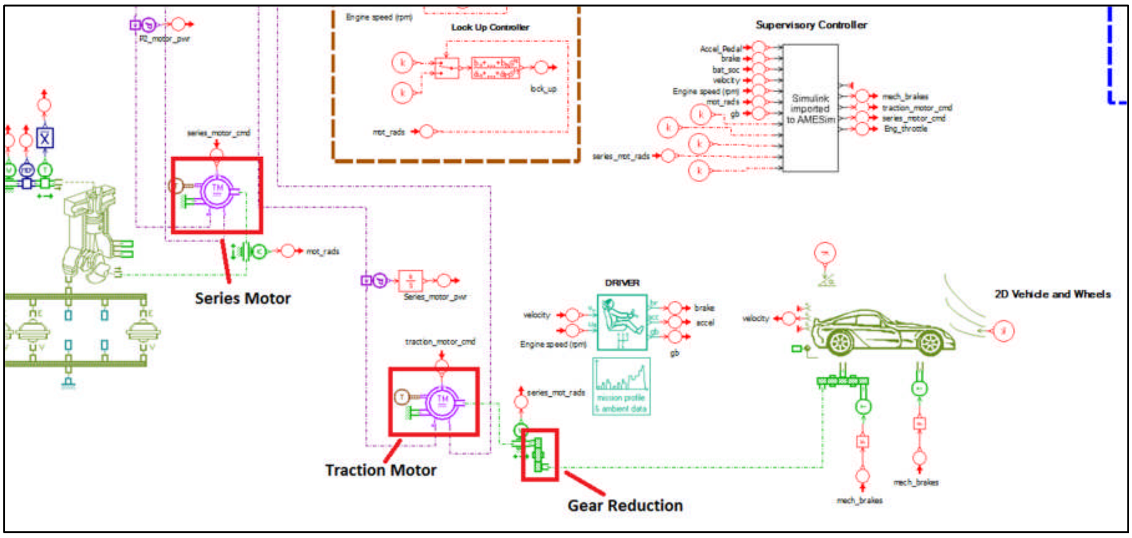

Figure 57 - Series Hybrid Model in AMESIM

Series-Parallel Hybrid Powertrain

A series parallel hybrid powertrain with two electric motor both in the P2 position (pre-trans) is also simulation in AMESIM. The first electric motor is directly connected to the engine and separated from rest of the powertrain with a clutch. The second electric motor is positioned directly after this clutch and before the transmission. This powertrain is capable of drive modes from both the series and parallel architectures. Figure 53 is the block diagram of this architecture.

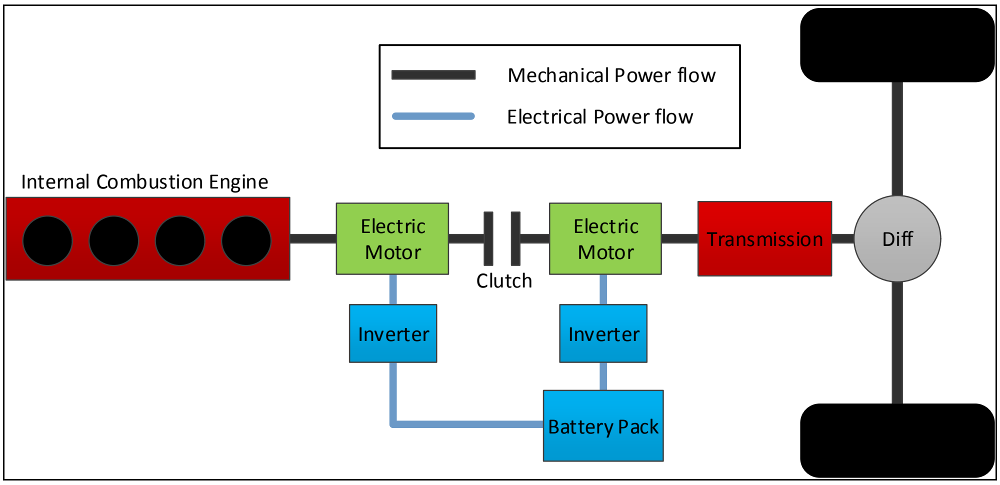

Figure 58 - Series-Parallel Hybrid Powertrain

Since this powertrain has two electric motors the shortfall in power from the engine alone is split between them. The first electric motor, known as the series motor, is sized to 40 kW. It is sufficient to let the motor and engine operate as a series genset. The second electric motor, referred to as the traction motor, is sized to 55 kW bringing the total power output of this system to 225 kW.

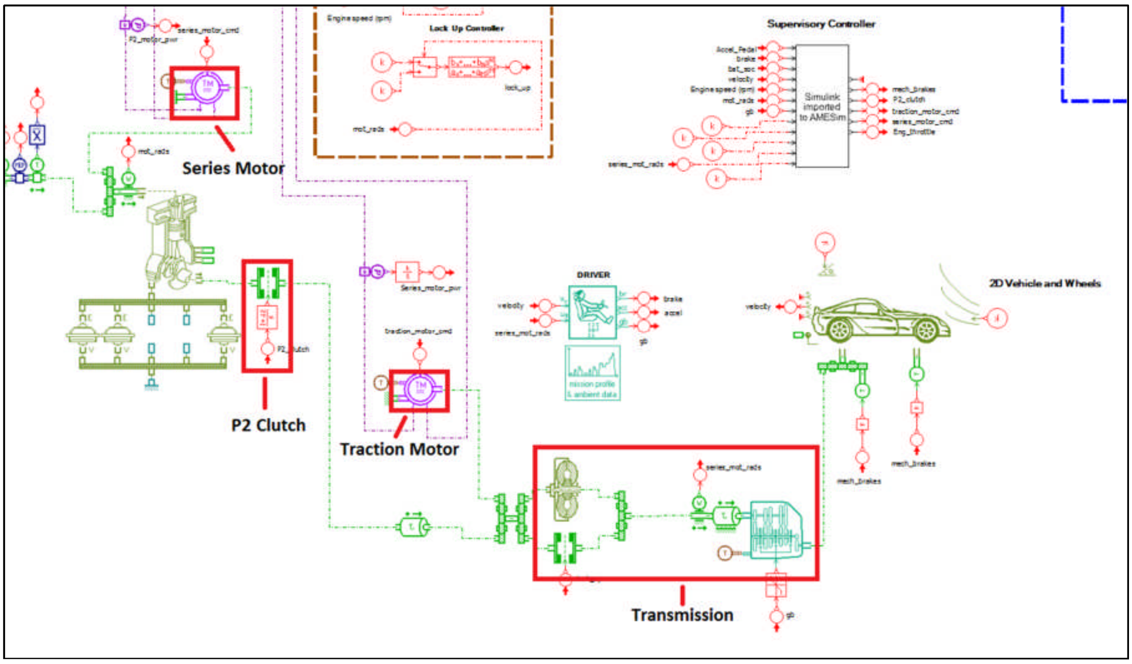

Figure 59 - Series-Parallel Hybrid Model in AMESIM

8. Hybrid Supervisory Control Units

Hybrid powertrains requires a top-level supervisory control unit to manage torque split between the ICE and electric motor(s). A supervisory control unit takes into account the state of all powertrain components, vehicle status and driver inputs then it sends a torque output command to each torque source in the vehicle. The supervisory controller will attempt to meet the torque command from the driver accelerator pedal while ensuring the powertrain is working at its maximum possible efficiency.

Every distinct powertrain architecture requires its own tailored supervisory controller and associated torque split/mode selection algorithm. The supervisory controller algorithm contains logic for mode switching depending on vehicle conditions and driver commands. The simplest and easiest to implement algorithm is known as a rules-based controller. In a rules-based supervisory controller the mode selection is based on predefined logical statements. These statements are created through experimentation and engineering experience to determine under which conditions should a powertrain operate and switch modes. For example if a powertrain is capable of an electric-only drive mode, the vehicle can use that for initial acceleration bypassing the low efficiency operating regions in an internal combustion engine. The disadvantage of rules-based supervisory controllers is the logic is preloaded and therefore cannot adapt to changing vehicle or powertrain conditions. Therefore this type of controller is not considered an optimized controller. Within this report all powertrain supervisory controllers are modeled using rules-based algorithms. Each supervisory controller is created using Stateflow within Simulink. Stateflow is a control logic tool within Simulink which uses finite state machines and flow charts. The supervisory controllers are created within Matlab 2014b and imported into the AMESIM model using the built in automatic C code generator.

All hybrid electric powertrains are capable of operating within two broad modes: charge-depleting (CD) and charge-sustaining (CS). In CD mode the electric motor will output a greater percentage of the drive requested torque. If the powertrain has high electrical power capability the electric motor(s) will fill 100% of the driver requested torque. As a results this mode depletes the battery state of charge over time. In CS mode the supervisory controller will modulate mode changing and electric motor operation to balance vehicle efficiency with battery SOC. Within standard drive cycle testing, when in CS mode, the net electrical energy used must be as close to zero as possible. In this report all powertrain simulations have been conducted to ensure delta SOC is within 2%.

P2-Parallel Hybrid

Within this powertrain the engine and electric motor are inline and therefore both can provide torque to the road. The electric motor is separated from the engine by a clutch to enable an electric-only drive mode. The goal is to use the electric motor for small torque requests and regenerative braking. The engine will operate during larger torque requests and during highway type higher vehicle speeds. The electric motor in this powertrain can also be used to provide a load on the engine. This will generate electrical power for storage within the battery pack and also push the engine operating points into a region of higher efficiency. The power flow diagrams for each mode within P2-parallel hybrid powertrain are given below.

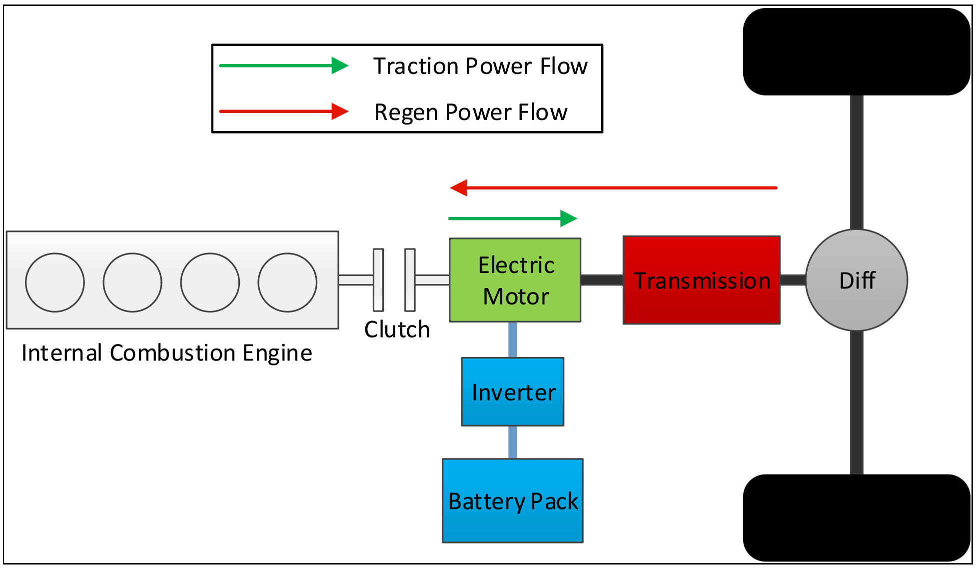

Figure 60 - P2 Parallel Electric Only Mode

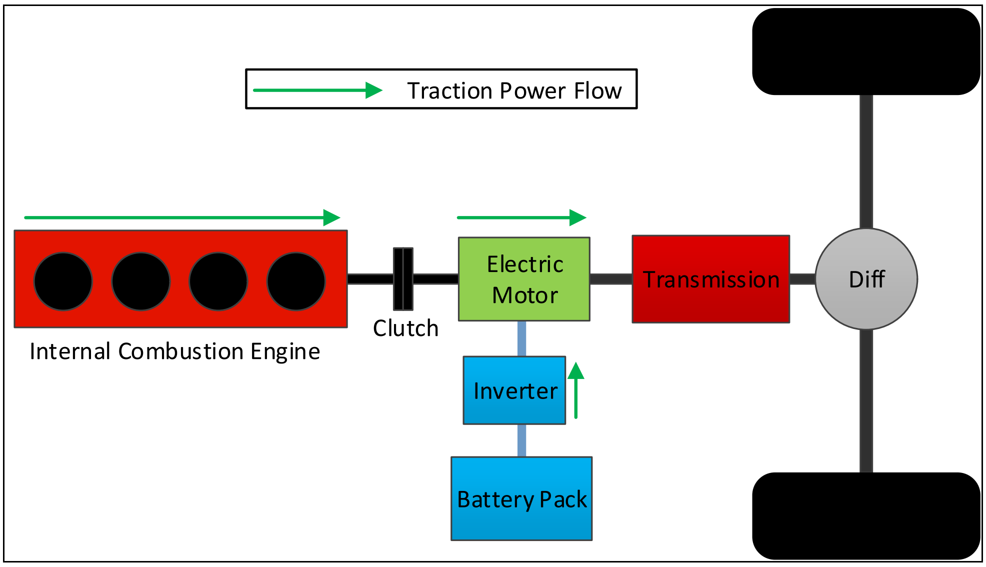

Figure 61 - P2 Parallel HEV Mode

In regular HEV mode the clutch is closed and the motor can supplement the ICE in providing power.

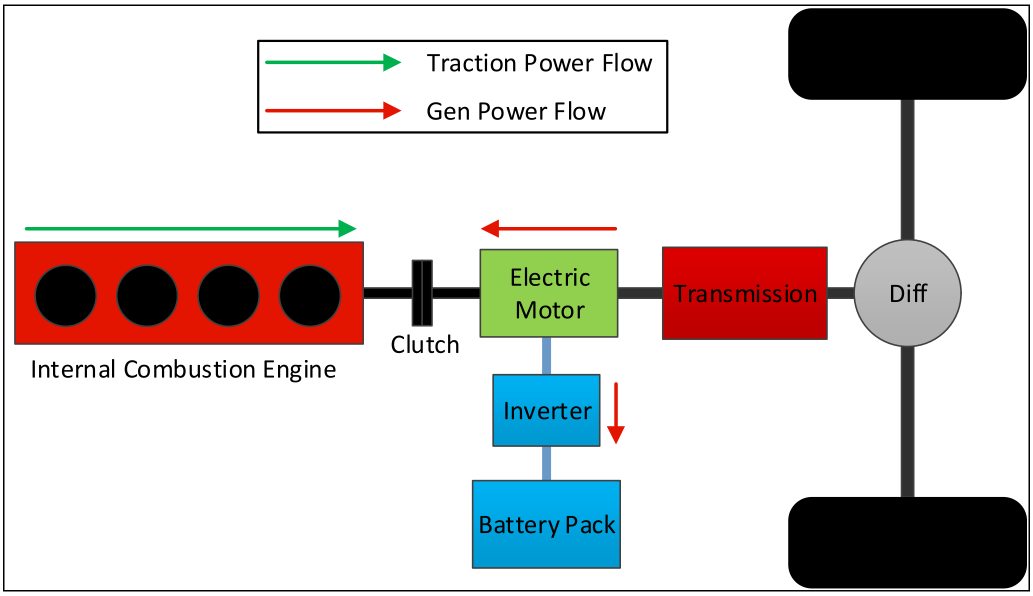

Figure 62 - P2 Parallel Motor Generator Mode

In generator mode the ICE produces extra power than is requested by the driver. This extra power is used by the electric motor to store electrical energy for later use. This mode also has the extra benefit of shifting the engine into its higher efficiency operating region during low torque requests.

The input/output signals for the P2 parallel hybrid powertrain is given in the table below:

Table 9: P2 Parallel Hybrid Stateflow I/O Signals

Input Signals (unit)	**Output Signals (unit)**
Accelerator Pedal (0-1)	Engine Throttle (0-1)
Brake Pedal (0-1)	Motor Torque Command (Nm)
Battery SOC (%)	P2 Clutch Command (0-1)
Vehicle Velocity (m/s)	Mechanical Brake Command (Nm)

Engine Speed (RPM)	Controller State
Motor Speed (RPM)	
Transmission Gear	
Motor Maximum Torque (Nm)	
Motor Maximum Power (W)	
Brake Maximum Torque (Nm)	
CD Mode (0-1)	
Battery SOC Target (0-1)	

The stateflow chart is broken up into two main states: braking and accelerating. Within braking the electric motor is configured to always apply maximum braking force and the shortfall is taken up with the mechanical brakes. The accelerating state is broken up into two parts, charge-depleting operation and charge-sustaining operation. In CD operation the electric motor fulfills as much of the torque request as possible. In CS mode the powertrain switches between electric-only, parallel and generator operation depending on the torque request and battery SOC.

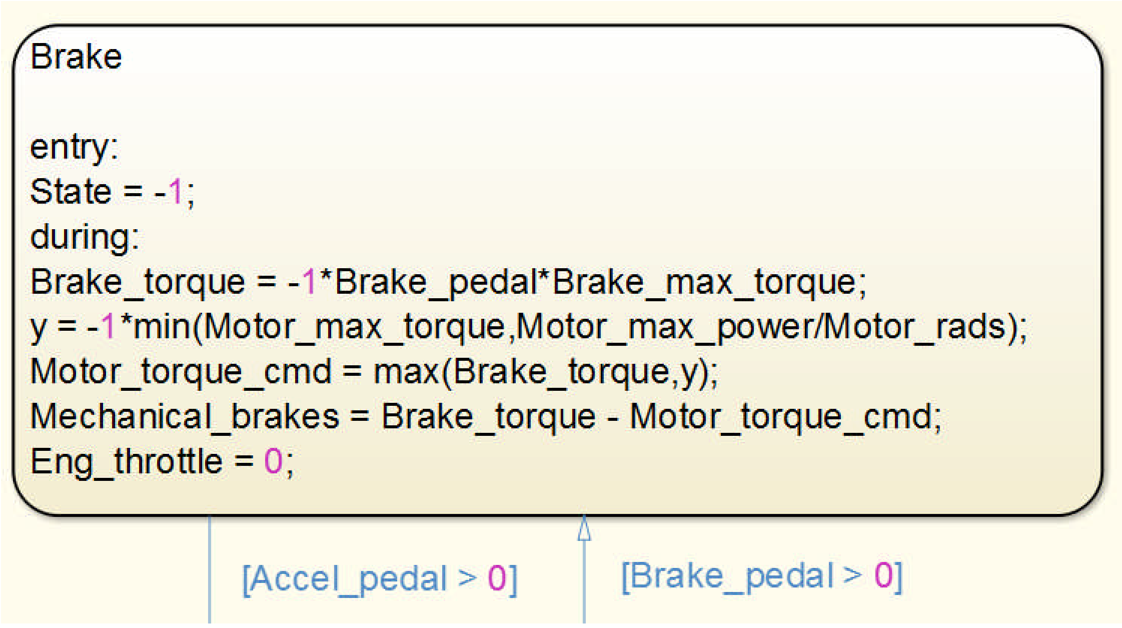

Figure 63 - P2 Hybrid Supervisory Controller Brake State

Figure 63 above is the Brake state where commands for both motor torque and mechanical braking is determined and output to the AMESIM plant model. The two statements at the bottom of the diagram are the possible transitions from the Brake state. Here if the accelerator pedal signal is greater than zero then the current controller transitions out of the Brake state.

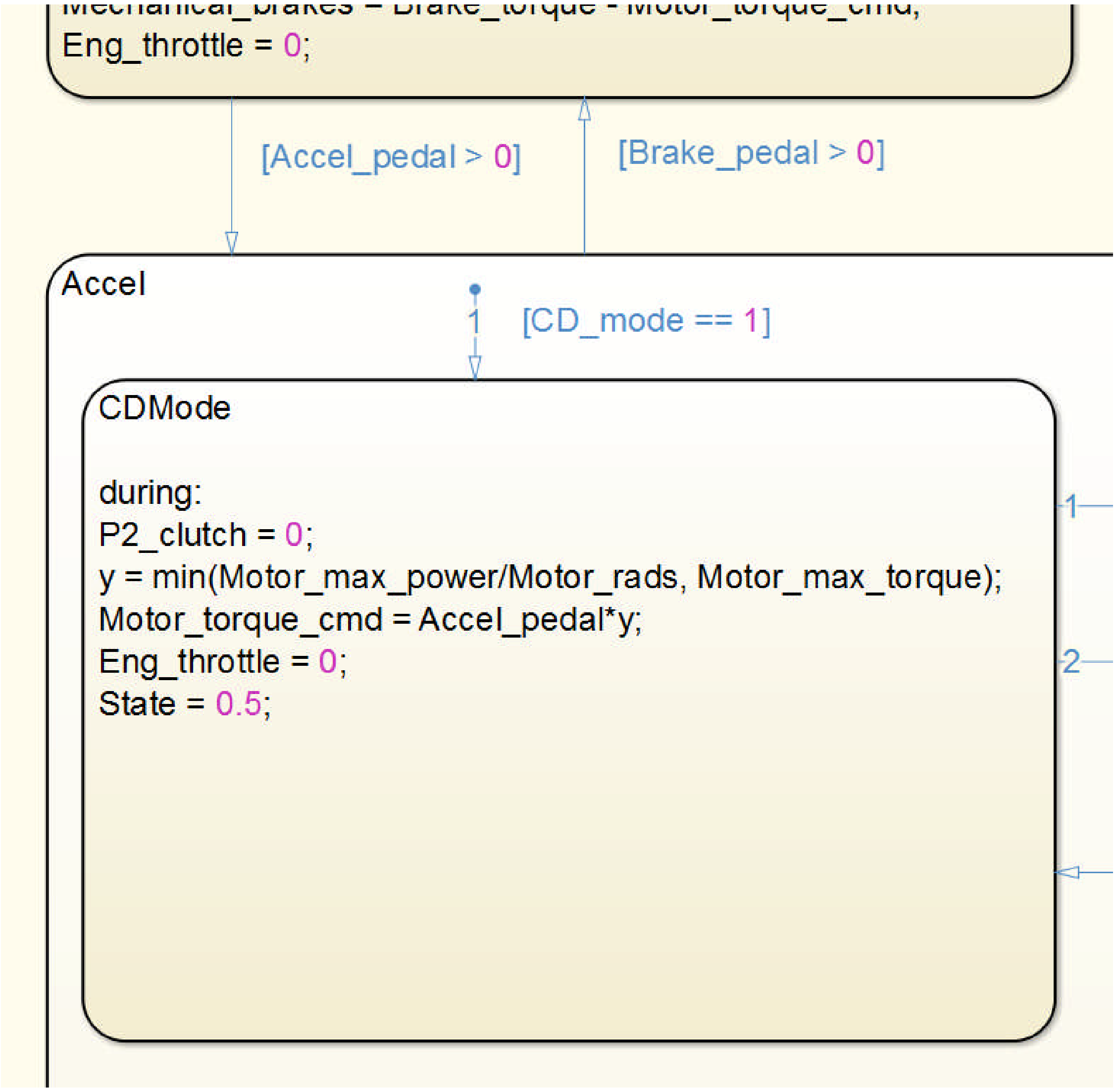

Figure 64 - P2 Hybrid Supervisory Controller CD Mode

In CD mode the clutch is open and hence the engine is disconnected from the rest of the powertrain. Only the P2 motor is used to satisfy drive accelerator command. A state command is output to keep track of controller state when this stateflow chart is compiled and imported within AMESIM.

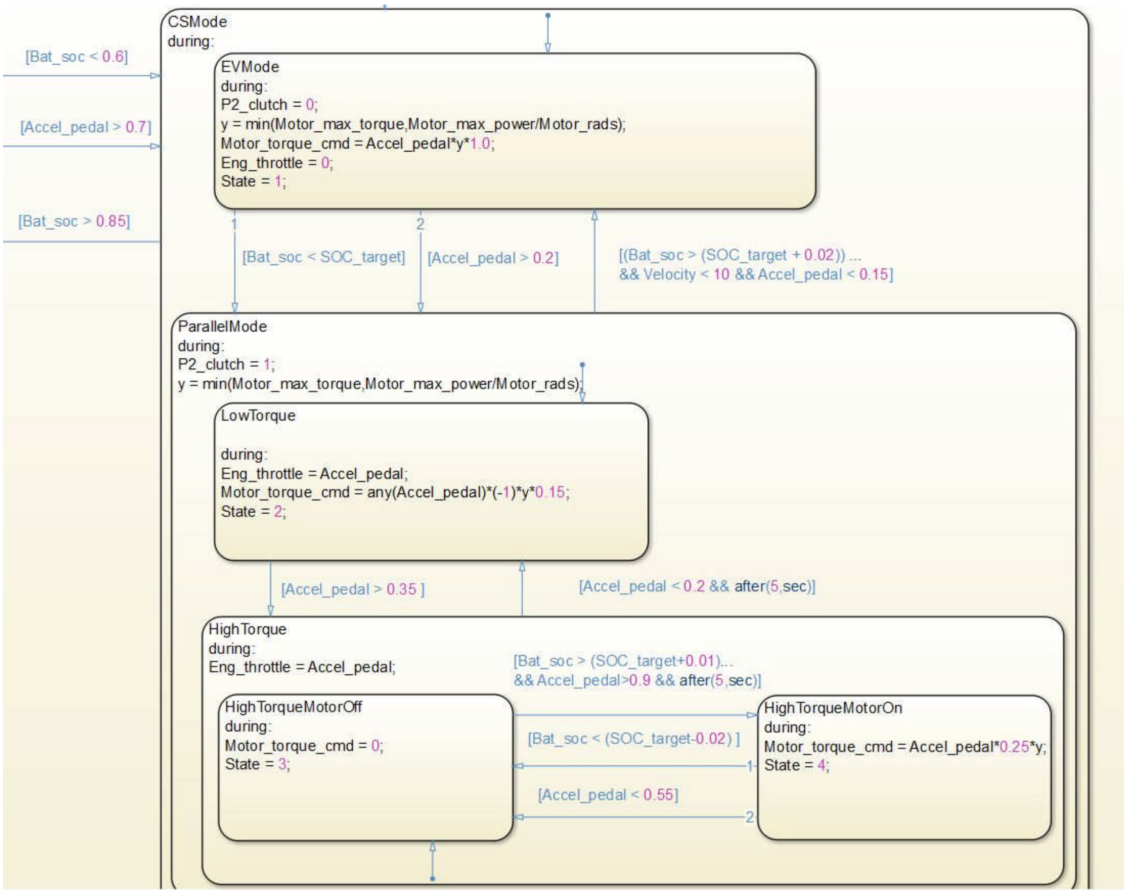

Figure 65 - P2 Hybrid Supervisory Controller CS Mode

CS mode is broken down into several states and sub-states. In the upper left corner of Figure 65 the transition into CS mode is when battery SOC dips below 60% or the driver torque request is above 70%. Within CS mode the powertrain can switch between all three drive modes: EV, HEV and generating. If the vehicle velocity and drive accelerator signals are low and battery SOC is above its set CS target the vehicle will operate in EV mode. If any of those conditions are not true then the clutch is engaged and the powertrain will operate with the engine on. Parallel operation is broken down further into two states: LowTorque and HighTorque. Within LowTorque state the engine will supply the requested driver torque while the P2 motor is in generator mode. If the accelerator pedal signal is above 35% the controller transitions into the HighTorque state. Here the motor is not allowed to operate in generator mode and if there is sufficient charge in the battery the motor will output tractive torque.

Series Hybrid

A series hybrid powertrain contains two main modes of operation. Electric only with the series generator off and when it is on. In a series hybrid only electric motor(s) connected to the wheels can provide tractive power to the road.

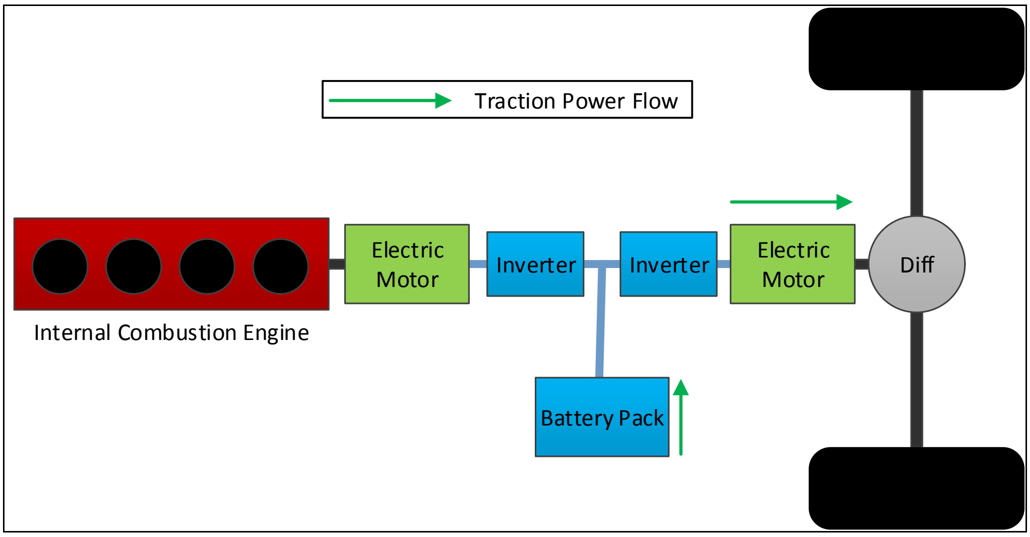

Figure 66 - Series Hybrid Electric Drive Mode

The other electric motor is coupled to the engine and only used when the battery SOC is below the target threshold. When the SOC does dip below the threshold the engine is turned on and runs at its most efficient operating point. Energy from the engine is converted to electricity by the generator motor. This electrical energy is either directly sent to the traction electric motor or stored in the battery pack for later use.

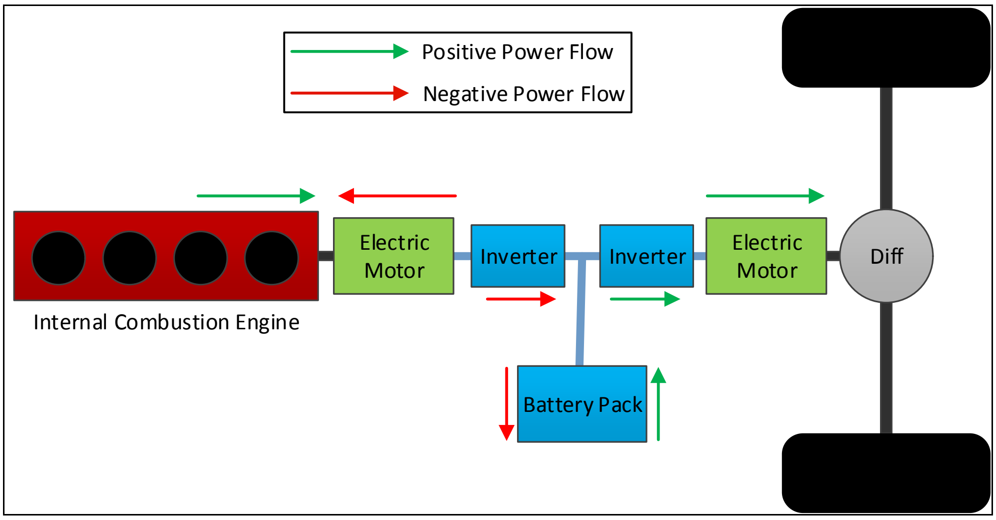

Figure 67 - Series Hybrid Series Mode Operation

The supervisory controller for series hybrid is also modelled using stateflow within Simulink. Table 10 below displays the input/output signals from the series hybrid supervisory controller.

Table 10: Series Hybrid Powertrain Stateflow I/O Signals

Input Signals (unit)	**Output Signals (unit)**
Accelerator Pedal (0-1)	Engine Throttle (0-1)
Brake Pedal (0-1)	Traction Motor Torque Command (Nm)
Battery SOC (%)	Series Motor Torque Command (Nm)
Vehicle Velocity (m/s)	Mechanical Brake Command (Nm)
Engine Speed (RPM)	Controller State
Traction Motor Speed (RPM)	
Transmission Gear	
Traction Motor Maximum Torque (Nm)	

Traction Motor Maximum Power (W)	
Brake Maximum Torque (Nm)	
Series Motor Speed (RPM)	
Battery SOC Target (0-1)	

The series hybrid supervisory controller stateflow is split into two top-level parallel states. Parallel states execute simultaneously whereas the P2 hybrid supervisory controller contained solely exclusive state execution. At the top-level the chart is broken up into a state for braking and applying traction torque to the road. The other state is responsible for controlling the genset system.

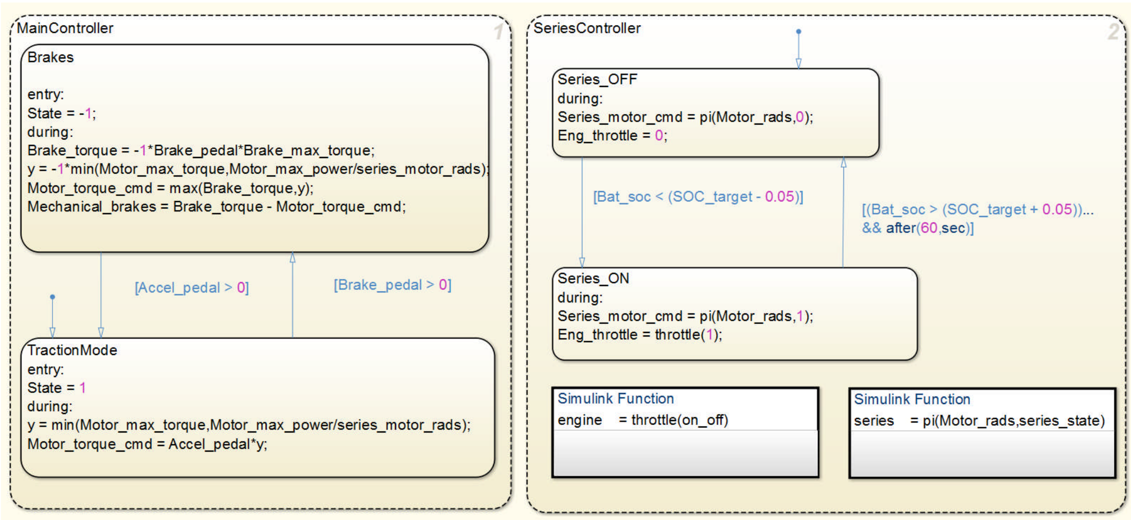

Figure 68 - Series Hybrid Supervisory Controller, Top Level

The first state, known as the 'MainController', contains a braking state similar to the one used earlier with the P2 hybrid controller. It splits commanded braking torque between regenerative and friction braking. The other state within this MainController is called TractionMode. This state directly takes driver accelerator pedal command and translates it to a torque command from the traction motor. In essence the MainController state handles direct torque commands relates to both the brake and accelerator pedals. A close-up of the MainController is shown in Figure 69.

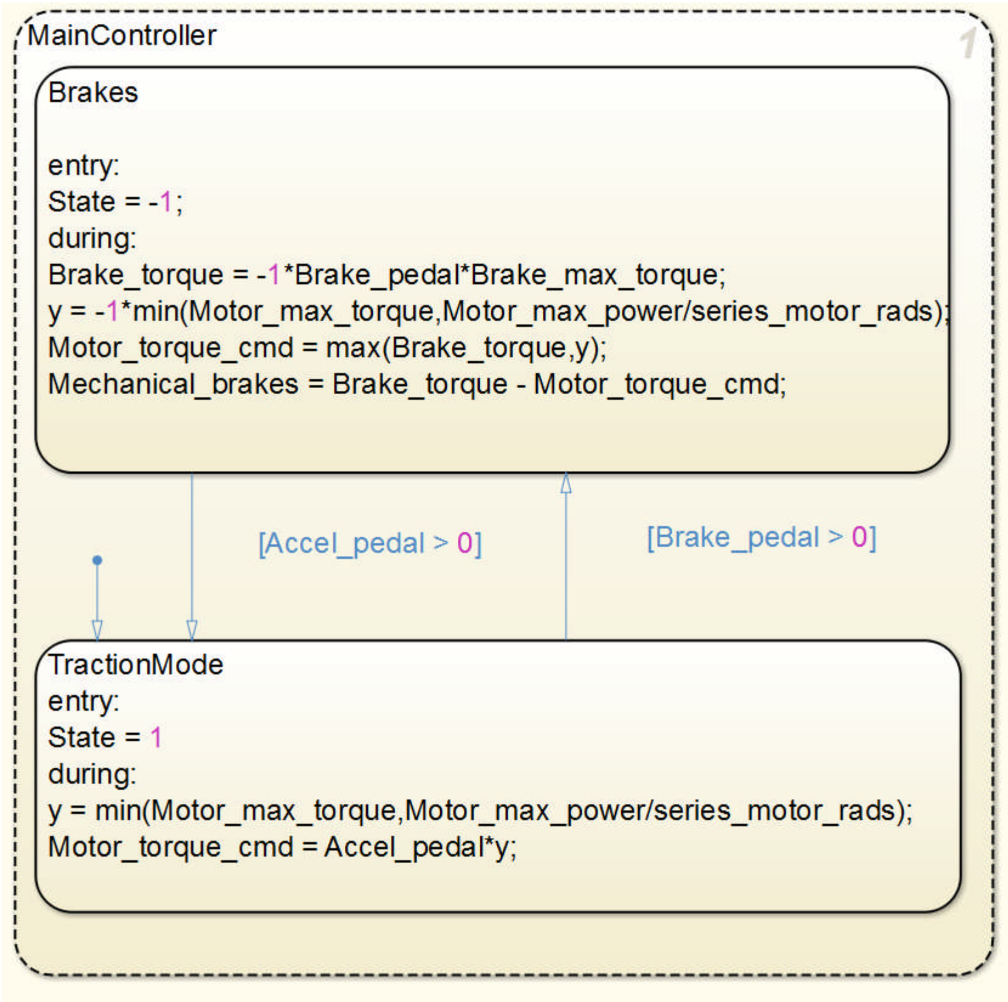

Figure 69 - Series Hybrid Supervisory Controller, Traction and Braking

The other parallel state is named SeriesController. This state controls the series ICE and generator system. Within SeriesController are two sub-states and two Simulink functions. The first state Series_OFF, output zero engine throttle and commands the series motor in speed mode to stay at 0 rpm. The second state, Series_ON, sets a constant engine throttle command and the series motor is also set to a constant speed command.

The throttle Simulink function outputs a constant value between 0 and 1 which is the engine throttle value. Within stateflow this function is used because when code is auto-generated a constant block within Simulink remains tunable in AMESIM whereas a line of code in stateflow would not be. The pi Simulink function seen below in Figure 71 takes in the current series motor speed and uses a proportional controller to set motor and ICE speed at the specified reference.

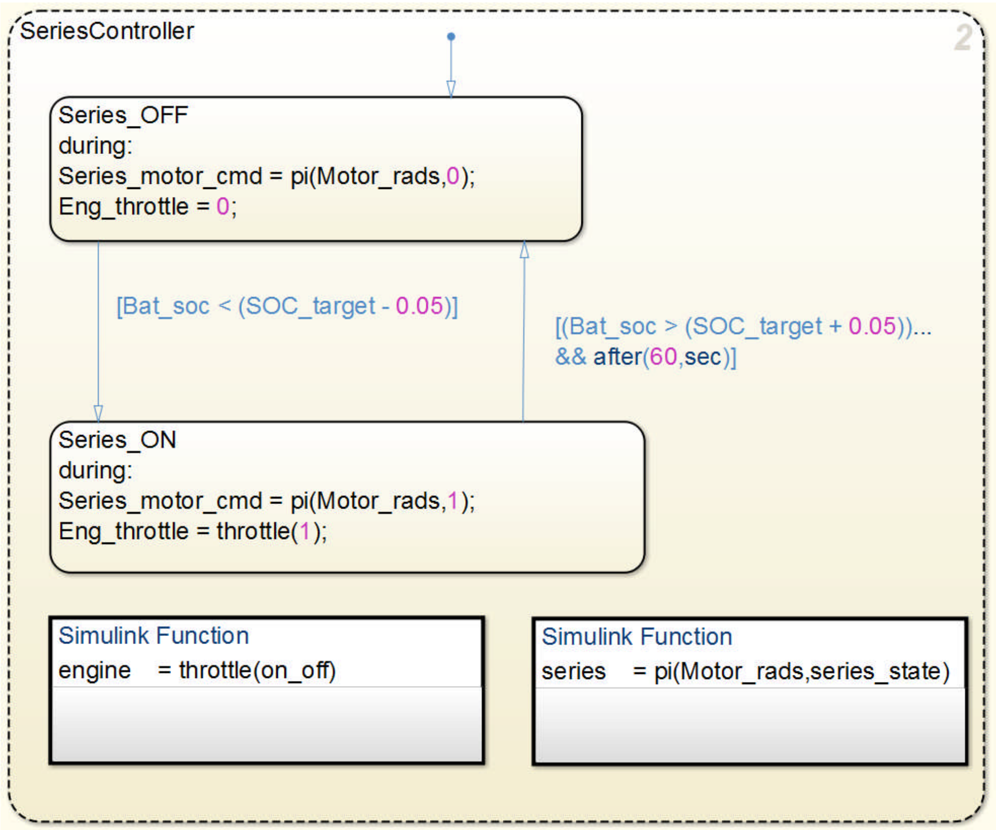

Figure 70 - Series Hybrid Supervisory Controller, Series Motor Genset

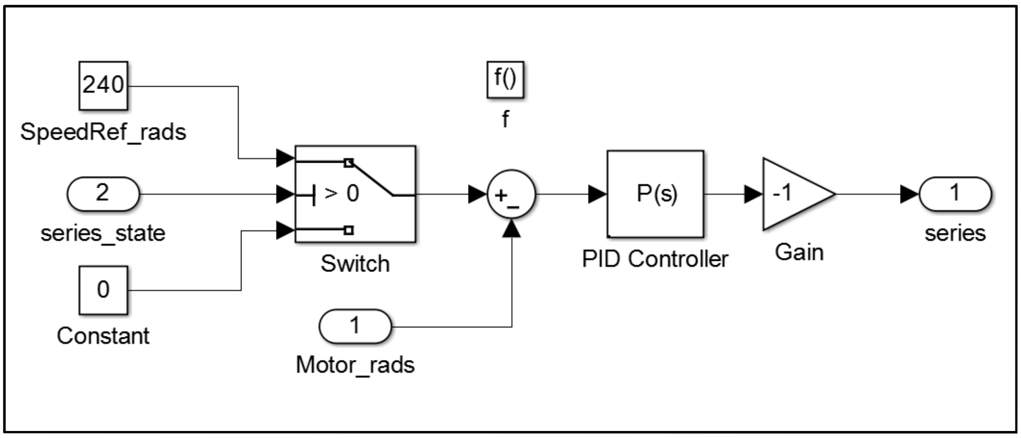

Figure 71 - Series Hybrid Supervisory Controller, Engine RPM Controller

Series-Parallel Hybrid

The series-parallel hybrid powertrain can use driving modes from both series and parallel hybrid powertrain architectures. If the clutch is open the powertrain can be operated in electric only drive mode or in series mode. The power flow for this is shown below in Figure 72.

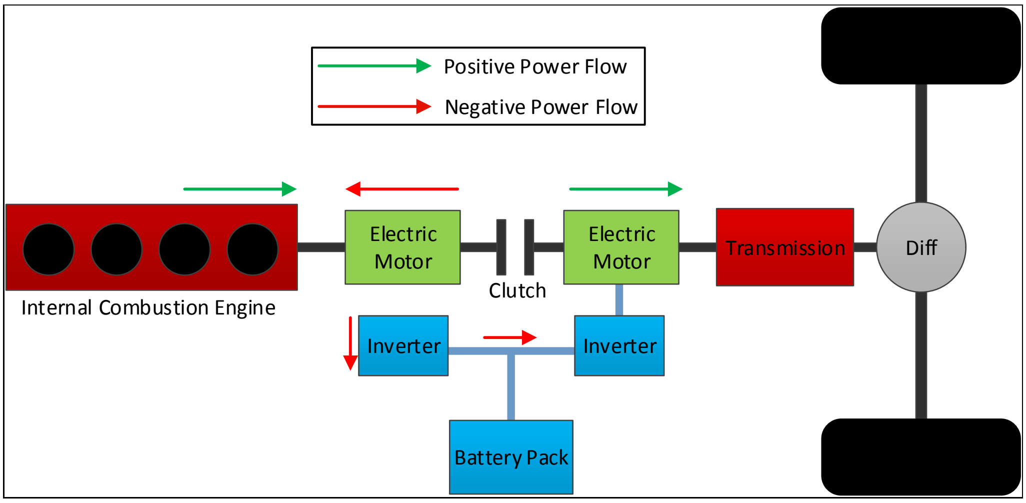

Figure 72 - Series-Parallel, Series Mode

With the clutch engaged the ICE can transfer power to the road. Here the electric motor(s) can add additional load to generate electrical energy for later use. The power flow for this mode is in the figure below.

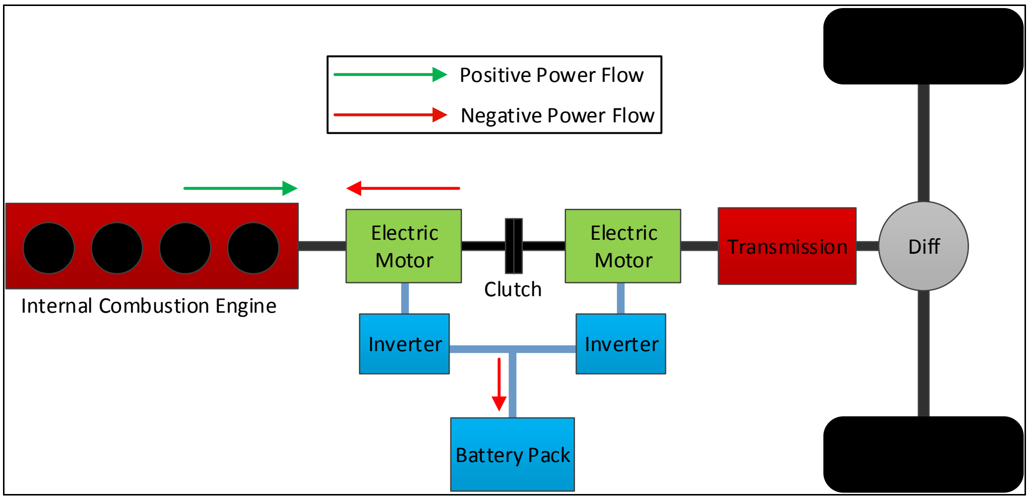

Figure 73 - Series-Parallel, Parallel Generator Mode

Furthermore unlike a series-hybrid this powertrain allows all torque producing components to deliver power to the road. This is shown in the figure below.

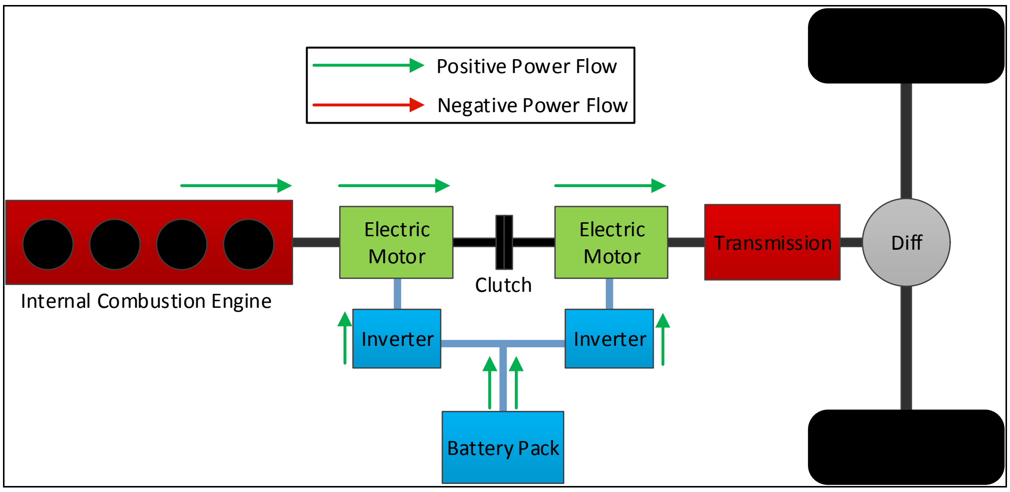

Figure 74- Series-Parallel, Parallel Mode

The supervisory controller I/O for this powertrain is similar to the one specified for series hybrid in the previous section in Table 10 with an added command for the clutch. The series motor here refers to the electric motor connected to the ICE and behind the clutch. At the top level the stateflow chart for this supervisory controller is also split into two parallel states. One state controls the traction motor and braking. The other controls the clutch, series motor and ICE.

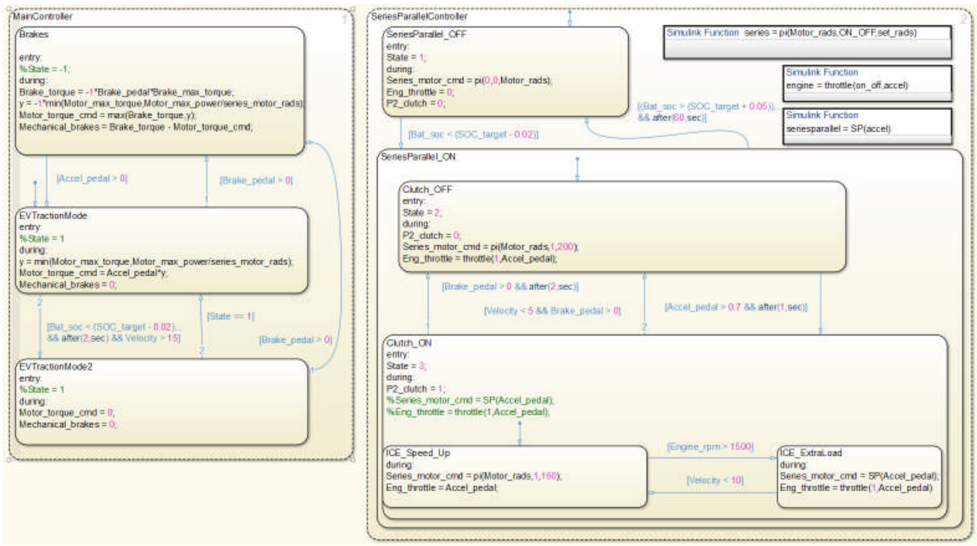

Figure 75 - Series-Parallel Hybrid Supervisory Controller, Top Level

The first state is similar to the one for series hybrid powertrain. It contains the exact same Brakes and EVTraction states. The difference here is an additional state for when the powertrain is operating with the clutch engaged and therefore in parallel mode. This other mode set the traction motor torque command to zero.

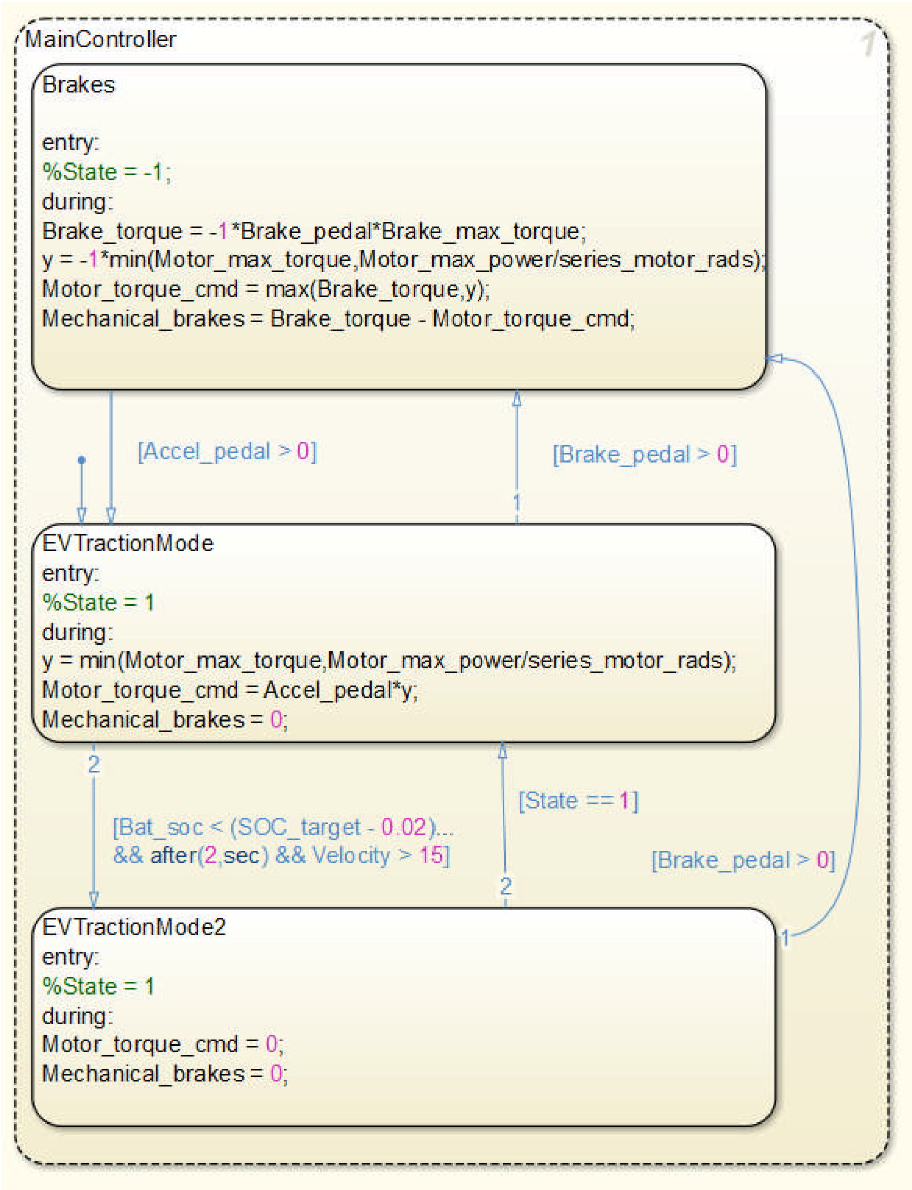

Figure 76 - Series-Parallel Hybrid Supervisory Controller, Brakes and EV Mode

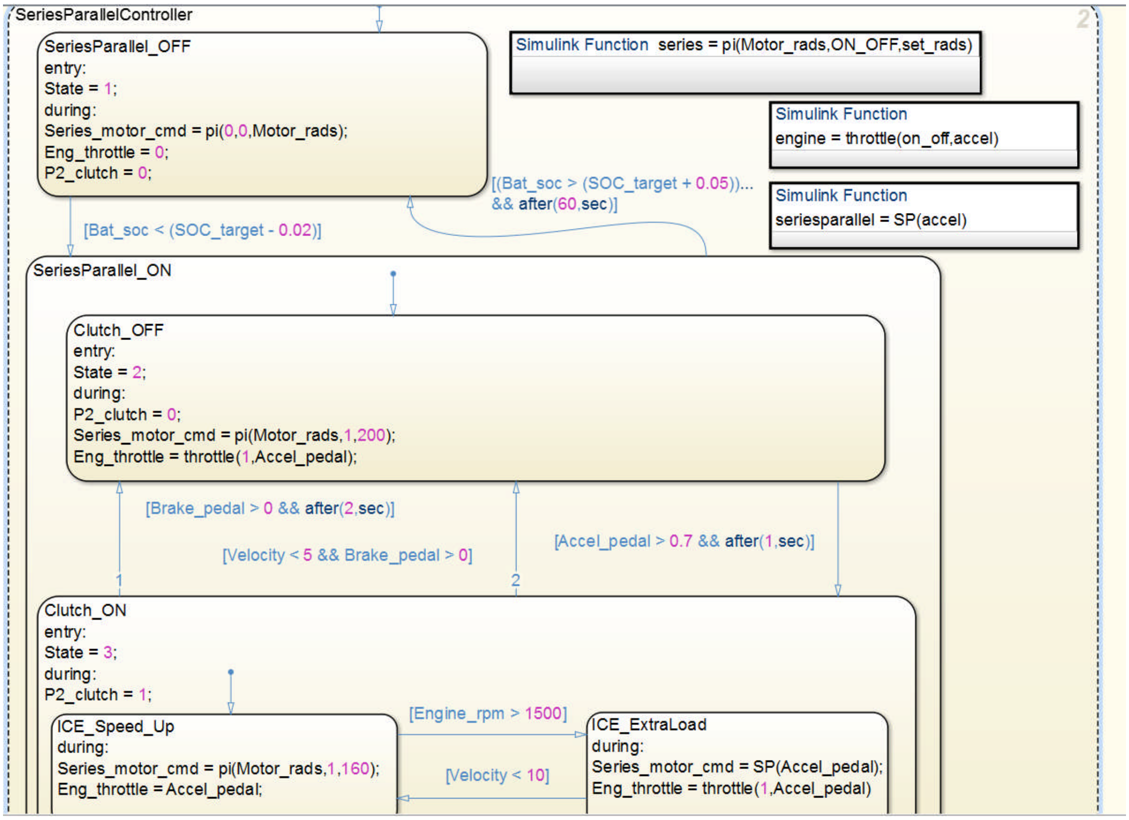

Figure 77 - Series-Parallel Hybrid Supervisory Controller, SeriesParallelController State

The second parallel state controls engine throttle, series motor torque and actuation of the clutch. At the upper level within this state there are two sub-states for engine on and engine off conditions. With the engine off the clutch is disengaged and series motor is commanded to reach zero rpm.

When battery SOC is below the transition threshold the controller state switches to the engine on-mode. With the engine on the controller can have the vehicle operate in either series or parallel mode. Initially the controller starts within the series state (titled Clutch_OFF in Figure 77). Here the engine is turned on and operated as a series generator until the driver accelerator command exceeds 70%. Then the controller transitions into parallel mode. In parallel mode there are two further sub-states for both electric motor assist and electric motor load. Vehicle and powertrain conditions determine the transitions between these two modes.

In this parallel state there are also three Simulink functions. These are used to set engine throttle and for series motor speed control. Similar to the series powertrain stateflow controller the series motor uses a PI function to match its torque with the ICE. The other two functions, Throttle and SP, are used to set engine throttle and motor torque during generator mode. Using Simulink functions allows these values to be tunable when the supervisory controller is compiled and imported within AMESIM.

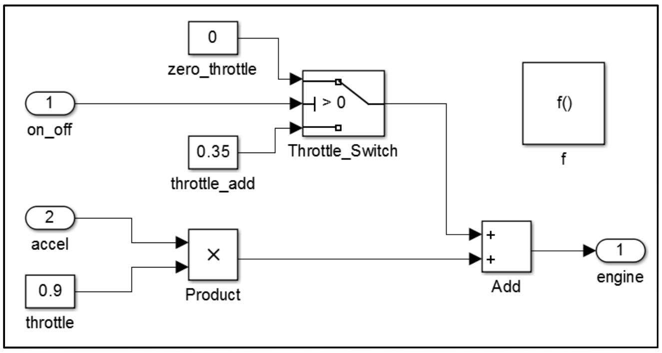

Figure 78 - Series-Parallel Engine Throttle Simulink Function

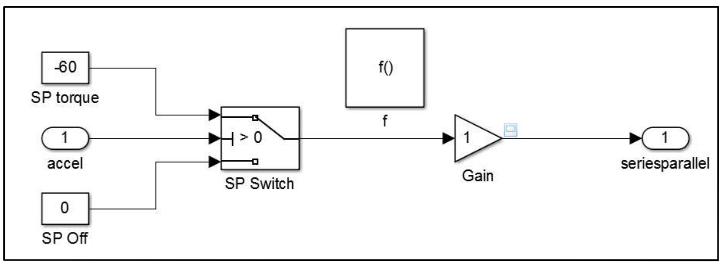

Figure 79 - Series-Parallel Generator Motor Simulink Function

9. Hybrid Powertrains with Electric Turbocharger Simulation Results

Standard Drive Cycle Simulation

Each hybrid powertrain is simulated over the US06, HWFET and UDDS cycles both with the electrified turbocharger system on and off. The overall benefits of the electrified turbocharger are then quantified within each hybrid powertrain architecture. Since electrification level is not considered, charge-depleting simulations are not conducted. All simulations are with the hybrid powertrain operating in charge-sustaining mode. This means all expended energy is either supplied by the ICE or by means of regenerative braking.

In charge sustaining mode typically the results are not perfectly state of charge neutral. The remaining battery SOC is converted to equivalent gasoline energy and counted against/for total energy consumption. Electrical energy is converted to equivalent grams of gasoline and multiplied by a set engine efficiency of 20%.Table 11 below summarizes the corrected energy consumption for the P2 parallel, series, and series-parallel hybrid powertrains with and without e-turbochargers.

Table 12 is a reproduction of earlier simulation results for the baseline conventional vehicle to compare against.

Table 11: Hybrid Powertrains Energy Consumption Results over Standard Drive Cycles

Powertrain	Energy Consumption with Electrified Turbocharger (Wh/km)				Energy Consumption without Electrified Turbocharger (Wh/km)			
	UDDS	HWFET	US06	Combined	UDDS	HWFET	US06	Combined
P2 Parallel Hybrid	715.1	559.6	744.3	645.1	716.2	552.7	749.6	642.63
Series Hybrid	396.1	519.4	652.2	452.6	405.3	522.3	685.1	457.9
Series-Parallel Hybrid	437.6	460.1	700.5	447.7	456.4	480.6	753.9	467.3

Table 12: Baseline Conventional Vehicle Results

	UDDS	HWFET	US06	Combined (City 55% / Highway 45%)
Fuel Economy (mpg)	24.5	31.8	22.4	27.8
Energy Consumption (Wh/km)	846.8	653.7	934.4	759.9

From simulation results the benefits of e-turbocharger systems within a wider hybrid powertrain range from 0.15% for the P2 parallel hybrid during UDDS cycle to 7% for the series-parallel hybrid during US06 cycle. Looking at the combined energy consumption, the greatest improvement from e-turbocharger system is for the series-parallel hybrid at a decreased energy consumption of only 19.6 Wh/km. This results suggests the e-turbocharger system does not offer any benefit in a hybrid powertrain during regular driving loads. Only during the demanding US06 cycle does the difference between powertrains with and without e-turbocharger systems become significant. The next few figures show e-turbocharger instantaneous power output for the three hybrid powertrains simulated over the three standard drive cycles. Negative power here indicated charging and positive power is discharge.

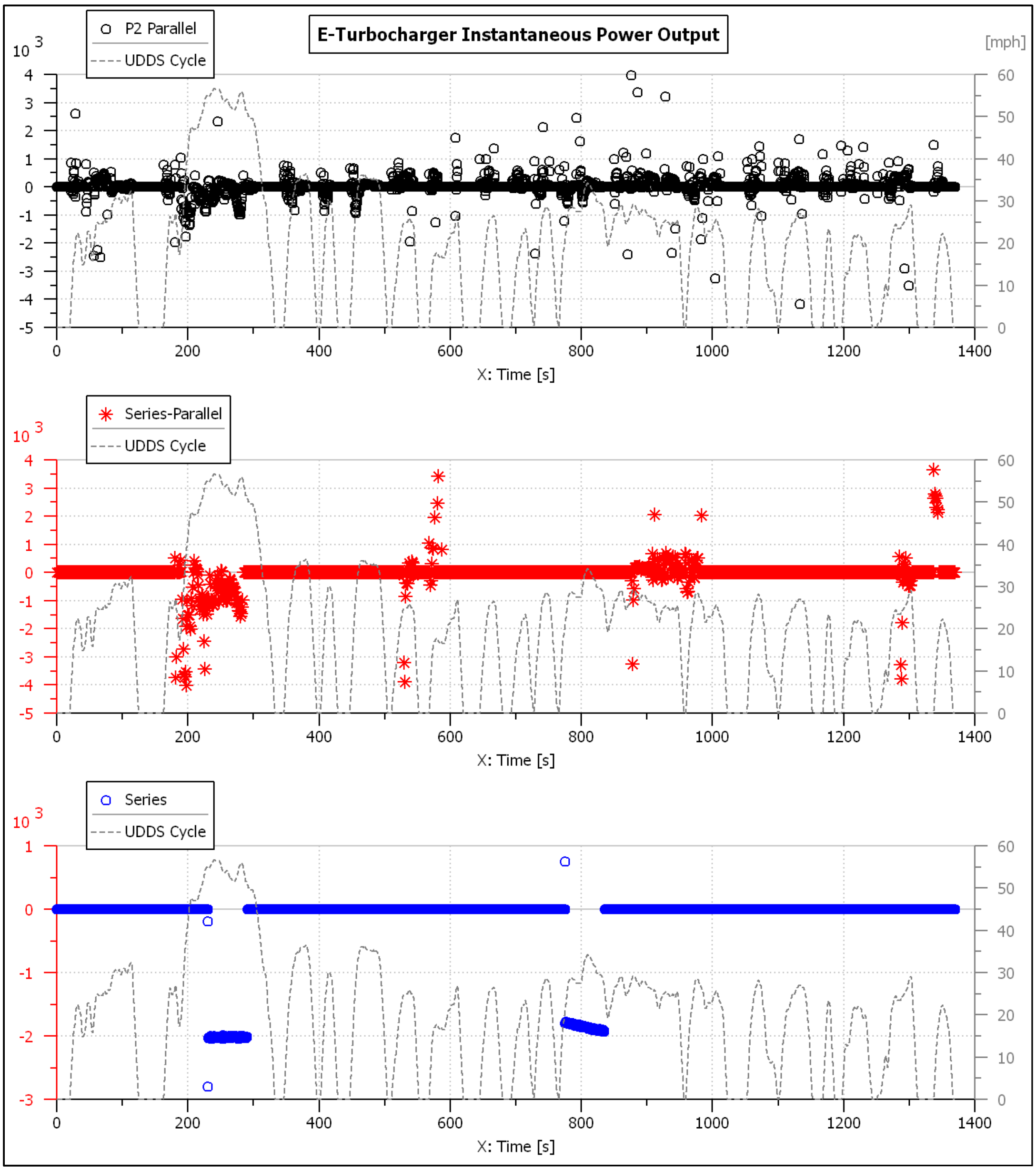

Figure 80 - E-Turbocharger Power Output over UDDS Cycle

Different modes of operation can be seen here. The P2 parallel powertrain and to an extent the series-parallel powertrain both have the ICE speed coupled to the vehicle speed. Therefore the amount of energy recovered from them varies on the drive cycle. Series powertrain in contrast output nearly a constant power through the system since the engine is at a set rpm and throttle level.

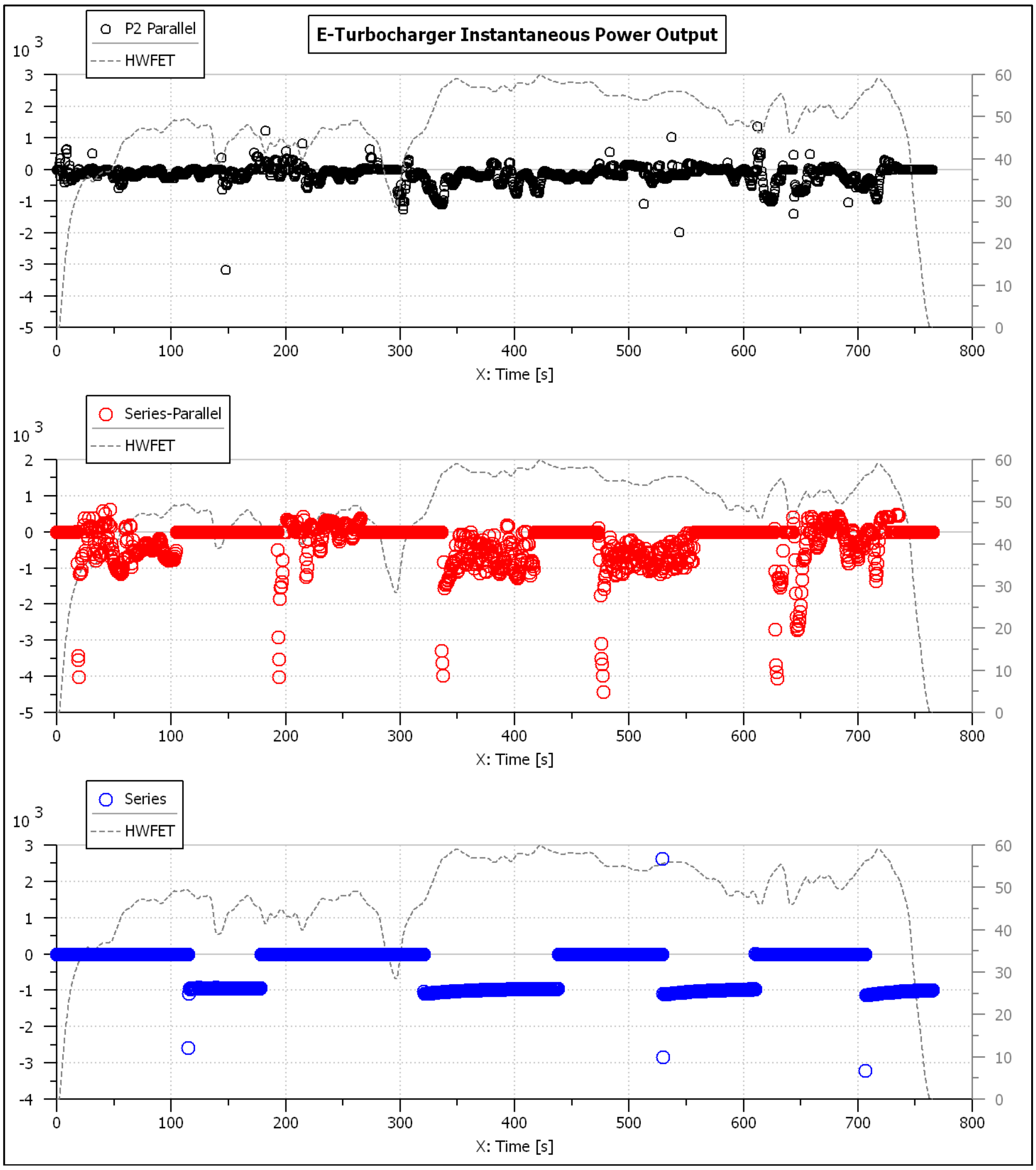

Figure 81 - E-Turbocharger Power Output over HWFET Cycle

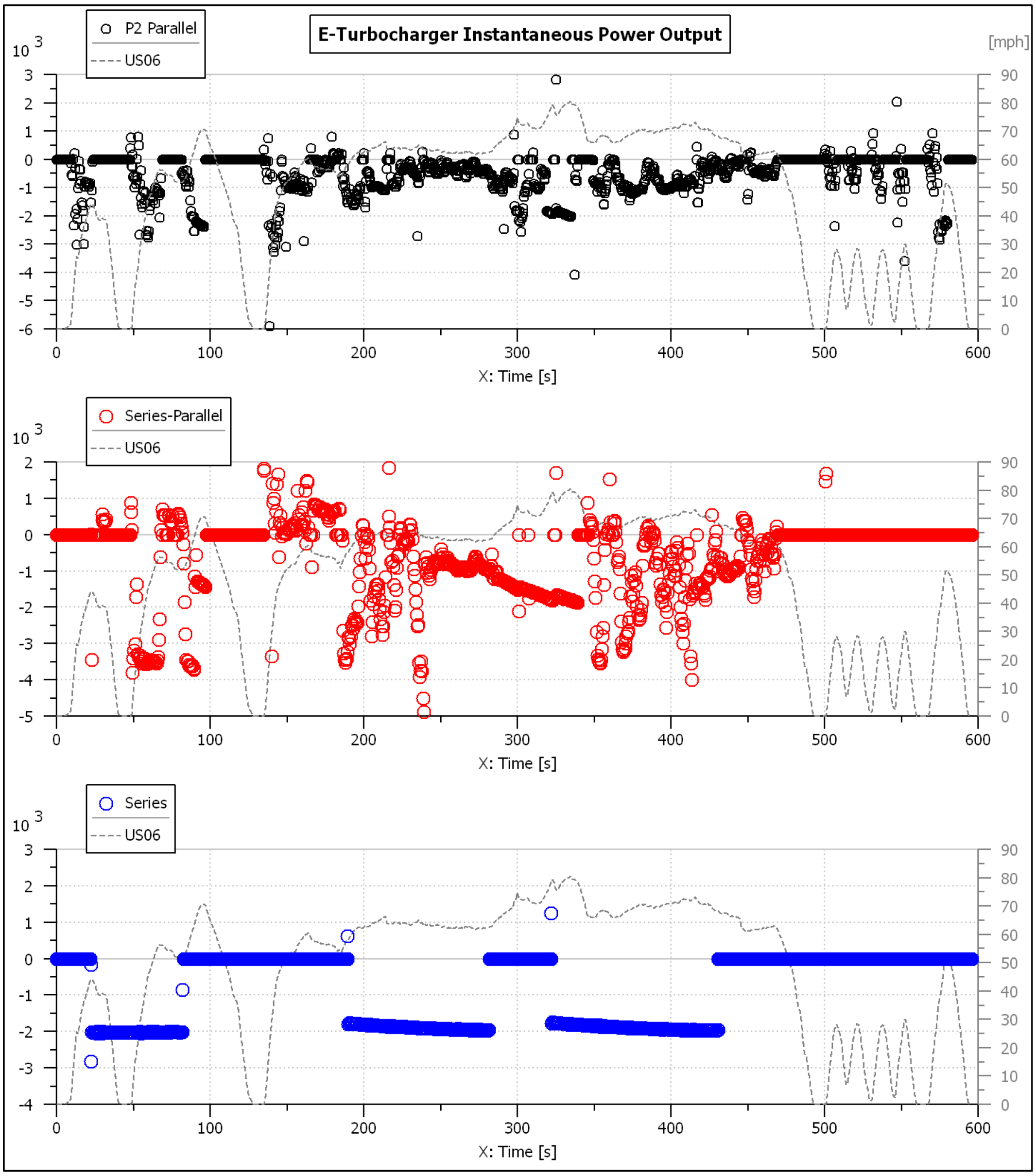

Figure 82 - E-Turbocharger Power Output over US06 Cycle

In the higher performance US06 cycle there is a marked increase in the amount of energy recovered from the turbocharger. A high load demand on the ICE leads to greater waste energy in the exhaust and consequently a higher amount recovered by the e-turbocharger.

Track Simulation

For sports cars and other similar vehicles an important part of their design is performance at a track. An increasing number of manufacturers are using track lap times in their marketing strategies to convince the consumer their product is better than the competition. For example lap times on the German circuit Nürburgring are often used to promote new high performance cars. When Porsche released the new 918 Spyder, a hybrid supercar, they announced the car had broken the 7 minute lap time barrier at the Nürburgring [55].

To simulate track performance with and without the e-turbocharger track drive cycles are generated using a program called Optimum Lap. Optimum Lap is a vehicle dynamics software which uses basic vehicle, tire and powertrain information to conduct lap time simulations around user defined tracks.

First a track is defined using a combination of straight lengths and constant radius turns. Here the Circuit of the Americas in Austin, Texas is modelled.

Type	Section Length (m)	Corner Radius (m)
Straight	242.329	
Left	29.211	1748.373
Straight	29.485	
Left	26.525	1225.987
Left	22.501	973.809
Left	18.658	1117.720

(a) Track Definition Cells

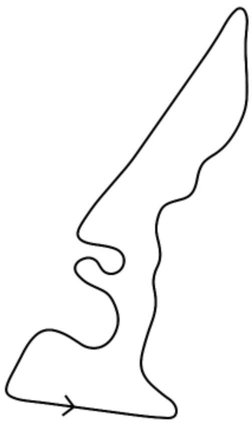

(b) Circuit of the Americas Track

Figure 83 – Circuit of the Americas Track as Defined in Optimum Lap

Then the following basic information about the vehicle, powertrain and traction is defined:

- Vehicle mass
- Drag Coefficient & Frontal Area
- Lateral/Longitudinal Friction Coefficient
- Tire Radius and Rolling Resistance
- Engine WOT Curve
- Transmission Gear Ratios and Shift Speeds
- Final Drive Ratio
- Total Driveline Efficiency

Optimum lap uses these basic parameters about the vehicle to calculate driving, braking and cornering forces. First the track is broken up into segments for braking, cornering and accelerating. Then the maximum cornering speed is calculated using the corner radius (R), vehicle mass (M) and vehicle downforce (Fy).

$$V_{cornering} = \sqrt{\frac{F_y * R}{M}} \tag{11}$$

Then the speed accelerating out the corners is calculated using vehicle lateral friction coefficient, engine WOT curve and the driveline model. Lastly the distance needed to decelerate the vehicle for the next corner is calculated. Using this method the performance of the vehicle over a lap is simulated.

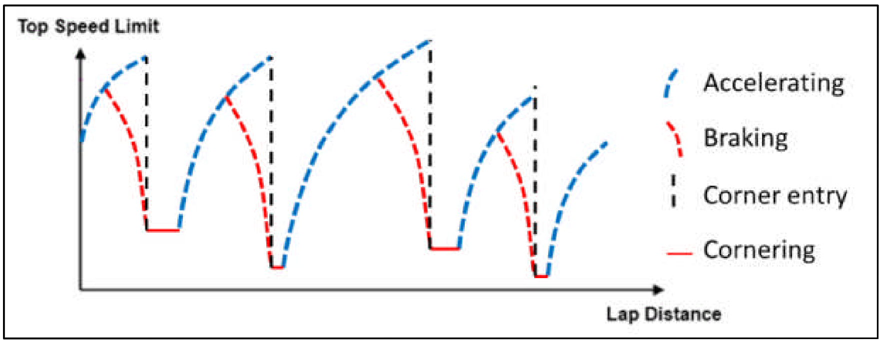

Figure 84 - Optimum Lap Calculation Process Illustration [56]

To generate a representative track drive cycle for testing with hybrid e-turbo models in AMESIM the baseline conventional vehicle as described earlier in this report is modelled and simulated over the Circuit of the Americas track in Optimum Lap. In the model an additional mass of 150 kg is added to compensate for added hybrid powertrain mass and the lateral/longitudinal friction is set at 0.95. The resulting drive cycle and track performance is displayed in the figures below:

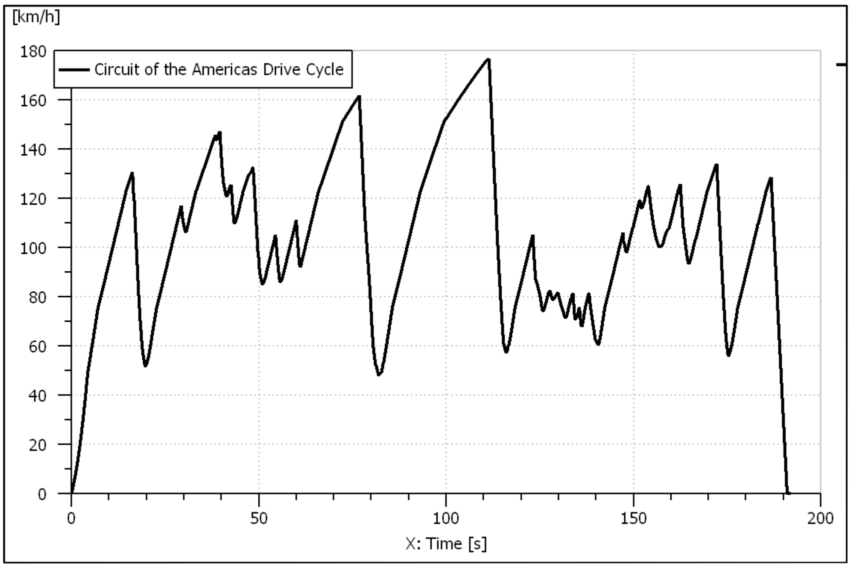

Figure 85 - Circuit of the Americas Drive Cycle from Optimum Lap

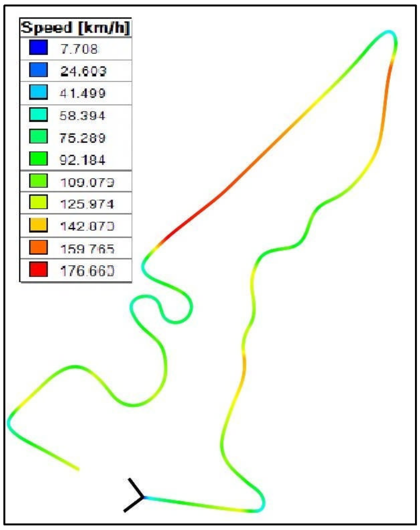

Figure 86 - Track Map Colored by Velocity

This new drive cycle trace is imported into AMESIM and used to evaluate performance with and without the e-turbocharger in the hybrid powertrain.

In both series and series-parallel hybrid powertrains the E-turbocharger system assists in sustaining the battery state of charge. For both powertrain architectures the extra energy provided by the system is sufficient to complete a lap of the Circuit of the Americas with the delta battery SOC within 1%.

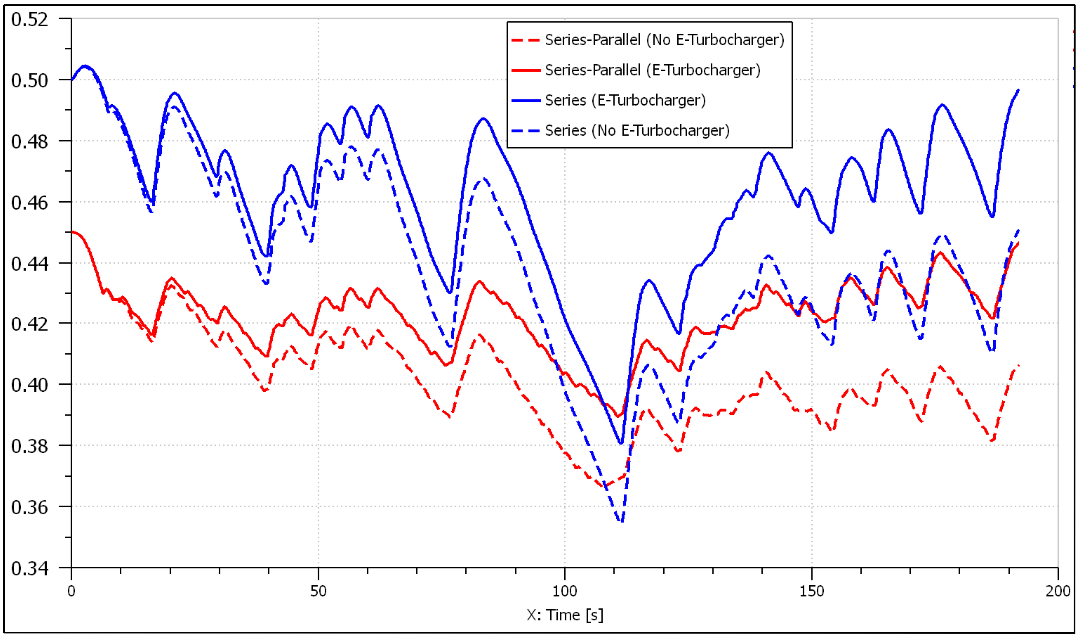

Figure 87 - Series-Parallel and Series Track Simulation Battery SOC Results

In Figure 87 battery SOC over a single lap simulation can be seen. In simulations with the e-turbocharger system enabled delta battery SOC is improved by almost 5% leading to an almost perfectly balanced charge-sustaining simulation. The energy consumption results are summarized in Table 13 below.

Table 13: Hybrid Powertrains Energy Consumption Results over Track Drive Cycle

Powertrain	**With E-turbocharger (Wh/km)**	**Without E-Turbocharger (Wh/km)**
Series	1230.8	1399.8
Series-Parallel	840.6	1045.1

Energy consumption is around 200 Wh/km lower due to the e-turbocharger system. In both powertrains the ICE operates at wide-open throttle leading to increased energy recovery from the e-turbocharger. This makes the e-turbocharger system more effective in this application.

In the P2 hybrid powertrain the vehicle was incapable of keeping up with the track drive cycle when in charge-sustaining mode. When in CS mode the supervisory controller will automatically de-rate the electrical system to a lower power output to avoid consuming more battery energy. It reduces the overall system power to a level where it is insufficient to follow the drive cycle. Even with the e-turbocharger system the P2 hybrid model can only match the track drive cycle in charge depleting mode.

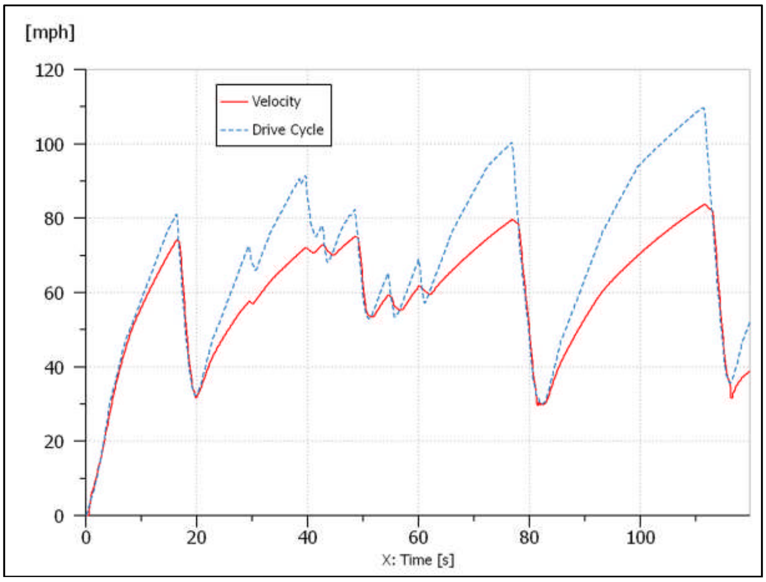

Figure 88 - P2 Hybrid CS Track Simulation

In the parallel hybrid configuration the ICE rpm is directly linked to the vehicle speed via the transmission and driveline. At higher speeds the ICE alone cannot supply the torque needed for acceleration, and since the electric motor is de-rated the vehicle's acceleration rate slows down around 80 mph.

10. Conclusion

An electrified turbocharger system in a consumer performance hybrid vehicle does not offer any substantial efficiency benefits during normal driving conditions. The system is not capable of recovering enough power when engine loads are low. Additionally in a hybrid powertrain high acceleration events generally use the electrical motor(s) to provide traction power keeping engine loads even lower than an equivalent conventional powertrain. In this research high-fidelity simulations have shown even under the US06 cycle the biggest energy benefit to a hybrid is around 50 Wh/km.

Under track performance conditions however the electric turbocharger can add close to 200 Wh/km of extra energy from the 4-cylinder engine. It is enough extra energy for the vehicle to successfully stay in charge sustaining mode during a lap of the Circuit of the Americas.

It should be noted the supervisory controllers and ECU used for these simulations are not optimized. A future opportunity would be to modify the ECU to take advantage of the electric turbocharger by taking engine transient conditions into account. Hybrid powertrain mode transitions and battery SOC management can also be optimized to maximize fuel economy.

References

[1] United States Environmental Protection Agency, August 2012. [Online]. Available: http://www.epa.gov/otaq/climate/documents/420f12051.pdf.

[2] National Highway Traffic Safety Administration, "CAFE - Fuel Economy," December 2014. [Online]. Available: http://www.nhtsa.gov/fuel-economy. [Accessed April 2015].

[3] Z. Yang, "Improving the conversions between the various passenger vehicle fuel economy/CO2 emission standards around the world," December 2014. [Online]. Available: http://www.theicct.org/blogs/staff/improving-conversions-between-passenger-vehicle-efficiency-standards. [Accessed April 2015].

[4] Center for Climate and Energy Solutions, "Comparison of Actual and Projected Fuel Economy for New Passenger Vehicles," 2014. [Online]. Available: http://www.c2es.org/federal/executive/vehicle-standards/fuel-economy-comparison. [Accessed April 2015].

[5] Cummins Inc., "Worldwide Emissions Regulations," 2014. [Online]. Available: http://cumminsemissionsolutions.com/ces/navigationAction.do?url=SiteContent+en+HTML+EmissionsTechnology+Worldwide_Emissions_Regualtions. [Accessed April 2015].

[6] Environmental Protection Agency, "EPA and NHTSA Set Standards to Reduce Greenhouse Gases and Improve Fuel Economy for Model Years 2017-2025 Cars and Light Trucks," Office of Transportation and Air Quality, Washington, 2012.

[7] J. Thomas, "Drive Cycle Powertrain Efficiencies and Trends Derived from EPA Vehicle Dynamometer Results," *SAE Int. J. Passeng. Cars - Mech. Syst.,* vol. 7, no. 4, pp. 1374-1384, 2014.

[8] M. Baglione, D. M. and a. P. G. , "Vehicle System Energy Analysis Methodology and Tool for Determining Vehicle Subsystem Energy Supply and Demand," *SAE International,* 2007.

[9] Department of Energy, "Where the Energy Goes: Gasoline Vehicles," 2015. [Online]. Available: https://www.fueleconomy.gov/feg/atv.shtml. [Accessed April 2015].

[10] Mazda Motor Corporation, "Skyactiv Technologies," 2015. [Online]. Available: http://www.mazda.com/en/innovation/technology/skyactiv. [Accessed April 2015].

[11] C. Corapi and G. Ott, "Mazda`s Skyactiv Technology," Pittsburg, 2012.

[12] T. Mark, "Next-generation Mazda engines to eclipse electric cars on emissions," March 2014. [Online]. Available: http://www.autocar.co.uk/car-news/industry/next-generation-mazda-engines-eclipse-electric-cars-emissions. [Accessed April 2015].

[13] Y. Cengel and M. Boles, Thermodynamics: An Engineering Approach, 7th ed., 2010.

[14] T. Grissom, "Turbocharging for Improved Engine Performance & Reduced CO2 Emissions," in *SAE International*, 2013.

[15] Ford Motor Company, "Ford Builds Two Millionth EcoBoost Engine as Consumer Demand Grows in Markets Worldwide," September 2013. [Online]. Available: https://media.ford.com/content/fordmedia/fna/us/en/news/2013/09/17/ford-builds-two-millionth-ecoboost-engine-as-consumer-demand-gro.html. [Accessed April 2015].

[16] J. Cobb, "December 2014 Dashboard," hybridcars.com, 6 January 2015. [Online]. Available: http://www.hybridcars.com/december-2014-dashboard/. [Accessed April 2015].

[17] a. Galindo et, "Surge limit definition in a specific test bench for the characterization of automotive turbochargers," *Experimental Thermal and Fluid Sci.,* vol. 30, no. 5, pp. 449-462, 2006.

[18] a. Saidur et, "Technologies to recover exhaist heat from internal combustion engines," *Renewable and Sustainable Energy Reviews,* vol. 16, no. 8, pp. 5649-5659, 2012.

[19] Honeywell International Inc., "Garret Performance Products," 2015. [Online]. Available: http://www.turbobygarrett.com/turbobygarrett/compressor_maps. [Accessed April 2015].

[20] H. Jaaskelainen, "Turbocharging Challenges," DieselNet Technology, April 2013. [Online]. Available: https://www.dieselnet.com/tech/air_turbo_challenge.php#lag. [Accessed April 2015].

[21] e. a. A. Pesiridis, Automotive Exhaust Power and Waste Heat Recovery Technologies, Hauppauge, NY: Nova Science Pub. Inc., 2012.

[22] W. De Ojeda and M. Rajkumar, "Engine Technologies for Clean and High Efficiency Heavy Duty Engines," *SAE International,* 2012.

[23] A. M. Noor, R. C. Puteh and S. Rajoo, "Waste Heat Recovery Technologies in Turbocharged Automotive Engine - A Review," *Journal of Modern Science and Technology,* vol. 2, no. 1, pp. 108-119, 2014.

[24] e. a. Wei Wei, "Comparative Study on Electric Turbo Compounding Systems for Gasoline Engine Exhaust Energy Recovery," in *ASME Turbo Expo 2010*, Glasgow, 2010.

[25] Audi AG, "Electric biturbo and hybridization," Audi MediaServices, 14 July 2014. [Online]. Available: https://www.audi-mediaservices.com/publish/ms/content/en/public/hintergrundberichte/2014/07/14/the_audi_tdi___tech/electric_biturbo_and.html. [Accessed April 2015].

[26] D. Carney, "Electric turbos promise big performance and efficiency gains in the near future," Autoblog, 8 August 2014. [Online]. Available: http://www.autoblog.com/2014/08/08/audi-electric-turbocharging-feature/. [Accessed April 2015].

[27] K. Buchholz, "Valeo's electric supercharger targeted for 2015-16 production," Automotive Engineering Magazine, France, 2012.

[28] BorgWarner, "eBooster," BorgWarner, 2015. [Online]. Available: http://www.turbos.bwauto.com/products/eBooster.aspx. [Accessed April 2015].

[29] AerisTech, "Full Electric Turbochager Technology," AerisTech, 2015. [Online]. Available: http://www.aeristech.co.uk/full-electric-turbocharger-technology. [Accessed April 2015].

[30] U. Hopmann and M. Algrain, "Diesel Engine Electric Turbo Compound Technology," *SAE International,* 2003.

[31] I. Arsie, A. Cricchio and C. Pianese, "A Comprehensive Powertrain Model to Evaluate the Benefits of Electric Turbo Compound (ETC) in Reducing CO2 Emissions from Small Diesel Passenger Cars," *SAE International,* 2014.

[32] Federation Internationale De L'Automobile, "2014 Formula One Power Unit Regulations," 2014. [Online]. Available: http://www.fia.com/sites/default/files/publication/file/FIA%20F1%20Power%20Unit%20leaflet.pdf. [Accessed April 2015].

[33] Mercedes AMG Petronas Formula One Team, "PU 106A Hybrid," Mercedes-Benz Grand Prix Ltd, 2015. [Online]. Available: http://www.mercedesamgf1.com/en/car/pu106a-hybrid/. [Accessed April 2015].

[34] Formula1 Dictionary, "2014 Formula 1 Rule change New Power Unit with ERS," 2014. [Online]. Available: http://www.formula1-dictionary.net/engine_power_unit_and_ers.html#index_top_page. [Accessed April 2015].

[35] M. Olszewski, "Evaluation of 2004 Toyota Prius Hybrid Electric Drive System," Washington, 2006.

[36] E. Karden, "Microhybrid Goes Mainstream: Battery Selection and Trends," in *Advanced Battery Conference* , Mainz, 2011.

[37] US Department of Energy, August 2013. [Online]. Available: http://www.fueleconomy.gov/feg/Find.do?action=sbs&id=33336&id=32655&id=33335&id=32516.

[38] Car and Driver, "Car and Driver," 2015. [Online]. Available: http://www.caranddriver.com/. [Accessed April 2015].

[39] P. Zal, "Automobile Catalog," 2015. [Online]. Available: http://www.automobile-catalog.com/. [Accessed April 2015].

[40] Ford Motor Co., "2015 Mustang," 2015. [Online]. Available: http://www.ford.ca/cars/mustang/. [Accessed April 2015].

[41] Fiat Chrysler Automobiles, "Dodge Challenger," 2015. [Online]. Available: http://www.dodge.com/en/challenger/. [Accessed April 2015].

[42] Chevrolet Canada, "Camaro eBrochure," 2014. [Online]. Available: http://www.chevrolet.com/content/dam/Chevrolet/northamerica/usa/nscwebsite/en/Home/Vehicles/Performance/Camaro/02_pdf/MY15%20Camaro%20eBrochure_102214.pdf. [Accessed April 2015].

[43] M. Juhala, "Improving vehicle rolling resistance and aerodynamics," in *Alternative Fuels and Advanced Vehicle Technologies for Improved Environmental Performance*, Woodhead Publishing Limited, 2014, p. 462–475.

[44] Environmental Protection Agency, "Fuel Economy Labeling of Motor Vehicles: Revisions To Improve Calculation of Fuel Economy Estimates," *Federal Register,* vol. 71, no. 248, 2006.

[45] United States Environmental Protection Agency, "Dynamometer Drive Schedules," 6 February 2013. [Online]. Available: http://www.epa.gov/nvfel/testing/dynamometer.htm. [Accessed 2014].

[46] Natural Resources Canada, "5-cycle Testing," 20 June 2014. [Online]. Available: http://www.nrcan.gc.ca/energy/efficiency/transportation/cars-light-trucks/buying/7495. [Accessed April 2015].

[47] Advanced Vehicle Technology Competition; Department of Energy, "Model Based Design for Vehicle Powertrains," National Training and Education Resource, Lemont, 2014.

[48] Argonne National Laboratory, "Autonomie," December 2013. [Online]. Available: http://www.autonomie.net/. [Accessed April 2015].

[49] A. Irimescu, L. Mihon and G. Pãdure, "Automotive transmission efficiency measurement using a chassis dynamometer," *International Journal of Automotive Technology,* vol. 12, no. 4, pp. 555-559, 2011.

[50] T. Read and D. Nordlicht, "Cadillac Introduces New 8-Speed Automatic on CT6," 20 March 2015. [Online]. Available: http://media.cadillac.com/media/us/en/cadillac/news.detail.html/content/Pages/news/us/en/2015/mar/0320-cadillac/0320-cadillac-8spd-trans.html. [Accessed April 2015].

[51] Cornell University Law School, "40 CFR 600.109-08 - EPA driving cycles.," 6 July 2011. [Online]. Available: https://www.law.cornell.edu/cfr/text/40/600.109-08. [Accessed April 2015].

[52] LMS Imagine Lab, "8.2.2 WIEBE Model," AMESIM Help Documentation, Detroit, 2014.

[53] G. Woschni, "A Universally Applicable Equation for the Instantaneous Heat Transfer Coefficient in the Internal Combustion Engine," *SAE International,* 1967.

[54] LMS Imagine Lab, "8.5.4. Woschni," AMESIM Help Documentation, Detriot , 2014.

[55] Porsche, "Porsche 918 Spyder Record Lap Onboard," YouTube , https://www.youtube.com/watch?v=2Yz8cizr6sI.

[56] Optimum G, "OptimumLap Help File," Optimum G, 2014.

Appendix

Engine Gas Model

All three gasses in the engine model are defined using a linear model. First this model requires the definition of these constants at two different temperatures (intake temperature and exhaust temperature).

- Intake reference temperature
- Exhaust reference temperature
- Cp (J/kg/K)
- Perfect gas constant, r, (J/kg/K)
- Viscosity (kg/m/s)
- Thermal conductivity (W/m/K)

Using these constants at two different temperature point the same gas properties at any other temperature point is calculated using linear interpolation.

For density the ideal gas law is used and the constant-volume specific heat is calculated with the Mayer law:

$$C_v(p,T) = C_p(p,T) - r$$

E-Turbocharger Track Simulation Results

In this appendix plots of vehicle velocity and battery state of charge are given for series-parallel and series hybrid powertrains with and without the electric turbocharger system under the track cycle.

Series CS without E-turbocharger

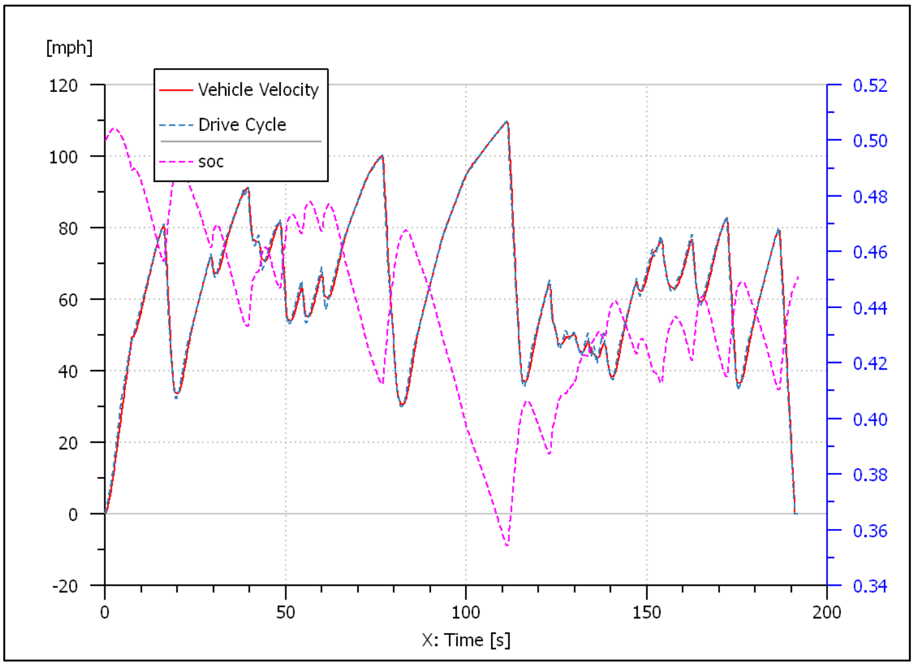

Series CS with E-turbocharger

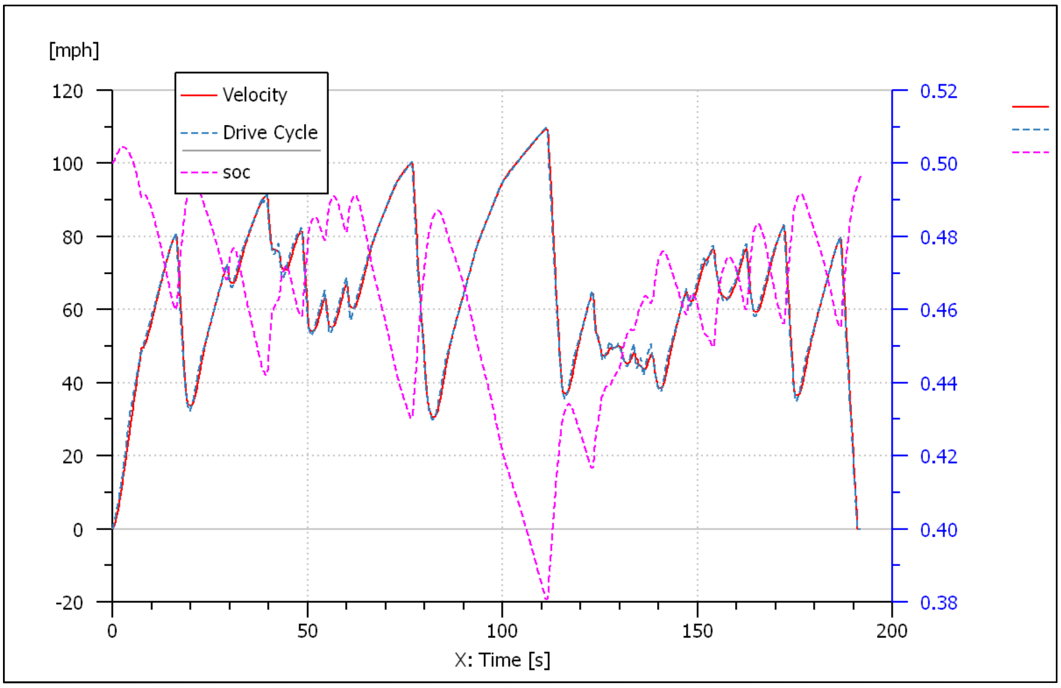

Series Parallel without E-turbocharger

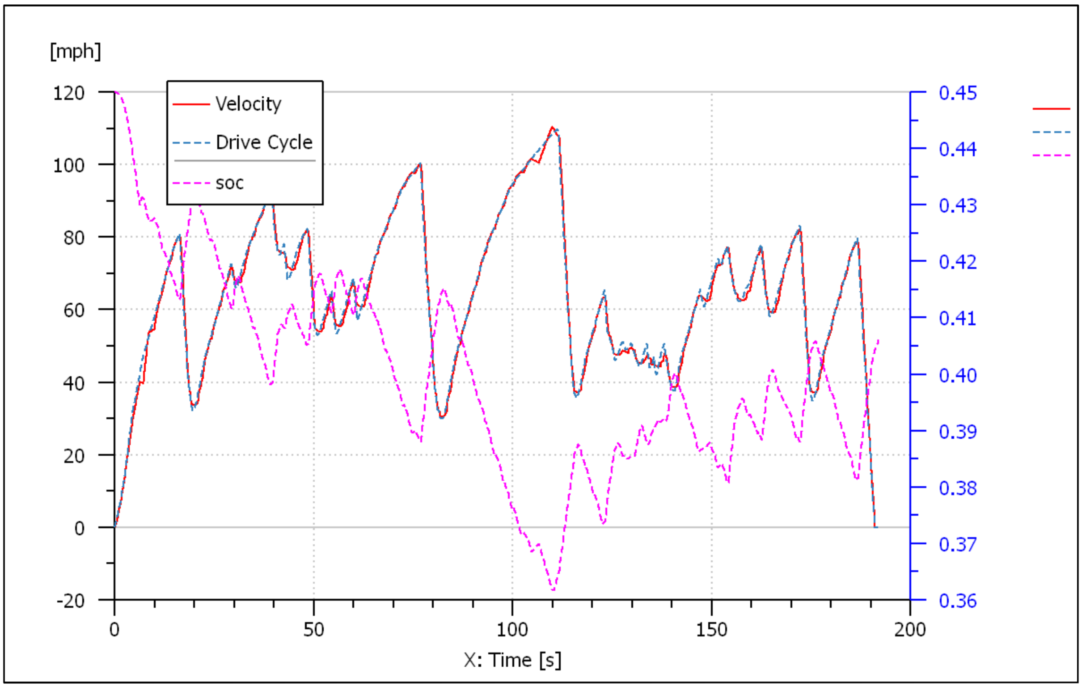

Series Parallel with E-turbocharger

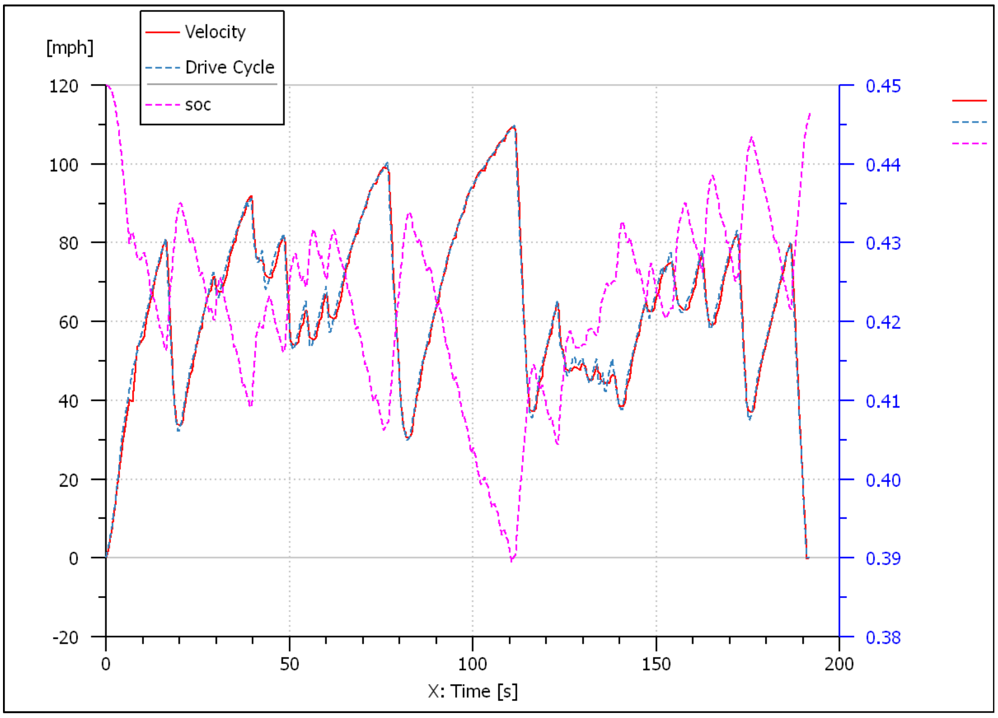

E-Turbocharger Standard Cycle Simulation Results

In this appendix the instantaneous engine efficiency and turbocharger electrical energy output are given for each hybrid powertrain under standard drive cycles.

Series-Parallel Hybrid UDDS Cycle

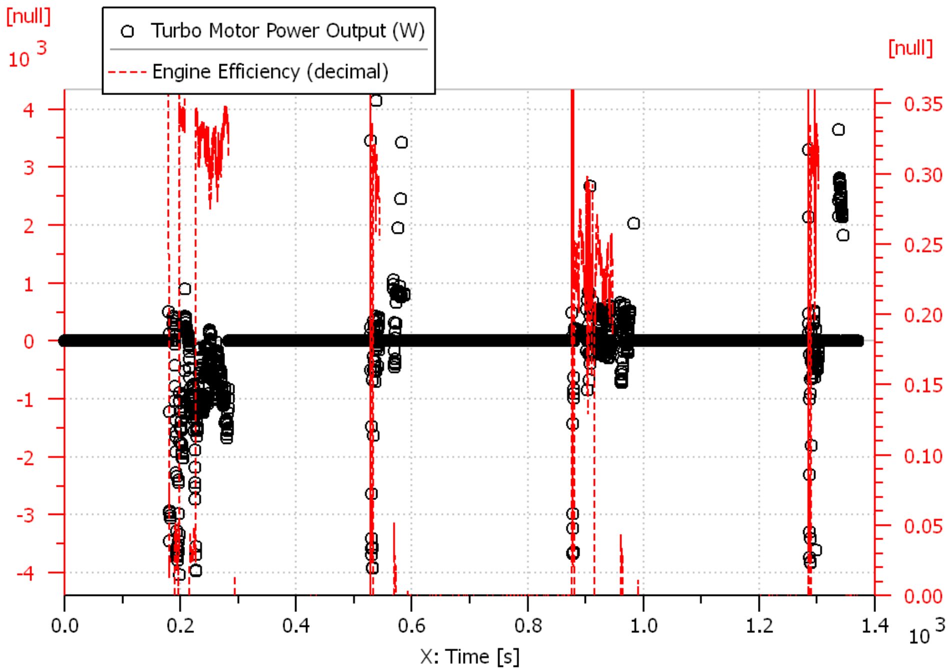

Series-Parallel Hybrid HWFET Cycle

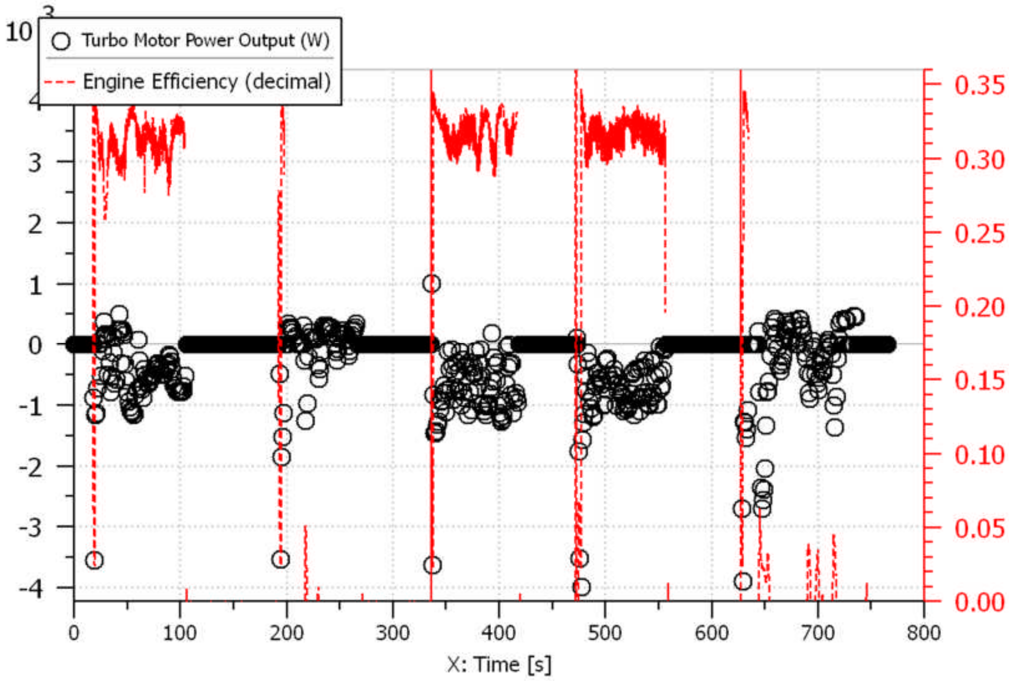

Series-Parallel Hybrid US06 Cycle

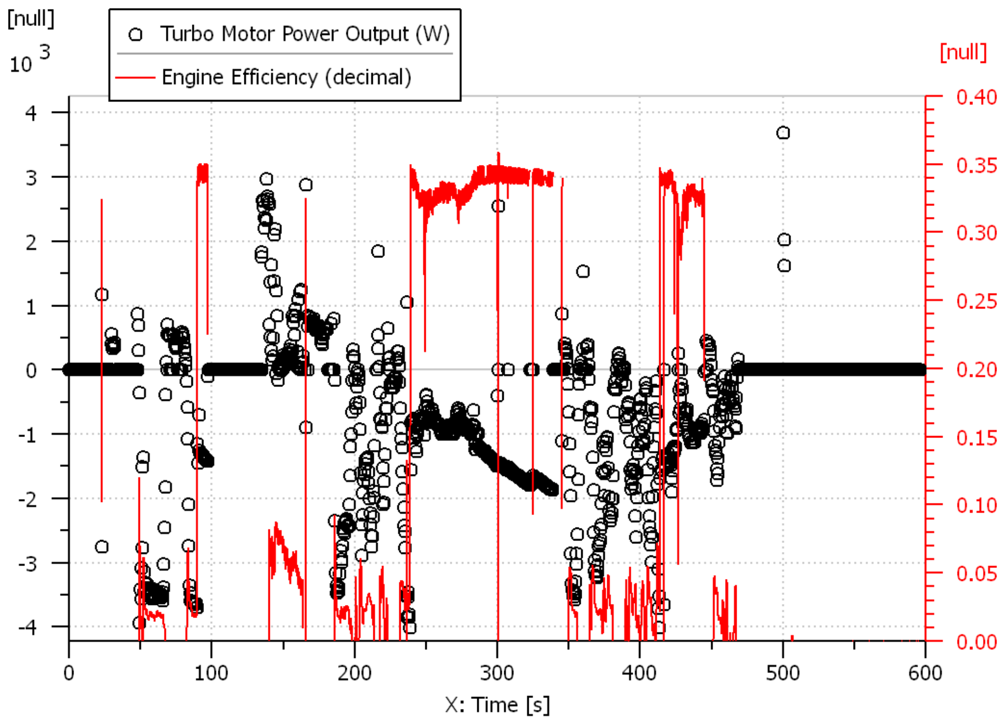

P2 Parallel Hybrid UDDS Cycle

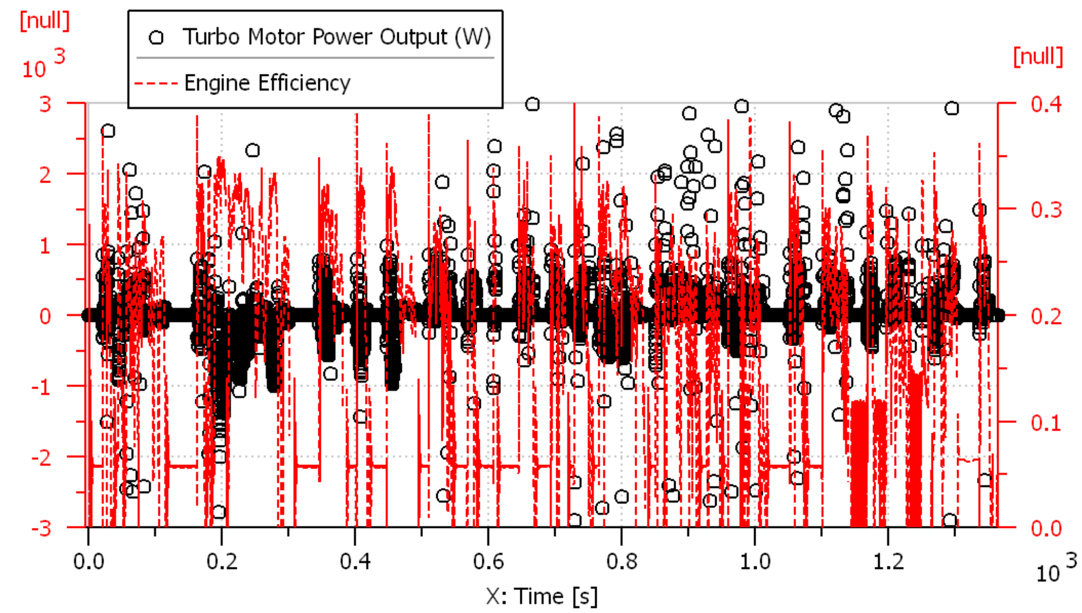

P2 Parallel Hybrid HWFET Cycle

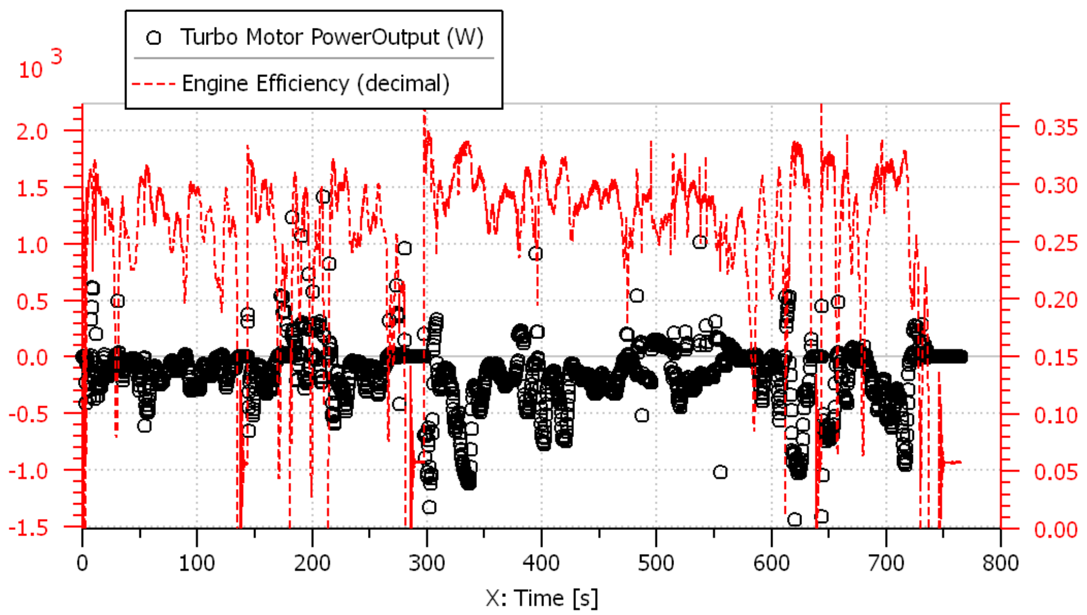

P2 Parallel Hybrid US06 Cycle

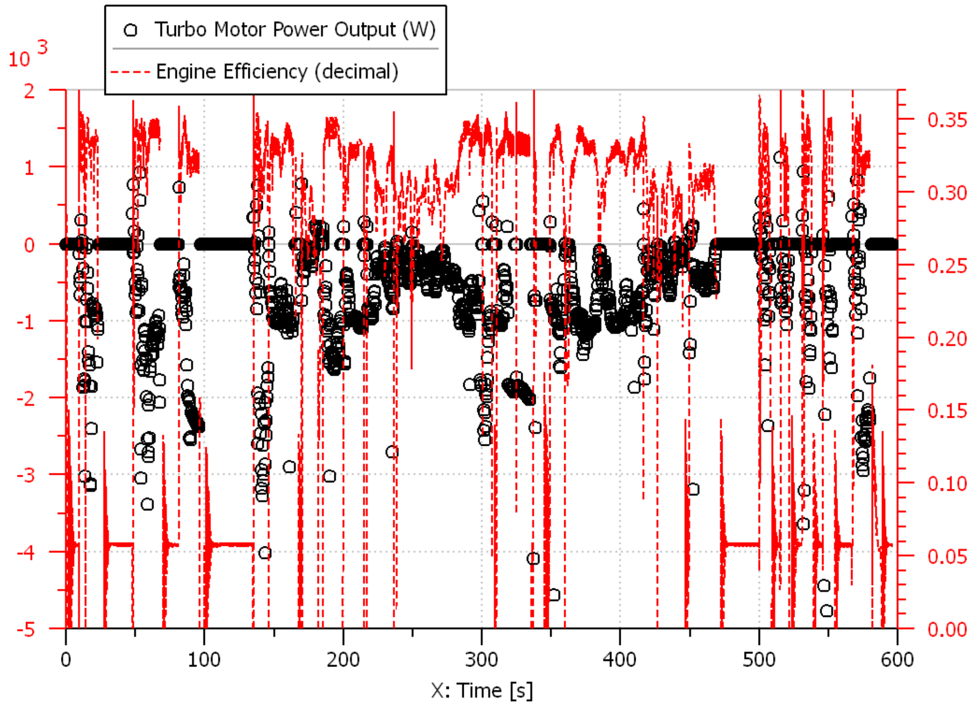

Series Hybrid UDDS Cycle

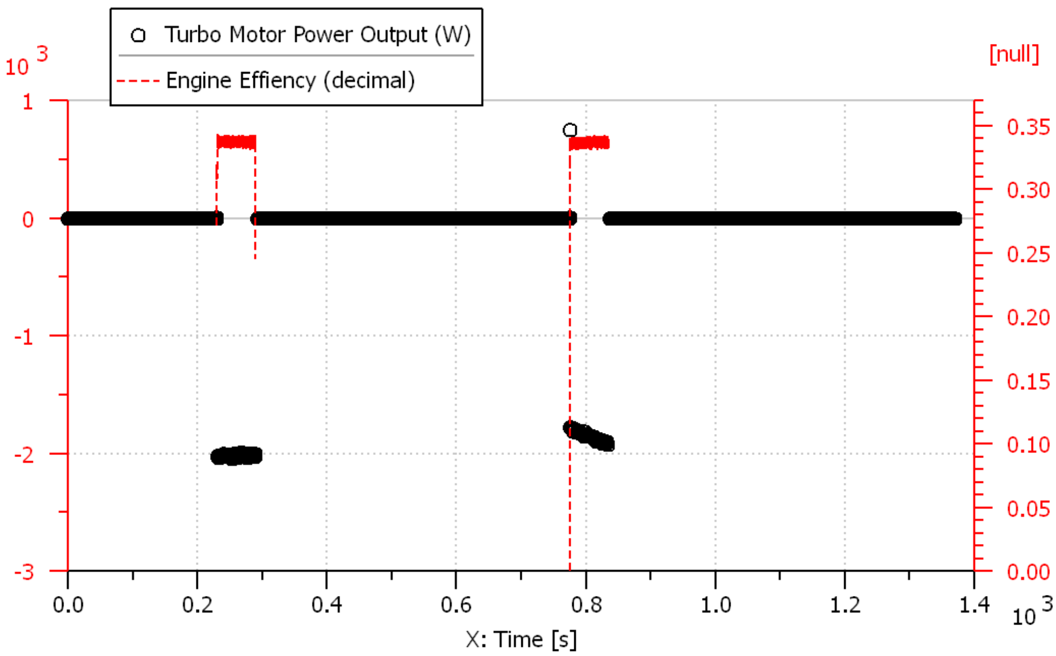

Series Hybrid HWFET Cycle

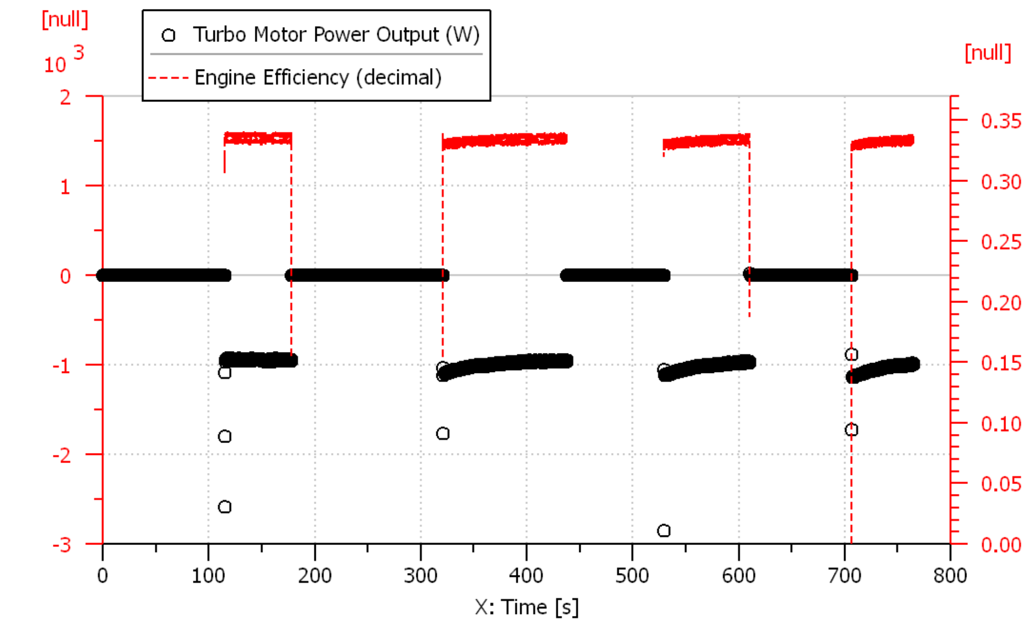

Series Hybrid US06 Cycle